



Broadband multispectral indices for remote sensing of vegetation
affected by oil spills in the mangrove forest of the Niger Delta,
Nigeria

Thesis submitted for the degree of
Doctor of Philosophy
at the University of Leicester

by

Bashir Adamu

Department of Geography

University of Leicester

2016

Broadband multispectral indices for remote sensing of vegetation affected by oil spills
in the mangrove forest of the Niger Delta, Nigeria

Bashir Adamu

Abstract

Detection of vegetation affected by oil spills in oil polluted environments such as mangrove forest can be challenging using in-situ measurements and laboratory-based analysis techniques. Satellite remote sensing has been shown to be an effective tool to detect and monitor vegetation health and status in polluted areas. The application of broadband multispectral vegetation indices (BMVIs) derived from remotely sensed satellite data to detect and monitor impacts of oil spills on vegetation health has not been fully evaluated through previous research. The study was conducted in the mangrove forest South-West of Port Harcourt City in Niger Delta, Nigeria. This study first investigated the potential for using BMVIs to detect the impact / the effects of oil pollution on vegetation health. A total of 20 BMVIs were evaluated using data acquired at the visible, near infrared and shortwave infrared wavelengths. In Chapter 4 a statistical analysis of the indices from 37 oil polluted and non-polluted (control) sites show that 12 BMVIs demonstrated significant differences ($p < 0.05$) between pre- and post-spill observations. For the control sites 11 of the 20 BMVI values did not indicate significant change and remained statistically invariant before and after the spill date ($p \geq 0.05$). Oil spills are therefore suggested to cause a biophysical and biochemical alteration of the vegetation, leading to changes in reflectance signature detected by these indices. Five spectral indices (normalized difference vegetation index (NDVI), soil-adjusted vegetation index (SAVI), adjusted resistant vegetation index (ARVI2), green near infrared (G/NIR) and green shortwave infrared (G/SWIR)) were found to be consistently sensitive to the effects of oil pollution on vegetation and hence could be used for detection of oil pollution in vegetated areas. This study sought to, secondly, investigate factors that have been assumed to be influential on the detection of the impacts on vegetation from oil spills such as oil spill volume, time gap (number of days between oil spill events and image acquisition date) and spatial distance using the five BMVIs (NDVI, SAVI, ARVI2, G/NIR and G/SWIR). Regression analysis, utilised to determine the relative influence of these factors over 56 oil spill sites, revealed a significant relationship between the volume of the oil spill and increased deterioration of vegetation condition ($p < 0.05$) for four of the indices (NDVI, SAVI, ARVI2 and G/NIR). The length of time between image acquisition and oil spill was observed to exert an influence on the ability to detect the biophysical effects of oil spills on vegetation. The longer the time gap between the date of image acquisition and the oil spill event, the lower the detectability of oil spill impacts on vegetation. The influence of spatial variation on the detection of vegetation impacts was evaluated using a directional flow model applied over a local neighbourhood; the results from which did not show any significant difference between the neighbouring pixels (first pixel-P1, second pixel-P2 and third pixel-P3). The study also attempted to assess and validate the techniques used in chapter 4 in a different study site (study site 2- SS2) with a relative climatic and environmental conditions using new oil spill data in 2014. The findings revealed that statistical results from five indices (NDVI, SAVI, ARVI2 and G/NIR) derived from Landsat 8 in SS2 are found to show similar results to the ones obtained in SS1 using Landsat 5 & 7. In conclusion, it was found that the BMVIs have potential capacity for detection

of vegetation affected by oil spills, not only are several factors found to exert a significant influence on the detection of oil spill impact on vegetation pollution using BMVIs, but also this method has the potential for replication in other over an oil-polluted environment.

Dedication

This Thesis is dedicated to my late mother (Amina Adamu), my son (Muhammad-Nabeel) and wife (Ikilimat Tamima). I am ever grateful to my dad (Adamu Usman).

Acknowledgements

I would like to express my very great appreciation to my main supervisor Professor Kevin Tansey for his valuable and constructive suggestions during the planning and development of this research work. I thank you Kevin for the patient guidance, enthusiastic encouragement and useful critiques of this research work. I would also like to thank my initial co-supervisors Professor Michael J. Bradshaw (University of Warwick) and Dr. Booker Ogutu (University of Southampton) for their advice and assistance while at the University of Leicester. My grateful thanks are also extended to Professor Heiko Balzter, Professor Alan Blackburn and Dr. Sue McLaren. I greatly appreciated and acknowledge the assistance provided by Dr. Virginia Nicola-Perea and Adam Cox for his technical support in software installations. I wish to acknowledge the advice and guidance before the start of the research work from Professor Mala Galtima, Professor A. L. Tukur and Professor Ademola Omojola.

I would also like to thank the USGS for providing free Landsat data for the study. I appreciate and thank the Petroleum Technology Development Fund (PTDF), Nigeria for funding this project. And many thanks to the Department of Petroleum Resources, Nigeria (DPR-N) and Shell Nigeria for the field data. To fellow colleagues in both the Department of Geography and Centre for Landscape and Climate Research (CLCR) at the University of Leicester I appreciate the good relationship and knowledge we have shared during this period. My special thanks are extended to Dr. Shittu J. Whanda, Dr. Umar Mohammed Bibi, Dr. Prem C. Pandey, Dr. Idris Mohammed Jega, Usman Isyaku, Yahya Ibrahim Zayyana, Ibrahim Sa'ad, Dr. Azad Rasul, Dr. Ramesh Ningthoujam, Ajoke Onojeghuo, Dr. Pedro Rodriguez-Veiga, (James Wheeler, Tom Potter and Chloe Barnes (help in proof-reading some parts of the thesis)), David Ackerley, Ana Maria Pacheco Pascagaza, Maryam Pourshamsi and Peshawa Najmaddin for contributing intellectual and technical ideas relating to this work. Thanks to David Lashley for the final proofreading of the entire theses.

Finally and most importantly my gratitude to wife (Ikilimat Tamima) for her patience and taking care of little Mohammed-Nabeel and myself all along.

Table of Contents

Abstract	i
Dedication	iii
Acknowledgements	iv
Table of Contents	v
Chapter 1 Introduction	1
1.0 Historical evolution of petroleum industry	2
1.1.1 Evolution of petroleum industry in Nigeria.....	4
1.1.2 Petroleum extraction and pipeline transportation.....	5
1.1.3 The impact of the oil industry on the environment	7
1.1.4 Monitoring the environmental effects of oil pipelines	9
1.1.5 Understanding the pipeline right-of-way (ROW).....	11
1.1.6 Pipeline routes and potential impacts on ecological systems	12
1.3 Thesis Structure	18
Chapter 2 : Literature review	20
2.0 Introduction	21
2.1 Hydrocarbon impact on vegetation.....	21
2.2 Effects of bidirectional reflectional distribution function (BRDF).....	23
2.3 Remote sensing and concept of spectral signatures	25
2.4 Reflectance characteristics of vegetation.....	26
2.4.1 Atmospheric effects on the radiation.....	28
2.5 Vegetation response to hydrocarbon leaks	32
2.6 Traditional method of monitoring environmental variables	33
2.7 Spectral vegetation indices for detecting impacts of hydrocarbon leaks	35
2.7.1 Broadband Multispectral Spectral Vegetation Indices (BMVIs)	35
2.7.2 Detection of oil pollution using BMVIs.....	36
2.7.3 Factors influencing detection of oil pollution	38
2.7.4 Importance of determining the flow direction of an oil spill.....	40
2.7.5 Tidal flow model	40
2.7.6 Research gap	41
2.8 Aim and objectives	42
Chapter 3 Study area, data and methodology	44
3.0 Introduction	45
3.1 Study Area - Niger Delta	45
3.1.1 Geology and Soil.....	46
3.1.2 Hydrology.....	47

3.1.3	Vegetation	49
3.1.4	Climate	51
3.2	Data sources.....	54
3.3	Data sampling and analysis	56
3.4	Landsat data.....	59
3.5	General methodology.....	62
3.5.1	Data pre-processing.....	63
3.6	Calculating vegetation indices.....	65
Chapter 4 : Investigating BMVIs for detection and analysis of vegetation affected by oil spill over time and space		67
4.0	Introduction	68
4.1	Data analysis and method.....	68
4.2	Results	70
4.2.1	Analysis of vegetation indices at the (P) and (NP) sites.....	71
4.2.2	Analysis vegetation indices before (<i>Ppre</i>), spill date (<i>Spill Date</i>) and after (<i>Ppost</i>) at the P and NP sites over time.....	74
4.3	Discussion.....	77
4.3.1	Spatial analysis of vegetation indices at the P and NP sites.....	77
4.3.2	Temporal analysis of vegetation indices at the P and NP sites	78
4.4	Summary.....	80
Chapter 5 : Analysis of factors influencing detectability of oil pollution using BMVIs		81
5.0	Introduction	82
5.1	Method.....	82
5.1.1	Volume of oil spill.....	82
5.1.2	Spatial distance.....	85
5.1.3	Time gap between spill and image acquisition date	86
5.2	Results	87
5.2.1	Influence of volume of oil spill on the selected BMVIs from 56 sample sites	87
5.2.2	Spatial analysis of oil spill on the BMVIs.....	92
5.2.3	Influence of time gap between spill and observation on BMVIs	96
5.3	Discussion.....	99
5.3.1	Influence of volume of oil spill on the selected BMVIs	99
5.3.2	Spatial analysis of oil spill on the BMVIs.....	100
5.3.3	Influence of time gap between spill and observation on BMVIs	101
5.4	Summary.....	101

Chapter 6 : Validation of vegetation spectral techniques for detection of oil pollution on vegetation.....	103
6.1 Introduction	104
6.2 Study area	104
6.3 Sources of data and method	107
6.3.1 Source of oil spill data.....	107
6.3.2 Image Data	107
6.3.3 Landsat 8 image processing	108
6.3 Method and data analysis.....	110
6.4 Results	113
6.4.1 Impact of oil spill on vegetation in the image of 2014.....	113
6.4.2 Change detection of vegetation at the oil spill sites	114
6.4.3 Changes in vegetation affected by oil pollution at the P sites (2013, 2014 and 2015)	120
6.4.4 Analysis of vegetation condition at the NP sites (2013, 2014 and 2015).....	122
6.4.5 Mapping likely stressed vegetation affected by oil pollution.....	123
6.5 Discussion.....	127
6.6 Summary.....	131
Chapter 7 : Discussion, conclusion and future work	132
7.1 Discussion.....	133
7.1.1 Are the BMVIs capable of detecting changes in the leaf pigments of vegetation affected by oil pollution in mangrove forests?.....	133
7.1.2 How do the identified factors influence detectability of vegetation affected by oil spills using spectral vegetation indices?.....	135
7.1.3 Can the method developed be implemented in a different part of the wider study area?	138
7.2 Conclusion.....	139
7.3 Future work.....	140
References.....	142

List of Figures

Figure 1.1: A Topology of Oil Pipeline and Facilities in the Niger Delta Nigeria	8
Figure 1.2: A Typical model of ROW	12
Figure 2.1: General reflectance spectra of some earth surface materials	24
Figure 2.2: Dominant factors causing leaf reflectance Source:	27
Figure 2.3: Spectral reflectance of healthy vegetation	28
Figure 2.4: The balance of incoming and outgoing radiation measured by satellites and shown in W/m ²	29
Figure 3.1: Oil pipeline and spill sites distribution within the study area (SS1).....	46
Figure 3.2: Nigeria vegetation zones.....	50
Figure 3.3: Distribution of annual rainfall in Nigeria (mm/yr)	52
Figure 3.4: Monthly average values of rainfall in the study area (closest towns) from 1931-1997	53
Figure 3.5: SRTM data used for generating flow direction model and oil spill sites	56
Figure 3.6: Landsat images used for the study site 1	58
Figure 3.7: (a) Number of spill events recorded over the years and (b) Observable number of sample spill sites by year of image	58
Figure 3.8: General methodology flowchart showing the four stages of analysis used for the study	62
Figure 4.1: Samples from oil polluted (P) and non-polluted (NP) sites.....	69
Figure 4.2 : Box plots show the minimum, 25% quartile, median, 75% quartiles and maximum values respectively of BMVIs from P and NP sites. The red color stands for P sites and green for NP sites. Note that the minimum and maximum for the GLI value is -11 and 14 respectively.	73
Figure 5.1: Illustrates coding of flow direction.....	86
Figure 5.2: Regression between BMVIs response and volume of oil spill between 1 – 3500 bbl	90
Figure 5.3: Regression between BMVIs response and volume of oil spill threshold between 201 – 3500 bbl.....	91
Figure 5.4: Calculated direction flow model from SRTM data	93
Figure 5.5: Regression plot for volume of oil spill on BMVIs based on spatial distance.....	95
Figure 5.6: Regression between the time gap between spill and observation date and selected BMVIs at the polluted sites.....	98
Figure 6.1: Location of the two study sites on Landsat 5 (SS1) and 8 (SS2).....	106
Figure 6.2: Landsat 8 and oil spill data used for the study site 2	110
Figure 6.3: Sample P and NP points on vegetation indices maps in 2014.....	112
Figure 6.4: Few sample sites illustrating on Google Earth maps how P and NP points were obtained from Landsat data.....	112
Figure 6.5: Box plot for the calculated mean of the 5 vegetation indices from polluted (P) and non-polluted (NP) sites in 2014	113
Figure 6: Areas identified as likely vegetation stress based on the NDVI	125

List of Tables

Table 1.1: Nigeria's Oil Production and Oil Spill from 1976-2009	6
Table 1.2: Environmental impact and monitoring methods of hydrocarbons from pipeline operation.....	17
Table 2.1: VIs evaluated for vegetation stress detection from oil polluted sites in this study	37
Table 3.1: Oil spills recorded over the years and available image data in spill sites 1.	57
Table 3.2: Oil spill data points used in the study	60
Table 3.3: Landsat data sensor and band specifications.....	61
Table 4.1: BMVIs statistics at 95% confidence level from P and NP sites	72
Table 4.2: Twelve (12) BMVIs temporal statistics at 95% confidence level from P sites.....	75
Table 4.3: BMVIs temporal statistics at 0.95confidence level from control or NP sites	76
Table 5.1: The mean of BMVIs and volume of oil from 56 spill sites	88
Table 5.2: Coefficient of determination (R^2) and between BMVIs response and volume of oil spill (statistics at 0.95 confidence level with p-value at 0.05).	89
Table 5.3: BMVIs obtained at spatial distance from polluted and neighbouring pixels	94
Table 5.4: Coefficient of determination (R^2) of BMVIs and spatial distance.	95
Table 5.5: Coefficient (R^2) time gap between oil spill and image date on BMVIs.....	96
Table 5.6: Time gap (days) between oil spill and image date and selected BMVIs.	97
Table 6.1: Oil spill data for the new study site 2 (SS2)	107
Table 6.2: A comparison of p-values from paired t-test analysis for the study sites (P and NP sites) in 2014	114
Table 6.3: Statistics of extracted vegetation indices from 9 P and NP sample oil spill sites in 2014.....	115
Table 6.4: Statistics of extracted vegetation indices from 9 P and NP sample oil spill sites in 2013 (pre-spill not polluted)	116
Table 6.5: Statistics of extracted vegetation indices from 9 P and NP sample oil spill sites in 2015 (post-spill not polluted).....	117
Table 6.6: Analysis of change detection using paired t-test statistics of means of vegetation indices at the P and NP in 2013, 2014 and 2015.....	118
Table 6.7: shows the statistical analysis of the mean values for indices of vegetation affected by oil spill at the P sites.	120
Table 6.8: Temporal comparison of means of indices using a paired t-test of vegetation indices at the NP sites.....	122
Table 6.9: NDVI values and oil spill data used for mapping likely SP in 2013 and 2014.....	124

Chapter 1 : Introduction

1.0 Historical evolution of petroleum industry

The United States Department of Labour, in its Oil and Gas Well Drilling and Servicing eTool, defined petroleum as “a substance occurring naturally in the earth in solid, liquid, or gaseous state and composed mainly of mixtures of chemical compounds of carbon and hydrogen, with or without other non-metallic elements such as sulphur, oxygen, and nitrogen”. In Schlumberger’s Oil Field Glossary it is defined as “a complex mixture of naturally occurring hydrocarbon compounds found in rock. Petroleum can range from solid to gas, but the term is generally used to refer to liquid crude oil. Impurities such as sulphur, oxygen and nitrogen are common in petroleum. There is considerable variation in colour, gravity, odour, sulphur content and viscosity in petroleum from different areas”. Petroleum in an unrefined state has been utilized by humans for over 5000 years. In fact, oil in some form has been used since early human history to keep fires ablaze, and also for warfare. Its importance in the world economy evolved slowly, though whale oil was used for lighting into the 19th century, and wood and coal used for heating and cooking well into the 20th century. The industrial revolution generated an increasing need for energy which was fielded mainly by coal, with other sources including whale oil. However, it was discovered that kerosene could be extracted from crude oil and used as light and heating fuel. Petroleum was in great demand, and by the 20th century had become the most valuable commodity traded on the world market. With regards to the modern history of the petroleum industry, Imperial Russia produced 3500 metric tonnes of oil in Baku in 1825 and doubled its output by mid-century (Krylov et al., 1998). After oil drilling began in what is now Azerbaijan in 1848, two large pipelines were built in the Russian empire; the 833km long pipeline to transport oil from the Caspian to the Black Sea Port of Batumi (Baku-Batumi pipeline), completed in 1906, and the 162km long pipeline to carry oil from Chechnya to the Caspian. At the turn of the 20th century, Russia’s oil output from the Absheron Peninsula accounted for half of the world’s production and dominated international markets (Aknerns, 2004). According to Hardt et al., (1995) nearly 200 small refineries operated in the suburbs of Baku by 1884. As a side effect of these early developments, the Absheron Peninsula emerged as the world’s first example of oil pollution and environmental negligence (Saiko, 2001).

In Canada, oil extraction began in 1858 in Oil Springs Ontario. In the USA oil drilling began in 1859 (Gordon, 2007), when it was successfully drilled in Titusville, Pennsylvania. By the 1920s, oil fields had been established in many countries including Canada, Poland, Sweden, the Ukraine, the United States, Peru and Venezuela. In the first quarter of the 20th century, the United States overtook Russia as the world's largest oil producer. In Nigeria, oil was discovered in 1956 (Falola and Heaton, 2008) in the Niger Delta region. Exploration of crude oil began in 1958 by the Shell British Petroleum (now Royal Dutch Shell) in a village called Oloibiri in the Niger Delta, Southern Nigeria. According to the CIA (2011), oil accounts for a large percentage of the world's energy consumption ranging from a low of 32% for Europe and Asia, up to a high of 53% for the Middle East, South and Central America 44%, Africa 41% and North America 40%. Also, a report by the European Energy Review in Sweden 2010, showed that the use of oil doubled in China between 2000-2009 and in 2009 the consumption of oil in the European Union (EU) was 1.6 times and North America 2.5 times that of China. Meanwhile, in 2009 the world usage of gas was 131% compared to the year 2000. This shows that 66% of the growth was outside the EU, North America, Latin America and Russia, the Middle East, Asia and Africa. In the same report, the gas supply from 2000-2009 also increased in the EU (8.6%) and North America (16.0%). In the BP Statistical Report of World Energy Report (2011), the world oil consumption rose from 84,714,000 barrels per day (bpd) in 2009 to 87,382,000 bpd in 2010 (3.1%) while production stood at 82,278,000 bpd in 2009 against 82,095,000 bpd in 2010 (2.2%), which did not match the rapid growth in consumption during the same period. Statistically, consumption in 1965 was 30,783,000 bpd less than the production which was slightly higher at 31,806,000 bpd. Inversely, consumption in 2010 was higher at 87,382,000 bpd than production at 82,095,000 bpd (BP, 2011). This shows consistent increase in both oil consumption and production between 1965 - 2010. From these statistics, it is assumed that these increases will also increase the development of more production chains and facilities, especially expansion in pipeline infrastructural network. At the same time, this will add pressure on the natural and human environment, where environmental regulations and standards are not adhered to.

Oil has become a vital commodity for government as a source of revenue and national economic growth (Bridge, 2008). It also serves as a source of energy for the maintenance of industrial civilization which has become a critical concern for many countries (Smil, 2010). Globally, energy consumption in almost all regions of the world has increased from 1965-2010, as has crude oil production (IEA, 2011, BP, 2011). The increase in both the oil production and demand has also contributed to the increasing world carbon dioxide (CO₂) emissions (IEA, 2011). Also, the increasing production and demand for this commodity has necessitated an increase in transportation from the producing or supplier regions to demanding or consumer regions. Improvements in methods and better techniques in pipeline construction and utilization after World War II have revolutionized the pipeline industry, especially in the parts of the advanced world where crude oil production has been increasing (Smil, 2010).

1.1.1 Evolution of petroleum industry in Nigeria

In 1908, the Nigeria Bitumen Company and British Colonial Petroleum were set up to search for oil in Nigeria, but the outbreak of World War I in 1914 halted the initiative. The search continued after World War I. In 1939 World War II disrupted the activities of the oil search until 1947. In 1951, the search was narrowed to an area covering 58,000 square kilometres in the present Niger Delta of Nigeria. By January 1956 the first successful oil well was drilled at a village called Oloibiri. The petroleum industry in Nigeria is the most viable industry and main generator of Gross Domestic Product (GDP) in the country. Nigeria's oil and gas exports account for more than 90% of export earnings and about 83% of Federal Government Revenue, as well as generating 40% of its GDP and 65% of government budgetary revenues. Nearly all of the country's primary reserves are concentrated in and around the Delta of the Niger River, but offshore rigs are also prominent in the well-endowed coastal region of the country. Nigeria has a total of 159 oil fields and 1481 wells in operation according to Nigeria's Ministry of Petroleum Resources. As a result of these numerous oil fields, an extensive and well developed pipeline network has been engineered and constructed to transport the crude petroleum and related products. The amount of oil extracted from Nigeria expanded from 274,000 bpd in 1965 to 2,402,000 million bpd in 2010 (BP, 2011). All petroleum production and exploration activity is taken under the auspices of joint ventures between foreign multinational corporations' and the Nigerian Federal Government. Six companies are operating in Nigeria, namely Shell (UK & Netherlands) Petroleum Development

Company of Nigeria Limited (SPDC), Chevron (USA) Nigeria Limited (CNL), Mobil (USA) Producing Nigeria Unlimited (MPNU), Nigerian Agip (Italy) Oil Company Limited (NAOC) and Total (France) Petroleum Nigeria Limited (TPNL), who all operate as a joint venture with the Nigerian National Petroleum Corporation (NNPC). The Shell Petroleum Development Company of Nigeria Limited (SPDC) and Nigerian National Petroleum Corporation (NNPC) account for fifty percent of Nigeria's total oil production from more than eighty oil fields, operating largely onshore on dry land or in the mangrove swamp of the Niger Delta. The company has more than 100 producing oil fields, and a network of more than 6,000 kilometres of pipelines flowing through 87 flow stations.

1.1.2 Petroleum extraction and pipeline transportation

Pipeline transport is the transportation of materials through a pipe, commonly liquids and gases. Any chemically stable substance can be sent through a pipeline. There are sewage, slurry, water, and even beer pipelines, but arguably the most valuable are those transporting fuels; oil, natural gas and biofuels. Dmitri Mendeleev first suggested using a pipe for transporting petroleum in 1863, though there is no clear evidence on who first suggested the use of pipes as a transportation medium. Oil pipelines are generally the most economical way to transport large quantities of oil, refined oil products or natural gas over land, compared to shipping by railroad and tankers. Pipeline operations under the sea are economically and technically challenging. Oil pipelines are made from steel or plastic tubes with inner diameters typically from 100 to 1200 mm. Most pipelines are buried at a typical depth of about 0.91 to 1.8 m and the rate of flow is from 1 to 6m per second. When a pipeline is built, the construction project not only covers the civil work to lay the pipeline and build the pump stations, it also covers all the work related to the installation of the field devices that will support remote operation.

The distribution of pipelines worldwide shows that the United States has the largest network with about 793,285km of pipeline, while the least is 20km in Liechtenstein. Nigeria is ranked 26th in the world with 11,647 km as of 2007 (Xu and Ratha, 2008). The construction of these pipelines and extraction of oil plays an important role and is responsible for the deforestation, degradation and destruction of land and ecosystems across the globe. According to the Organisation of the Petroleum Exporting Countries (OPEC, 2011) ,Nigeria has approximately 9,793 kilometres including gas, crude and products pipelines. This figure falls short of an earlier CIA report in 2008 which shows

that there is about 11, 647 kilometres. There are no statistical figures to show trends in the network expansion at the time of presenting these figures, but figures on oil production and quantity of oil spills from 1976-2009 (NNPC, 2011) are shown in the table below;

Table 1.1: Nigeria's Oil Production and Oil Spill from 1976-2009

Oil Production and Quantity Spilled (Average Barrels/Day)		
	Production	Spilled
1976-1980	2,084,800	68,602
1981-1985	1,369,800	37,199
1986-1990	1,514,200	15,302
1991-1995	1,883,400	52,345
1996-2000	2,025,600	65,788
2001-2005	2,309,000	85,143
2006-2009	2,224,250	54,655

Source: (NNPC, 2011)

These processes in oil pipeline activities often result in the release of toxic products into local rivers. In the case of extraction, oil spills result from persistent pipeline leakages. In addition the construction of roads for accessing remote oil sites, opens up wild land to settlers and land developers. For example, Nigeria, Colombia, Peru, Ecuador and Bolivia, have substantial oil operations in rainforests. As such, oil extraction and transportation can be destructive to the natural environment. Spills from burst pipelines and toxic drilling by-products may be dumped directly into local channels and rivers (CIA, 2005). The multiplier effect of this environmental destruction will result in the deterioration of the environment through the depletion of resources such as air, water, vegetation and soils, the loss of ecosystems and extinction of wildlife. The adverse effects are the reduction of the capacity of the environment to meet social and ecological objectives and needs. As such, if the improper use of the natural environment where these oil operations are carried out is not curtailed or minimized, short term impacts like loss of water, soil quality and biomass will result.

1.1.3 The impact of the oil industry on the environment

The Niger Delta is the major oil producing area in Nigeria comprising 70,000 square kilometres of wetlands formed primarily by organic matter deposits. It is home to about 40 million people from different ethnic groups and the floodplain makes up 7.5% of Nigeria's total landmass (923,768 square kilometres). It is the largest wetland in West Africa and maintains the third largest drainage in the African continent. The Delta's environment can be broken down into four ecological zones; coastal barrier islands, mangrove swamp forests, freshwater swamps and lowland rainforests. The ecosystem supports an abundant flora and fauna, arable terrain that can sustain a wide variety of crops, economic trees, and species of freshwater fish. In 1983, the NNPC issued a report on the environmental degradation resulting from oil operations in the Niger Delta. On p11 it stated;

“We witnessed the slow poisoning of the waters of this country and the destruction of vegetation and agricultural land by oil spills which occur during petroleum operations. But since the inception of the oil industry in Nigeria, more than twenty-five years ago, there has been no concerned and effective effort on the part of the government, let alone the oil operators, to control environmental problems associated with the industry”.

The NNPC Report in 1983 was supported by the UNEP, (2011) which reported that pollution from over 50 years of oil operations in the Ogoniland, Nigeria, has penetrated further and deeper than many may have supposed. It is considered to be the world's most wide ranging and long term oil clean up exercise and is estimated to take up to 30 years for environmental clean-up and restoration. During their study, The UNEP confirmed that lack of satellite images of the study area that show the environmental status of the sites before oil industry operations commenced in the Ogoniland in the 1950s, has been one of the shortcomings of the study. Thus, baseline comparison dating back to this period was not possible. In the absence of 1950s and 1970s remote sensing data, the 1986 imagery was used by the UNEP and serves as baseline data for the Ogoniland environmental analysis. UNEP, (2011), reported that land cover between 1960 and 1985 was not available which means that the state of vegetation cover, water and soil could not be ascertained.

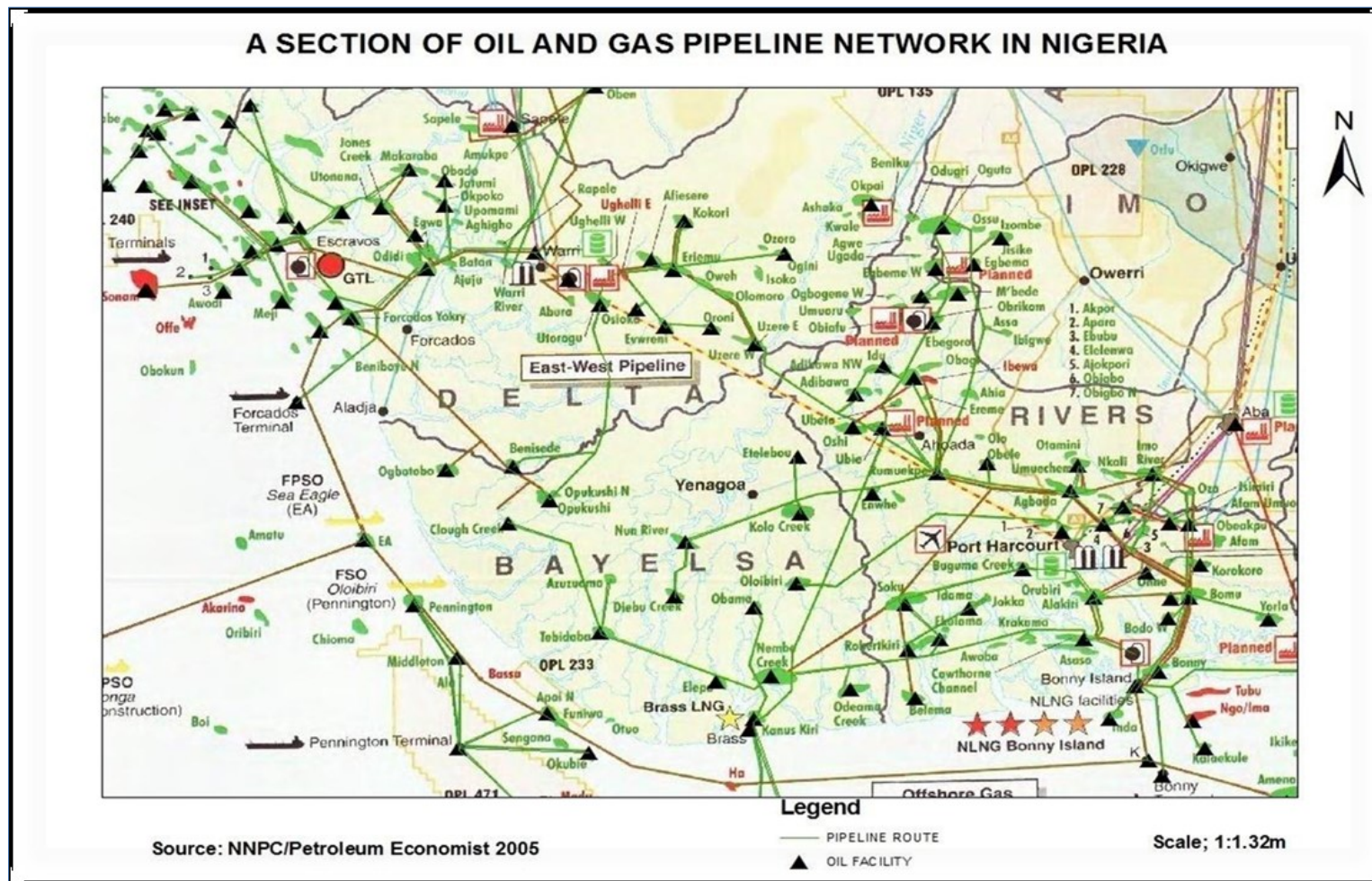


Figure 1.1: A Topology of Oil Pipeline and Facilities in the Niger Delta Nigeria

Source: (NNPC/Petroleum Economist, 2005)

Between these periods (1950 – 1986), oil operations were going on as well as oil spillages taking place. It could have been significant if the UNEP assessment was able to show the trend and rate of land cover change in the study area as well as provide valuable information about the status of land cover before and after oil operations. It is fair to conclude that in the absence of reliable baseline information on Ogoniland, the report was based on the observed situation compared with a presumed baseline condition. During the course of this study, access to topographic maps of the study area to determine the vegetation conditions before oil operations in the Nigeria was a great challenge. An attempt to obtain these maps from the Nigeria Surveyor General Office and Ordnance Survey London has been difficult and proved abortive.

1.1.4 Monitoring the environmental effects of oil pipelines

One of the critical global environmental problems is human and ecological exposure to hazardous wastes from agriculture, industrial, military and mining activities. These wastes often include heavy metals, hydrocarbons and other organic chemicals (Slonecker et al., 2010). According to the European Environmental Agency EEA (2007), about 242,000 contaminated sites in European Economic Area (EEA) countries are in need of clean-up. The main source of contamination are municipal and industrial waste disposals, mining and military sites no longer in operation, and present and past industrial plants such as metallurgical, chemical, oil and wood industries (Agostini et al., 2007). The amount of waste has been predicted to increase by up to 50% by 2025. The EEA also reported in 2007 that primary pollutants identified heavy metals and mineral oil as the cause of soil contamination in 37.3% and 33.7% of cases respectively. The use of remote sensing for oil or hydrocarbon leaks monitoring dates back to the 1970s using aerial photographs or data (Casciello et al., 2007). In their studies, they concluded that ultraviolet (UV), TIR and microwave sensors have the potentials to detect oil, which has been supported by a number of studies reporting the use of remote sensing data and methodology for this purpose. Furthermore, recent developments in geospatial sensors, data analysis and communication technologies present new opportunities. There are a number of commercial satellite images that are potentially applicable to pipeline transportation studies, including airborne and satellite radar, LIDAR and hyperspectral and multispectral sensors used to enhance monitoring of environmental changes caused by anthropogenic processes. The need for regular information on land cover conditions is important to policy makers and environmental observers. Satellites repeatedly and

simultaneously observe wide areas on the Earth's surface and continually acquire spatial information of ground features and any environmental changes. Satellite sensors detect electro-magnetic radiation from features on the Earth's surface over a wide range of spectrum within visible, invisible and infrared wavelengths and record this in digital format/images. Since satellite images are analysed or interpreted mostly by computer, this gives it the ability to acquire different information simultaneously rather than the manual visual method of interpretation.

There are a number of studies that demonstrate the use of remote sensing for pipeline detection, vegetation stress from hazardous liquid leakage, quantification of pollution/stress level and monitoring after remediation (van der Werff et al., 2008). These have demonstrated the capability of remote sensing in detecting environmental stress resulting from oil leaks from pipelines, without direct contact or mounting monitoring devices on the pipelines. An increasingly common application of remotely sensed data is in change detection. Change detection is the process of identifying differences in the state of an object or phenomenon over different periods of time. Change detection is an important process in monitoring and managing natural resources and urban development (Singh and Lin, 2008). The process of discovering, characterizing and remediating polluted sites is typically a long and costly endeavour (Slonecker et al., 2010). In the hazardous waste remediation process, one of the key steps is site characterization; the determination of the spatial extent, concentrations and nature of the contamination. Site characterization traditionally require extensive field sampling and laboratory analysis (Slonecker et al., 2010). As a result of the expense and time involved in the traditional method of investigating environmental contamination or pollution, remote sensing is a new and the most efficient tool which is a time saving, cost effective, and non-destructive investigation method. . It is one technology that has been valuable in detection and clean-up efforts that shows promise in providing alternative sampling methods. Timely and accurate monitoring of vegetation dynamics is essential for sustainable management and also to improve the effectiveness of vegetation monitoring. The linear trend analysis (LRA) method was used to compare degraded vegetation areas from two remotely sensed imageries of the same area (Zhang et al., 2011). The effective 'real time' imaging is used in responding to the spillage of hazardous materials. Such images are used to determine the extent and location of visible spillage and release, vegetation damage and threats to natural drainage and human welfare (Lillesand et al., 2008). On the other hand, historical

images are often used to conduct intensive site analysis of waste sites, augmenting these with current images when necessary.

1.1.5 Understanding the pipeline right-of-way (ROW)

According to Henry Campbell Black's (1995) law dictionary, a ROW is a strip of land that is granted, through an easement or other mechanism, for transportation purposes such as foot rail, driveway, rail line or highway. A ROW is reserved for the purposes of maintenance or expansion of existing services within the ROW. In the case of easement, it may revert to its original owners if the facility is abandoned. In the United States, rail road ROW is considered private property by the respective rail road owners and by applicable state laws. In the United Kingdom, rail road companies reserved the right to assume land for a ROW by a private Act of Parliament. Pipelines cross the landscape to deliver products over long distances as well as crossing channels, streams, highways and roads, farm fields, parks and may be close to homes, businesses or other community centres. The initial working space during pipeline construction may be temporarily wider but the permanent ROW width varies depending on the easements (in legal terms, this means the right held by one property owner to make use of the land of another for a limited purpose), the pipeline system, the presence of other nearby utilities and the land use along the ROW. Many ROW are 50 feet (15.24 m) wide, but may be wider or narrower in specific locations. These rights-of-way are kept clear to allow the pipeline to be operated safely, aerially surveyed and properly maintained. According to the Canadian National Energy Board (NEB, 2006) pipeline companies are responsible for maintaining their ROW to protect the public and environment. The strip of land for the ROW is usually between 5.0 m and 46.0 m wide containing the pipeline. In Nigeria, it is 30 m wide. Figure 1 below is a typical model of a pipeline right-of-way:

According to a (Breagh, 2010) Project Breagh report , a temporary site is required to support the construction and installation of the pipeline which comprise purpose-made temporary accommodation units to provide office, facilities, a workshop, storage and welfare facilities. After a pipeline is constructed, the right-of-way and temporary work areas (see Figure 1) of the pipeline are restored to a condition similar to the surrounding environment and consistent with the current land use (NEB, 2006). After a pipeline is constructed this area is maintained as a permanent ROW to allow for future maintenance, operational safety, aerial surveys of the pipelines and equipment. This area is contained

work side during construction and buried pipelines within the area at a specified distance are permitted by the regulatory agency or easements.

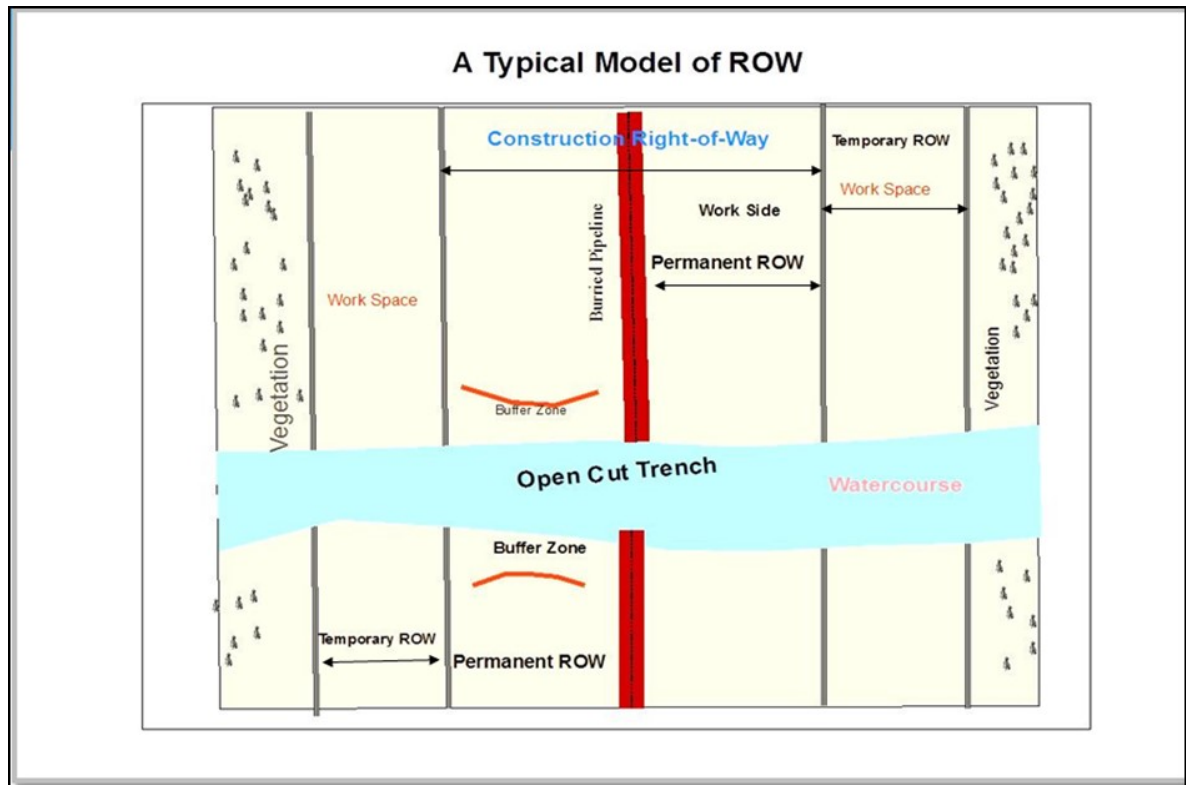


Figure 1.2: A Typical model of ROW Source: (NEB, 2006) Modified (2015)

Open-cut crossings of tracks and roads, the pipeline trench is excavated to allow the pipe to be lowered into the trench and is usually completed in a single day (Breagh, 2010).

1.1.6 Pipeline routes and potential impacts on ecological systems

Oil pipeline planning and development considers a number of factors during route selection, construction, operational and decommissioning phases of the project. Since the impact at every phase varies, the initial planning at these phases will minimise potential impacts on the natural and human environment. This section will discuss environmental impacts associated with oil pipeline projects, from route selection to decommissioning phase. Generally, oil pipelines can have different environmental impacts depending on the type and size of the pipeline, causing damage to natural, physical and ecological resources and to human life. There is a need to incorporate environmental considerations from conceptual planning to various stages in the lifecycle of oil pipeline projects. The pipelines are constructed both onshore and offshore which have a varying degree of environmental impacts (Cáceres et al., 2007). This section focuses on

onshore pipeline route selection, construction, operation and decommissioning impacts on the natural and human environment. There is, however, a paucity of scientific research on the monitoring of ROW, thus, materials used in the discussion are general literature on environmental impact issues related to oil pipeline corridors. The table below highlights general environmental impacts of oil pipelines on various environmental elements from route selection to the decommissioning phase of the pipeline project. It also highlights both ecological and human/socio-economic impacts of the pipeline project, though some are supported with various studies while others were not due to weak literature in that area. The aim and emphasis of this study is to use remote sensing techniques for detecting the impacts of pollution from oil pipelines on these ecological systems in the study area highlighted in table 2.

Pressure Testing under Section 7 of the Canadian National Energy Board, before putting a pipeline into service, a company shall develop a program in respect of pressure tests to be conducted for pipe and components used in its pipeline and shall submit it to the Board when required to do so (NEB, 2006). At this phase there are impacts which might be on various scales ranging from small leaks to major leaks or spills which are immediate and catastrophic to the environment when compared to the construction phase. When oil spills occur, it degrades air quality due to emissions and leads to loss of vegetation and soil productivity (Obire and Nwaubeta, 2002). Operations can cause noise pollution to humans and wildlife especially seismic surveys, drilling, pumping and processing oil facilities and contamination of ground water aquifers (UNEP, 2011). Land surfaces are also affected by these activities. In addition, waste generated at the pump and transfer stations are major potential contaminants to soil surface and groundwater. In the case of ruptures and oil leaks from pipelines, depending on the type and size, they may result in significant environmental damage. In this work the right-of-way width distance of 100 m may be used instead of the 30 m wide Nigerian standard. This is to allow identification of the impact of the oil pipeline beyond the 30 m wide ROW when considering the pixel resolution of the satellite for the study. The Canadian National Energy Board (NEB, 2006) reported that on the 8 and 28 November 2006, there were incidences of hydrocarbon spills of 100 cubic meters and 80 cubic meters respectively within the same oil pipeline right-of-way, resulting from technical failure. They also reported that a landowner identified a leak in August 2006 that stained a patch of soil in his pasture and also affected the soil and groundwater confined within the right-of-way.

Oil facilities, including pipelines, are decommissioned if they are no longer in operation. In the Department of Petroleum Resources DPR-Nigeria regulations handbook (Environmental Guidelines and Standards for the Petroleum Industry in Nigeria – EGASPIN [<https://dpr.gov.ng/index/egaspin/>]), there are a number of factors to be considered before a project facility is decommissioned. These include economic, ecological, health, fire and safety hazard, socio-cultural and technological impact on water, land, air and allied resources that could be a threat to public health. These factors determine the decommissioning of a project if it becomes necessary, but there are other environmental measures to be taken into account, which include; removal of contaminated soils and bottom sediments from contaminated streams and rivers, that waste removed should be deposited in an environmentally sound manner, and that uncontaminated soil from a clean unpolluted land is used to replace contaminated soil removed, while the recovery of the soil is achieved through planting of rapidly growing crop varieties, monitored for oil and hazardous substances through laboratory analysis (UNEP, 2007). Surface water rehabilitation involves restoration of fish into the water bodies and can be monitored through chemical and biological laboratory studies (UNEP, 2011b). It is also necessary and appropriate to make remediation plans in order to consider both positive and negative environmental impacts of the plans during the decommissioning of any project. It has been reported by EEA (2007) that European countries spent millions of Euros every year for cleaning up hydrocarbon contamination while Sweet et al., 2006 reported that in the US about 2 billion Dollars are needed for remediating polluted sites. Most of these are preliminary investigations which were carried out through traditional methods that are time consuming, expensive and destructive during the taking of soil, vegetation and water samples as well as drilling and geotechnical analysis (van der Werff et al., 2007). Wasted time, cost and destruction could have been spared using remote sensing methods to investigate hydrocarbon contaminated or polluted sites (van der Werff et al., 2008). The impact at this phase is highly dependent on how the first three stages contained the risks associated with the pipeline project.

Table 1.2 summarises the inherent impact from oil pipelines on various environmental elements (water, soil and vegetation) and some of the traditional methods used for monitoring this pollution. There are advantages and disadvantages of both the traditional and remote sensing method of monitoring hydrocarbon pollution in a polluted environment. Traditionally, monitoring oil pollution in such an environment will provide

detailed and accurate laboratory analysis of the affected environmental variables. But it is limited in coverage of the area affected, time consuming and costly, since it involved labour for field sample collection. It is also destructive to the environment since it entails clearing path ways for navigating within the affected areas to access the spill sites, as well as taking samples from the affected environmental variables. One other disadvantage of this method is the temporary lack of monitoring and analysis of these polluted sites. Oil pipelines cover large distances and it may not be possible to cover this distance when it must be done by foot patrol or flown aircraft (Van Persie et al., 2004). On the other hand, remote sensing (which simply means accessing information on an object without coming into contact with it), whilst not as detailed and accurate compared to ground or field laboratory analysis, is reliable, saves time and is cost effective. It has the advantage of covering kilometres of oil pipelines and can access information on environmental variables affected by pollution through their spectral characteristics. Where the oil spill sites are in remote areas and difficult to access, remote sensing can be used as the viable option. Many studies have demonstrated the application of remote sensing data and techniques in addressing environmental problems relating to oil pollution.

The use of remote sensing for oil or hydrocarbon pollution monitoring dates back to the 1970s using aerial photographs or data, (Casciello et al., 2007). Infrared sensors such as ultraviolet (UV), TIR and microwave sensors (Brekke and Solberg, 2005, Zhao and Li, 2007) have the potential to detect oil spill and this has been supported by a number of studies reporting the use of remote sensing data and methodologies for this purpose. Recent developments in geospatial sensors, data analysis and communication technologies present new opportunities. Studies have shown that hyperspectral sensors e.g. Airborne Visible/Infrared Imaging Spectrometer (AVARIS) and Airborne Imaging Spectrometer for Application (AISA) have the capability to detect oil spills (Jha et al., 2008, Landgrebe, 2005). Active sensors such as Radar operates in a radio wavelength which can detect the presence of oil in offshore areas (maritime shores) through the reduction of ocean reflectance (Brown and Fingas, 2003). Microwave sensors have been studied on how to detect oil spill and their thickness (Jha et al., 2008) and Laser-acoustic oil thickness sensors have been used for detecting oil mechanical properties instead of its optical and electromagnetic properties (Goodman, 1994). The onshore oil pollution monitoring in forest areas with these sensors has been limited due to its lack of availability and cost in countries like Nigeria, thus, it is worth considering available, free and

assessable data such as Landsat data. The Landsat data compared to sensors previously discussed are readily available globally, free and accessible. The sensor can repeatedly and simultaneously observe wide areas on the Earth's surface and continually acquires spatial information of ground features and any environmental changes. The sensors can also detect electro-magnetic radiation from features on the Earth's surface over a wide range of spectrum within visible, invisible and infrared wavelengths and record this in digital format/images. In other parts of the world, successful examples of using remote sensing techniques have been reported to be effective in detecting and monitoring vegetation affected by oil pollution on the ground (Hörig et al., 2001). In Nigeria, there were recent attempts, for example (Anejionu et al., 2015, Anejionu et al., 2014), to develop a technique for detecting and estimating gas flaring using MODIS and Landsat data in the Niger Delta. However, little or no research has been done on the monitoring of oil impact on vegetation from satellite data (e.g. Landsat data) and reliable methods to extract vegetation change/stress due to oil pollution. Thus the study used spectral vegetation indices (broadband multispectral vegetation indices - BMVIs) derived from optical data (Landsat data) to detect changes in vegetation physiological status resulting from oil pollution in the Niger Delta mangrove forest.

Table 1.2: Environmental impact and monitoring methods of hydrocarbons from pipeline operation

S. No	Environmental Elements	Operational Impact	Hydrocarbon Monitoring Methods	
			Remote Sensing	Field/Ground Investigation
1	Water	a) Contamination of surface and groundwater due to hydrocarbon leaks	Through remotely sensed data water anomaly can be detected using spectral reflectance. Though, the optical remote sensing literatures on this are found to be weak compare to soil and vegetation.	Field investigation and laboratory analysis of the water sample (Nduka and Orisakwe, 2011)
		b) Where there is large volume of leakage may cause oil slick on water surface		
2	Soil	c) Loss of soil productivity due to contamination from hydrocarbon leaks	Soil PH/anomaly can be detected through spectral reflectance (Schumacher, 1996, Yang et al., 2000, Xu et al., 2008)	Field investigation and laboratory analysis of the soil sample (Osuji and Opiah, 2007)
		d) Changes in soil PH and causes toxicity to microorganism in soil due to hydrocarbon concentration		
3	Vegetation	e) Concentration of hydrocarbons may affect vegetation health and vigour due to leakage (van der Meer et al., 2002, van der Werff et al., 2007, van der Meijde et al., 2009)	Vegetation health/anomaly can be detected using remote sensing techniques (Spectral characteristics) (Smith et al., 2005, van der Meer et al., 2000, Noomen et al., 2012, van der Meijde et al., 2009)	Field investigation and laboratory analysis of the vegetation sample (UNEP, 2011b).

1.3 Thesis Structure

The thesis comprises seven (7) chapters:

Chapter 1: This chapter provided a background that lead to the entire research, the rationale and objectives of the study. The evolution, extraction and transportation of petroleum were discussed. The chapter also discussed the impact of the petroleum industry specifically that of the oil spills arising from the pipeline transportation of these products on the natural environment. The historical evolution of the petroleum in Nigeria was also highlighted. The aims and objectives were developed based on the problems identified for detection and monitoring of oil pollution impacts on vegetation.

Chapter 2: This chapter discussed the concepts and literature relating to the use of remote sensing techniques for monitoring hydrocarbon contaminated sites. The concepts of remote sensing and spectral signatures were reviewed relating to oil polluted environments and methods adopted in detecting oil spill impacts resulting from pipelines. The chapter also assessed related studies that used vegetation spectral reflectance or indices for the detection of oil pollution impacts on vegetation. Twenty broadband multispectral vegetation indices were examined and reviewed as the main techniques employed for the study.

Chapter 3: The chapter provides details on methods used in addressing the main objectives and research questions developed in section 1.2. The description of the study area was necessary in order to understand the nature of the environment which will help in choosing data and method for addressing the research questions/objectives. The satellite and field data sampling, processing and analysis used in the thesis were fully described. The chapter also described how the Landsat data were pre-processed and how vegetation indices from the polluted and non-polluted sites were extracted for spatial and change detection analysis.

Chapter 4: The chapter investigated and analysed the capacity of the vegetation indices used for the detection of oil pollution impacts on vegetation. The vegetation indices obtained at the polluted and non-polluted sites were statistically analysed. Also, statistical temporal (before and after spill) analysis of these polluted sites were compared with the ones from the non-polluted sites. This chapter has shown that some vegetation indices

performed better and were capable of detection of oil pollution impact on vegetation in polluted areas, while others did poorly.

Chapter 5: The chapter focused on methods used in the investigation and determined factors influencing the detectability of oil pollution in vegetated areas which were not addressed in Chapter 4. The chapter used regression analysis to determine the relationships between the volume of oil spill, time gap between oil spill and image date, and spatial distance with vegetation indices. The chapter aimed at identifying factors influencing the detectability of oil pollution impacts on vegetation in an oil polluted environment using these vegetation indices.

Chapter 6: The chapter assessed the validity of the technique used and results obtained in order to test the transferability of the method used in chapter 4. The results have shown that results obtained in the two study sites were similar, but with small variations which could be due to local environmental and sensor characteristics.

Chapter 7: This chapter summarised results from the individual result chapters which were synthesised. Conclusions were derived from the results chapters on the potential and capabilities of BMVIs for detection and monitoring of oil pollution impacts on vegetation derived from multispectral Landsat data. Factors influencing the detection of oil pollution impact on vegetation using vegetation indices are critical areas and some of the challenges and implications relating to future studies.

Chapter 2 : Literature review

2.0 Introduction

This chapter reviews literature on remote sensing concepts and techniques relating to remote sensing of vegetation and hydrocarbon monitoring. Methods for detection and monitoring of oil contaminated sites with particular emphasis on the use of vegetation spectral techniques from the remotely sensed data are discussed. The aim of this review is to identify current research gaps and use them in addressing the research questions and objectives stated in chapter 1. The research focuses on the Niger Delta region, dominated by tropical mangrove forest, where oil exploration activities are carried out. The region's mangrove forest (described in section 2.9) has been affected through anthropogenic induced changes from oil spills and pollution.

2.1 Hydrocarbon impact on vegetation

Vegetation health and vigour can be affected by hydrocarbons (van der Meijde et al., 2009) through spillage onto roots, stems, leaves and soil (UNEP, 2011). Hydrocarbons can reach vegetation when dissolved in the groundwater in the root zone and sometimes via the air surrounding it. The uptake through roots and direct contact between soil and plants' tissues are also a medium in which organic contaminants enter plants (Lin et al., 2002). The effects may depend on the type and quantity of chemicals involved and the vegetation type. Different vegetation has varying sensitivity to hydrocarbons (UNEP, 2011). Vegetation can be affected by hydrocarbon-oxidation bacteria resulting from hydrocarbon leakages, causing reduction in soil oxygen concentration and at the same time increasing the concentration of carbon dioxide (CO₂) and organic acids (Yang et al., 2000) . As a result of these changes plants are affected by lack of solubility of trace elements due to the changes in soil pH (i.e a measure of the acidity or basicity in soils) and Eh (i.e. soil reduction/oxidation potentials) (Schumacher, 1996). The changes can also affect the root structure of the plants or vegetation, which later affects the plants' overall vigour and thus spectral reflectance (Feder and Penfield, 1985). Vegetation anomalies can be assessed using remote sensing through morphological changes in plants induced by deficiencies in available soil nutrients (Brooks et al., 1996). Crawford (1987), reported that poor health of vegetation could be as a result of the presence of methane in the root zone, resulting in seepage-induced geochemical changes in soil and groundwater. In another study carried out in the San Francisco basin in central Brazil, where spectral data were collected over anomalous and non-anomalous vegetation sites, the

corresponding bands showed higher reflectance values in chlorophyll absorption bands for the sites under hydrocarbon influence compared to sites outside the anomalies. Thus the study suggested that the presence of hydrocarbons seems to produce a change in the internal structure of the plant, which results in low reflectance values, and gas affected areas may also be responsible for low vegetation density in the area (Oliveira et al., 1997). Smith et al. (2004) indicated that vegetation growing near leaking gas pipelines revealed changes in the geobotany (which is the relationship between specific plant species and the substrata from which they receive their nourishment) and reflectance, and a strong relation between plant vitality and gas can be assessed using spectral indicators (van der Meer et al., 2000).

The normal spectral signature of healthy vegetation is controlled by chlorophyll in the visible (VIS) part of the electromagnetic spectrum (EMS) (at 430nm and 660nm, and 450nm and 640nm for chlorophyll a and b respectively), by cell wall structure in near-infrared (NIR) and by water content in shortwave infrared (SWIR) regions (Jensen, 2014). Noomen (2007) studied the effect of natural gas, methane and ethane for two different species of plants using controlled laboratory and field conditions. The study found, after testing several existing vegetation indices that reduced band depths in the water (1370nm – 1570nm and 1870 nm – 2170nm) and chlorophyll (550 nm – 750nm) absorption features correlates to an increase in the Photochemical Reflectance Index (PRI). The outcome proposed that hydrocarbon gases could be responsible for the decrease in photosynthetic activity of the plants (Noomen, 2007). Vegetation stress indices such as the Carter Stress Indices (Carter, 1994) and Red Edge Position Index (Baret and Guyot, 1991) were applied and tested by (van der Meijde et al., 2009) in order to detect vegetation anomalies around leaking pipelines. The results showed a lower vegetation index above the pipeline than further away indicating leakage had caused stress for the aboveground vegetation. These laboratory results were advanced using airborne imagery by (van der Werff et al., 2008), whose novel automated image processing technique applied both spectral information of stressed vegetation and knowledge of pipeline route or location in order to detect hydrocarbons over large areas. The results of the study were obtained without validation data though; the polluted sites were identified in different land cover areas using an automated procedure that has been challenged in (Wulder et al., 2007). This study will focus on the long term effect of hydrocarbon leaks, since bacterial oxygen depletion is likely to take place and effects of high gas concentration may be noticeable on

environmental elements (soil and vegetation) (Noomen et al., 2008). This is in contrast to the short term, where the effect of bacterial oxygen depletion resulting from hydrocarbon leaks might not be noticed. The study of the long term effect of hydrocarbons is suitable for the area under investigation, because most of the pollution from leaks is noticed after at least several weeks and sometimes after up to a year, and in most cases is reported by the local people and the patrol teams when it has become visible or impacted on the site. In addition to this, it is suitable in areas where environmental monitoring regulations are weak and accessibility to areas of oil pipeline routes are difficult e.g. in developing countries like Nigeria.

2.2 Effects of bidirectional reflectance distribution function (BRDF)

Surface reflectance, or albedo, is important in many geophysical applications, and is the proportion of the incident light or radiation that is reflected by a surface (Henderson-Sellers et al., 1993). Most retrieval algorithms emphasise only the removal of atmospheric attenuation due to molecular and gaseous aerosol scattering and absorption (Trischenko et al., 2000). Surface reflective properties can be retrieved from satellite observations and the targets may be viewed from different directions leading to diversity of surface properties (Li et al., 1996). BRDF can simply be described as how light is reflected when it makes contact with surface materials (Lubin and Massom, 2006, Wynn, 2000). BRDF is determined by the incoming light direction and outgoing direction in return that forms a ratio of reflected lights along the part of incidents on the surface from direction (Schaepman-Strub et al., 2006). BRDF properties can determine and correct the differences in surface properties recorded in an image by a satellite sensor, to produce a better final product (Trischenko et al., 2000). When light interacts with the surface, different wavelengths (colours) of light may be absorbed, reflected and transmitted to varying degrees, depending on the physical properties of the material itself. This also means that BRDF is a function of wavelength and therefore its properties (i.e. positional variance) can be noticed or observed in material (Wynn, 2000).

The knowledge of energy interactions with different surfaces helps us in interpreting the remotely sensed image. A given feature will have different reflection properties in different wavelengths of the energy spectrum. Therefore, a combination of information obtained in multispectral regions help in better interpreting an image. Energy interacts

with the Earth's surface, especially with the three major features of vegetation, soil and water. Evans et al. (1999), reported that each spectral signature is unique to the object or an object class and is based on the target's surface structure and molecular composition and on the incident radiation. For example when electromagnetic energy is incident on any given earth surface feature, three fundamental energy interactions with the features are possible. Various fractions of the energy incident on the element are reflected, absorbed, and or transmitted, applying the principles of conversion of energy;

$$E_i(\lambda) = E_g(\lambda) + E_a(\lambda) + E_T(\lambda) \quad \text{Eq. 1}$$

Where E_i = incident energy, E_g = reflected energy, E_a = absorbed energy, E_T = transmitted energy, λ = function of wavelength

Reflectance characteristics of earth surface features are quantified by measuring the portion of the incident energy that is reflected.

Spectral reflectance = Energy of wavelength (λ) reflected/ Energy of wavelength (λ) incident x 100.

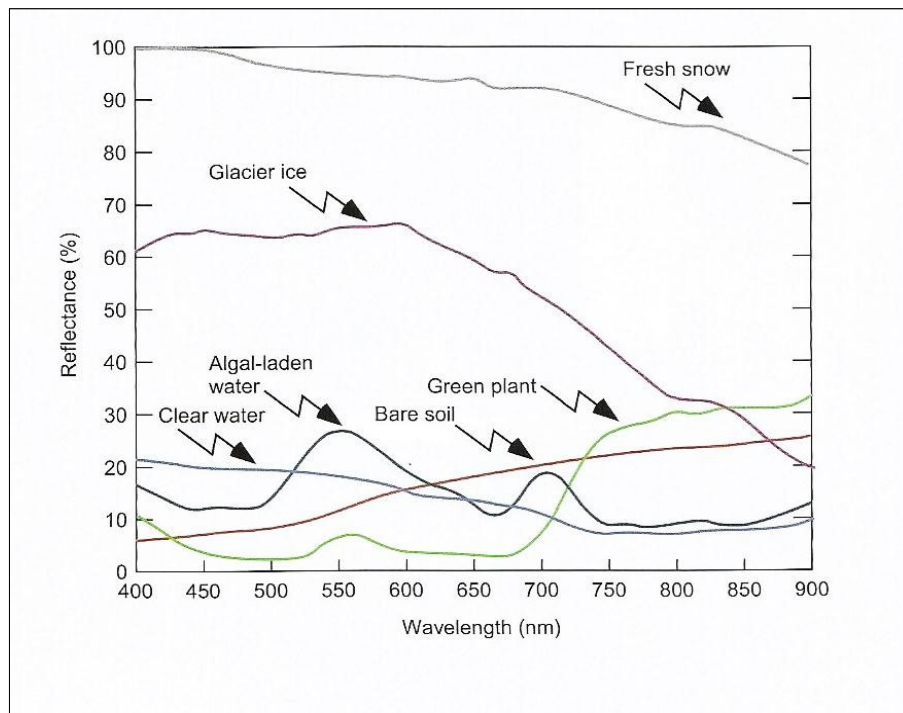


Figure 2.1: General reflectance spectra of some earth surface materials Source: Purkis and Klemas (2011)

Two points about the above given relationship (expressed in the form of an equation) should be noted. The proportions of energy reflected, absorbed, and transmitted will vary for different earth features, depending upon their material type and conditions. These

differences permit us to distinguish different features on an image. The wavelength dependency means that, even within a given feature type, the proportion of reflected, absorbed, and transmitted energy will vary at different wavelengths.

2.3 Remote sensing and concept of spectral signatures

Remote sensing is the acquisition of information about an object or phenomenon without making physical contact with the object. Today, the term generally refers to the use of aerial sensor techniques to detect and classify objects on the Earth by means of propagated signals (electromagnetic radiation emitted from aircraft or satellites (Schowengerdt, 2007). In another definition (Lillesand et al., 2008), remote sensing is the science of obtaining information about an object, area or phenomenon through the analysis of data acquired by a device that is not in contact with the object, area or phenomenon under investigation. The process involves making observations using sensors mounted on platforms which are at varying heights from the Earth's surface and recording the observation on a suitable medium. There are two main types of remote sensing, passive remote sensing and active remote sensing (Liu and Mason, 2009). Passive remote sensors detect natural radiation that is emitted or reflected by the object or the surrounding area being observed (reflected sunlight, film photography, infrared, radiometers). Active sensors emit energy in order to scan objects and areas whereupon a sensor then detects and measures radiation that is reflected or backscattered from the target. Examples include Radio Detection and Ranging (RADAR) and Light Detection and Ranging (LIDAR), where time delay between emission and return is also measured, which establishes the location, height, speed and direction of an object. Remote sensing works by converting observed measurements into information about physical objects or systems that we are interested in. It can be used to collect data over dangerous and inaccessible areas such as thick forest and glacial areas in Arctic and Antarctic regions.

Remote sensing is an essential tool for long term documentation of oil pipeline induced vegetation cover change that has important implications for efficient remediation, restoration and recovery planning (Li et al., 2005). Comparing traditional multispectral and hyperspectral remote sensing is potentially the best approach to assess oil-induced environmental problems in inaccessible areas, sites with potentially hazardous contamination, and sites where information about the spatial context of such conditions is critical to understanding the location, distribution, or spread of adverse conditions.

Remote sensing images provide sufficient spectral resolution to describe diagnostic absorption signatures (band position, depth, width and symmetry) and allow for differentiation between vegetation species, and the separation of vegetation from different types of soil minerals. The differentiation of vegetation species from background soils is crucial in the assessment of vegetation stress in arid and semi-arid regions where vegetation is sparsely distributed. Successful examples of using remote sensing techniques have been reported to be efficient in detecting hydrocarbons on the ground surface (Hörig et al., 2001). In Nigeria, however, little or no research has been done on long term monitoring of oil induced vegetation cover change because of a lack of a satellite data time series and reliable methods to extract change/stress information for remotely sensed data analysis; this was also acknowledged in a report by the United Nations Environment Program (UNEP) on the Environmental Assessment of Ogoniland, Nigeria (UNEP, 2011).

2.4 Reflectance characteristics of vegetation

Vegetation has a unique spectral signature which enables it to be distinguished readily from other types of land cover in an optical/near-infrared image. The reflectance is low in both the blue and red regions of the spectrum (Sims, 2002) because of the absorption of chlorophyll for photosynthesis. It has a peak at the green region. However, in the near infrared region (NIR- is an electromagnetic radiation with longer wavelengths than those of visible light, extending from the nominal red edge of the visible spectrum at 740 nm to 1300 nm), the reflectance here is much higher than that in the visible band due to the cellular structure in the leaves (Purkis and Klemas, 2011, Mather and Koch, 2011). Therefore, vegetation can be identified by high NIR but generally low visible reflectance. The spectral characteristics of vegetation can be detected in three major electromagnetic spectrum (EMS) regions; EMS describes the full range of frequencies, from radio waves to gamma rays that characterise light. Figure 2.2 below is a spectral response characteristic of green vegetation. Chlorophyll contained in a leaf has strong absorption at 450 nm and 670 nm and high reflectance in the NIR (700-1200 nm). In the SIR, vegetation displays three absorption features that can be related directly to the absorption spectrum of water (blue line) contained within the leaf.

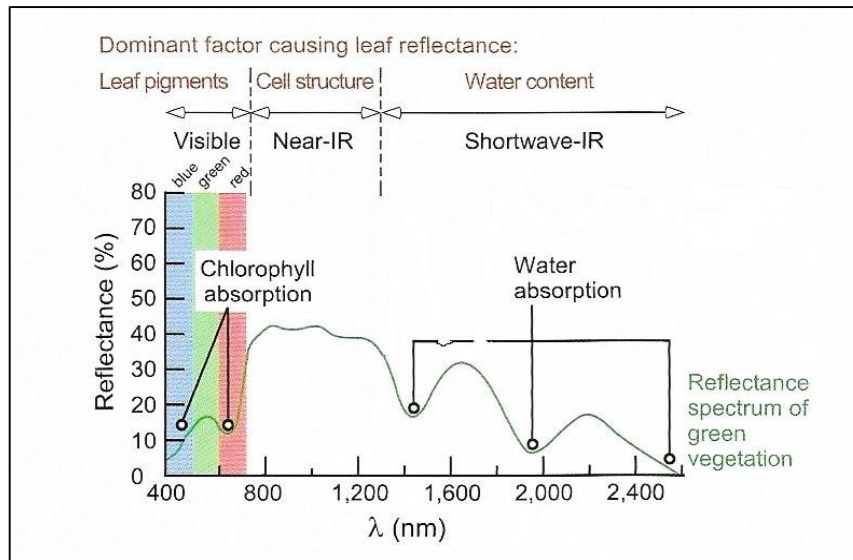


Figure 2.2: Dominant factors causing leaf reflectance Source: Purkis and Klemas 2011

Figure 2.2 illustrates the dominant factors that cause changes in the leaf reflectance in respective spectral wavelength. For leaf reflectance in the visible bands (blue, green and red), leaf pigments are the dominant factors, in NIR, the cell structure of the leaf is the main factor, and in SWIR bands it is water content. The below text summarises characteristics of and response in respective wavelengths (between 400 – 2500nm) on vegetation health.

Visible region (400-700nm) – low reflectance, high absorption, and minimum transmittance

NIR region (700-1350nm) – high reflectance and transmittance, very low absorption

MIR (1350-2500nm) – as wavelength increases, both reflectance and transmittance generally decrease from medium to low while absorption increases from low to high

There are a number of studies that show the capabilities of remote sensing or hyperspectral remote sensing in monitoring the health condition of plants or leaves in relation to their environment. Jensen (2014) and (Purkis and Klemas, 2011) demonstrate that remote sensing systems can provide valuable spectral information to measure the functional health of vegetation. The studies further confirmed that remote sensing is now a viable alternative to predict or monitor vegetation's biophysical and biochemical characteristics. The spectral reflectance of curves for healthy green vegetation almost always manifests itself at the peak-and-valley. The valleys in the visible portion of the

spectrum are dictated by the pigments in plant leaves. For example, chlorophyll strongly absorbs energy in the wave length bands centered at about 450 and 650nm, so that when the amount of chlorophyll decreases it means the plant is subject to some form of stress (Sims, 2002). As a result of less chlorophyll absorption in the blue and red bands, often the red reflectance increases to the point that we see the plant turn yellow. In the infrared portion of the spectrum at about 700nm, the reflectance of healthy vegetation increases dramatically. In the range from about 700 to 1300nm, a plant leaf reflects about 50% of the energy incident upon it and the rest of the energy is transmitted since the absorption in the spectral region is minimal (Mather and Koch, 2011). Similarly, many plants' stresses alter the reflectance in this region, so sensors operating in this range are often used for vegetation stress detection (Purkis and Klemas, 2011).

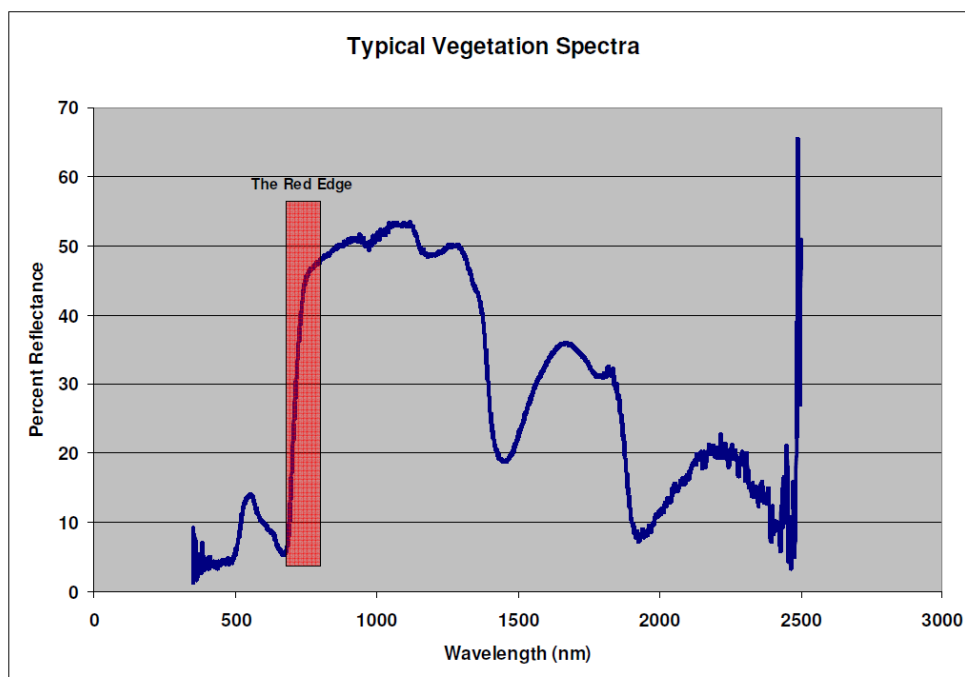


Figure 2.3: Spectral reflectance of healthy vegetation Source: (Slonecker et al., 2010)

Figure 2.3 shows the spectral characteristics of healthy vegetation which has strong absorption at 450nm and 670nm due to chlorophyll contents in the leaf with high reflectance in the near-infrared (700 -1,200nm).

2.4.1 Atmospheric effects on the radiation

Atmospheric effects have several impacts on the radiation at the Earth's surface, which include a reduction in the power of solar radiation due to absorption, scattering and

atmospheric reflection, and changes in spectral content of the radiation as a result of wavelength absorption or scattering. In addition, atmospheric effects can introduce an indirect component into solar radiation and there are also local variations in the atmosphere (e.g. water vapour, clouds and pollution). Absorption, scattering and atmospheric reflection reduce solar radiation, as when it passes through the atmosphere, the gases, dust and aerosols absorb the incident photons (Schneider, 1972). For example, ozone (O₃), CO₂ and water vapour (H₂O) have very high absorption of some specific photons (Hu and White, 1983).

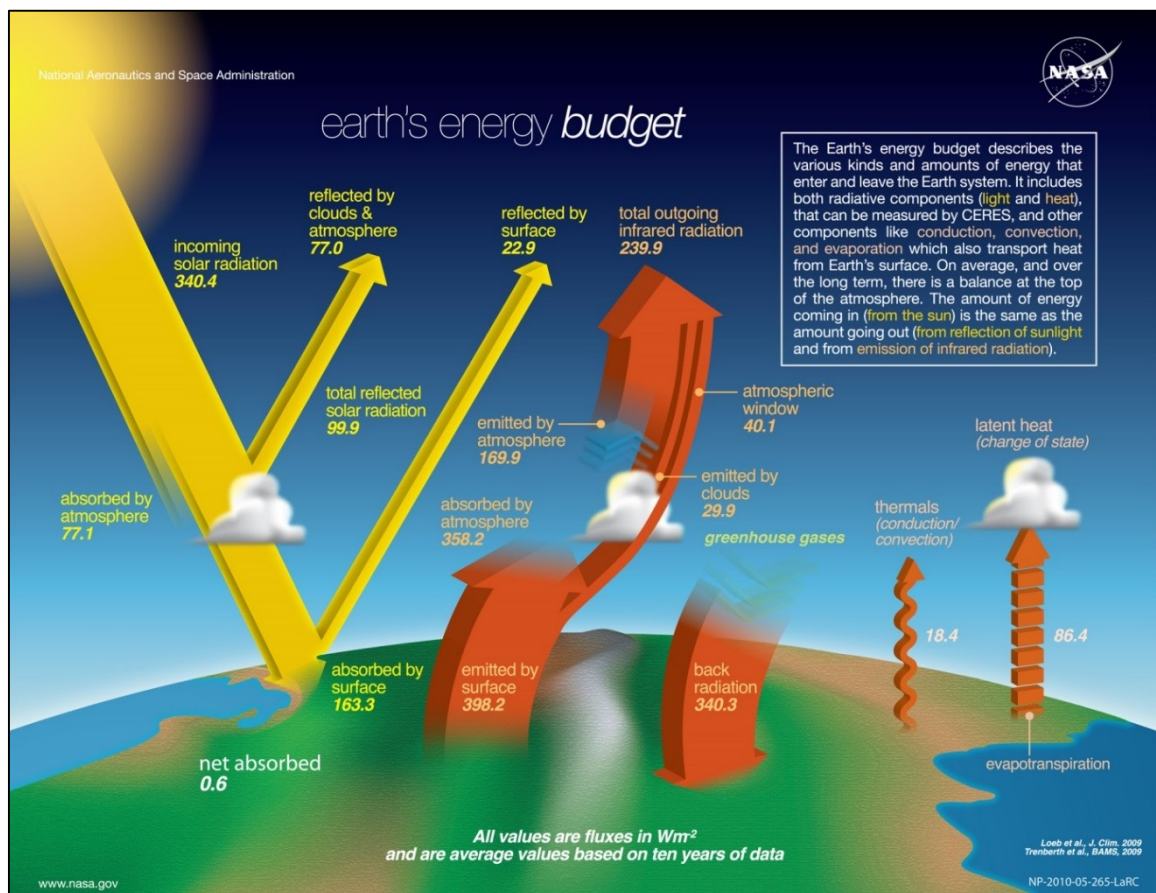


Figure 2.4: The balance of incoming and outgoing radiation measured by satellites and shown in W/m² Source: (NASA)

There are some specific gases in the atmosphere that change the spectral content of the terrestrial solar radiation with relatively minor impact. However, the major factor causing reduction in solar radiation power is the absorption and scattering of light due to air molecules and dust (Sekuler and Blake, 1985). The effects of cloud and local variations in the atmosphere are dependent on the type of cloud cover where the incident power is reduced (Mack, 1979). These atmospheric effects have an impact on the information recorded by satellite sensors and the data obtained by the sensors may contain unwanted noise in the images. This is because when solar energy strikes an object there are several interactions that are possible; transmission, absorption, reflection, scattering and emission of energy. Satellite sensor channels are designed to reflect and emit energy. For example, Landsat's Enhanced Thematic Mapper Plus (ETM+) converts the raw solar energy collected by the sensor to absolute units of radiance (Chander et al., 2009). Radiance is defined as incidences of energy per solid angle leaving a unit surface area in a given direction. To obtain a radiance image from an uncalibrated image, a gain and offset must be applied to the pixel values. These gain and offset values are retrieved from image metadata from the data provider (Chander et al., 2009). They are used for correction of DN (digital numbers) values to radiance. This study uses radiance images as input to the Fast Line-of-sight Atmospheric Analysis of Hypercubes (FLAASH) module in ENVI which converts to an output with units $\mu\text{W}/(\text{cm}^2 \cdot \text{sr} \cdot \text{nm})$. To convert calibrated DN (Qcal) in a Level (L1) Product of Landsat data back to at-sensor spectral radiance ($L\lambda$), knowledge is needed of original scaling factors using the following equation (Chander et al., 2009);

$$L\lambda = \text{"gain"} * \text{QCAL} + \text{"bias"} \quad \text{Eq. 1}$$

which is expressed as:

$$L\lambda = ((L\text{MAX}\lambda - L\text{MIN}\lambda) / (\text{QCALMAX} - \text{QCALMIN})) * (\text{QCAL} - \text{QCALMIN}) + L\text{MIN}\lambda \quad \text{Eq. 2}$$

where:

$L\lambda$ = Spectral Radiance at the sensor's aperture in watts/(meter squared * ster * μm)

"gain" = Rescaled gain (the data product "gain" contained in the Level 1 product header or ancillary data record) in watts/(meter squared * ster * μm)

“bias”= Rescaled bias (the data product "offset" contained in the Level 1 product header or ancillary data record) in watts/(meter squared * ster * μm)

$L_{MAX\lambda}$ = the spectral radiance that is scaled to Q_{CALMAX} in watts/(meter squared * ster * μm)

$L_{MIN\lambda}$ = the spectral radiance that is scaled to Q_{CALMIN} in watts/(meter squared * ster * μm)

Q_{CAL} = the quantized calibrated pixel value in DN

Q_{CALMAX} = the maximum quantized calibrated pixel value (corresponding to $L_{MAX\lambda}$) in DN = 255

Q_{CALMIN} = the minimum quantized calibrated pixel value (corresponding to $L_{MIN\lambda}$) in DN

= 1 for LPGS products

= 1 for NLAPS products processed after 4/4/2004

= 0 for NLAPS products processed before 4/5/2004

Radiance is the radiation reflected from the surface, rebounding from the neighbouring pixels and clouds above the area of the pixel. They are also affected by source of radiation for optical imagery from the sun. For any quantitative analysis from multispectral and hyperspectral image, radiant images are required to be corrected to reflectance images. Reflectance is the proportion of radiation which is reflected when it strikes a surface material. Reflectance spectra are used in identifying different surface materials, thus it is the first task toward identifying features in an image. The reflectance values that include contributions from clouds and atmospheric aerosols and gases which are measured by a space-based sensor flying higher than the atmosphere, are known as top-of-atmosphere-reflectance (TOA) (Shippert, 2013). Meanwhile, surface reflectance is the reflectance of the surface of the earth. Clouds and other atmospheric components do not affect surface reflectance spectre. They are basically derived from calibrated radiance images, using example model-based atmospheric corrections in an atmospheric correction module. Summarily, radiance corresponds to brightness in a given direction toward the sensor

while reflectance is the ratio of reflected versus total power energy. Radiance is measured at the sensor and is dependent on reflectance (Shippert, 2013).

In order to analyse a relatively clear Landsat scene, a reduction in scene variability is required, which can be done through a normalisation of solar irradiance by converting the spectral radiance (Chander and Markham, 2003) as shown above, to exoatmospheric reflectance. The advantages of converting radiance to TOA reflectance from different sensors are that the cosine effect of different solar zenith angles due to the time difference between the data acquisition can be removed, and that it compensates for different values of the exoatmospheric solar irradiances arising from spectral band difference (Chander and Markham, 2003).

2.5 Vegetation response to hydrocarbon leaks

In response to hydrocarbon concentration, the colour of plant leaves changes and subsequently lose photosynthesis pigments as colours change from green to pale-green, yellowish-green, and yellow. Photosynthesis in plants reduces due to of the restricted entry of carbon dioxide CO₂ into the leaf when oil is spilled and coated on plants (Pezeshki et al., 2000). Leaf spectral reflectance can be measured to determine whether leaf reflectance responses to plant stress may differ according to the agent of stress and species (Carter, 1993). Visible reflectance is most sensitive to stress in the 535 - 640 nm and 685 -700 nm wavelength ranges and sensitivity minimum occurred consistently near 670 nm. Remote sensing for vegetation stress detection is based upon vegetation response to solar radiation (Raghavan, 2000). The spectral response of healthy plants to solar radiation is, in general, similar though differences exist between plants due to morphology and physiology, background soil types, and the climate. Healthy plants have diagnostically high reflectance in the near infrared region of the solar region because of strong internal scattering of incident light from cell walls and intercellular spaces (Houborg and Boegh, 2008). When plants become senescent or stressed, however, the mesophyll tissue begins to desiccate and cell walls collapse, which results in substantially reduced intercellular surface area and air space (Mather and Koch, 2011). Thus senescent and stressed plants reflect more red light, but much less in the near-infrared region

compared to green healthy plants (Delalieux et al., 2008). Greater reflection of red light is due to the loss of photosynthetic pigments, resulting in less absorption.

Detection of hydrocarbon seepage/leakage of both surface and underground gas pipelines is an important environmental issue in many countries including Nigeria. The general practice of detection of leakage involves drilling and the subsequent geochemical analysis of soil and water samples, which is time consuming and expensive (Studer et al., 2007). The mineral alteration that occurs in the soil and geobotanical (e.g. abnormal behavior of vegetation) has become evidence for detecting hydrocarbon leakage (Noomen and Skidmore, 2008). Geobotanical anomalies occur as a result of the effect of light hydrocarbons on the growth of the vegetation. Reflectance properties of vegetation in the visible part of the spectrum are dominated by the absorption properties of photosynthetic pigments including chlorophyll, having absorption at 660 nm and 680 nm (Smith et al., 2004a). The changes in the chlorophyll concentration produce spectral shifts of the “red edge” absorption near 700 nm. Studer et al. (2007), confirmed that “traditional plant phenology provides very accurate information on individual plant species, but with limited spatial coverage. Satellite phenology allows monitoring of terrestrial vegetation on a global scale and provides integrative view at the landscape”. Change in leaf colour, stems and trunks are very good indication of a plant’s response to oil concentration or stress (Guyot et al., 1992, Noomen et al., 2012). The leaves gradually lose photosynthetic pigments resulting in colour change from green to pale-green, yellowish-green, and yellow (Raghavan, 2000). The stems become ash-brown, dark-brown or darkened after exposure. The exhibition of chlorosis is due to the loss of chlorophyll observed after an oil spill (Ustin et al., 1998). In their experiments they showed the adverse effect that oil-contaminated soil has on the plant growth, reducing germination, seedling growth and development.

2.6 Traditional method of monitoring environmental variables

At present there are various methods for monitoring oil pipelines, which include surveillance on foot, by helicopter and flown aircraft (van Persie et al., 2004). These methods are expensive and time consuming. Oil and gas pipelines can leak for a long period without being noticed (Noomen, 2007). In order to curtail the potential danger of long term gas leaks at an early stage, it is ideal to carry out continuous surveillance using the remote sensing approach, which is time saving, efficient and less expensive

(Hausamann et al., 2003). However, some pipelines are buried underground to a depth of 1m and that makes it difficult to detect leaks using foot patrols or aircraft, especially if the leak is minor and continuous. Polluted or contaminated sites can be detected using remote sensing techniques coupled with ancillary data (pipeline maps, land use maps, etc.). The cumulative effect of small leaks are damaging while major leakages or spills have both immediate and catastrophic impacts on the environment. TransCanada documents ((Zhou et al., 2008)), show a scenario that a slow leak of less than 1.5 percent of the pumping rate could go undetected for up to 90 days. Where the pipeline inspection is scheduled every few weeks it is likely that the oil leak would reach the surface and be detected before the entire 90 days elapsed. In this case, if a pipeline is buried at a depth of 10 ft and the 1.5 percent leak (75,802 ft³/d) is on the bottom of the pipe, oil would fill the pore spaces in the soil mostly in a downward direction, but it would also be forced upward toward the surface. Assuming that the oil initially fills a somewhat conical volume that extends twice as far below the pipeline as above it, the oil would emerge at the surface within about one day (the volume of a cone 30 feet deep with a base diameter of 30 feet is 7,068 ft³). Therefore, the leak would likely be detected in 14 days during the next inspection (assuming bi-weekly inspections). A 1.5 percent spill at a pumping rate of 900,000 Bbl/d over 14 days would result in a release of 189,000 Bbl (7.9 million gallons). (Noomen, 2007) which support the above report indicated that hydrocarbon leaks can affect plant health within 14 to 20 days. Therefore, minor leaks can lead to longer term damage to the environment than major leaks or spills which are noticeable in a short period of time. In this case, use of remote sensing techniques is appropriate especially in inaccessible or remote areas with weak regulatory environmental standards. In a major leakage or spill, containment is possible if the patrol team can respond quickly enough.

There are two identified ways of gas seepage from pipelines or reservoirs, macro and micro seepage. Macro seepage is a visible presence of oil and gas seeping to the surface and micro seepage is where gas or hydrocarbons seep probably vertically or near vertically from the reservoir to the surface. Micro seepage can be directly monitored using a remote sensing approach to detect oil seeping by identifying tonal anomaly (van der Meer et al., 2002). Macro seepage meanwhile, can be indirectly detected through anomalies in soil mineral composition (Xu et al., 2008), water quality and vegetation health (Noomen et al., 2012) as a result of hydrocarbon concentration.

2.7 Spectral vegetation indices for detecting impacts of hydrocarbon leaks

Vegetation indices are mathematical combinations of various satellite bands (Jensen, 2014) and have been used by scientists since 1960s. The indices are derived from satellite data as the main source for monitoring vegetation conditions (Teillet et al., 1997) and mapping land cover change. Vegetation stress within the oil producing facilities may be assumed to be as a result of hydrocarbon leaks. The mineral alteration that occurs in the soil and geobotanical anomalies have become evidence for detecting hydrocarbon leakage (Noomen and Skidmore, 2008). Several studies have shown the effect of hydrocarbons on vegetation health (van der Meijde et al., 2009) when the contaminants enter the plants (Liu et al., 2007). It has also been suggested that presence of hydrocarbons seems to produce a change in the internal structure of the plant that results in low reflectance values, and gas affected areas may also be responsible for low vegetation density in the area (Oliveira et al., 1997). Also, vegetation growing near leaking gas pipelines revealed changes in geobotany and reflectance and a strong relation between plant vitality and gas can be assessed using spectral indicators (van der Meer et al., 2002). Blackburn (2007), noted that the reflectance spectra of leaves can vary independently of pigments due to differences in cellular structure, surface characteristics, moisture content and other biochemicals.

2.7.1 Broadband Multispectral Spectral Vegetation Indices (BMVIs)

Vegetation indices are optical vegetation canopy (greenness) which is a composite property of leaf chlorophyll, leaf area, canopy cover and architecture (Jiang et al., 2008). Satellite vegetation indices products are commonly used in a wide variety of terrestrial science applications aimed at monitoring and characterising Earth's vegetation cover from space (Myneni et al., 2002) and (Saleska et al., 2007). Also, combining principal components and different vegetation indices (VIs) was used in order to obtain a strong contrast between pixels. This is done to create new images to improve image classification techniques. Running et al. (1994); Huete et al. (1999b) show how to maximise sensitivity to plant biophysical parameters using linear responses of different vegetation conditions, validation and calibration of the index. There are many vegetation indices and few more widely used (Jensen 2014) as those contained in (Running et al., 1994) and (Lyon et al., 1998) which provided summaries of some indices where the

inverse relationship between red and NIR bands reflectance was associated with healthy vegetation (Jensen 2014). The vegetation indices such as NDVI have been in use for over three decades to assess or monitor vegetation phenological patterns. This is based on linearity regressing NDVI values obtained from various satellite imageries, along with in situ measurements, though the empirical approach adopted in recent times does not really require in situ measurements (Jensen 2014). The empirically derived NDVI products seem to be unstable due to soil colour and moisture, and bidirectional reflectance distribution function (BRDF) effects on atmospheric conditions (Qi et al., 1995). An accurate empirically derived NDVI product needs to be constant without calibration using in situ measurements, even when atmospheric and soil conditions change (Jensen, 2014). Most of the improved vegetation indices such as NDVI, benefited from adoption of sensor calibration and have been useful in estimating vegetation characteristics (Running et al., 1994). Other improved vegetation indices such as the soil adjusted vegetation index (SAVI) (Huete, 1988, Huete et al., 1992), incorporated an adjustment factor of canopy background and atmospheric conditions to address noise found in NDVI. In this study 20 indices will be exploited to find the most appropriate for detecting the impact of oil on vegetation. Though NDVI has its shortcomings, such as poor indication of vegetation biomass where the ground cover is low, for example in arid regions, (Huete and Jackson, 1987) as well as saturation and loss of sensitivity in densely vegetated areas (Huete et al., 2002). This study adopted the use of broadband multispectral vegetation index (BMVI) over narrow band hyperspectral data as it has been found to be reliable and valuable in the absence of hyperspectral data (Zhu et al., 2013). NDVI obtained from BMVIs is still considered to have great potential for applications in environmental monitoring because of its low cost compared to hyperspectral data (Broge and Leblanc, 2001). Thus, in this study the BMVIs use the following broadbands; blue (450–515 nm), red (630–690 nm) and near-infrared (750–900 nm). Twenty vegetation indices used for the study were reviewed in Table 2.1.

2.7.2 Detection of oil pollution using BMVIs

Hydrocarbons may reach vegetation when dissolved in the groundwater in the root zone and sometimes via air surrounding it. The uptake through roots and direct contact between soil and plant tissues are also media in which organic contaminants enter plants (Liu et al., 2007). The effects may depend on the type and quantity of chemicals involved and the vegetation type. Different vegetation types have varying sensitivity to hydrocarbons

(UNEP 2011). Simonich and Hites (1995) showed that the settling down of hydrocarbon particulates and their gaseous contents on leaves and intake via leaf stomata, may affect the health of vegetation. Other researchers have also reported the impacts of oil pollution from hydrocarbon leakages on vegetation health and vigour (van der Meer et al., 2002, van der Meer et al., 2000, van der Meijde et al., 2009). Remote sensing approaches and techniques such as vegetation spectral indices have proven to be effective in detecting and monitoring impacts of hydrocarbon leaks on vegetation health (van der Meer et al., 2000, van der Meer et al., 2002, van der Werff et al., 2007, Noomen et al., 2015). The mineral alteration that occurs in the soil and geobotanical anomalies have been used as evidence for detecting hydrocarbon leakages (Noomen et al., 2012).

Table 2.1: VIs evaluated for vegetation stress detection from oil polluted sites in this study

Indices	Formula	Author
1. ARVI2	$-0.18 + 1.17 * (NIR - Red / NIR + Red)$	Kaufman and Tanre (1992)
2. CIGreen	$(NIR / Green) - 1$	Gitelson et al. (2003)
3. EVI	$2.5 * [(NIR - Red) / (NIR + 6 * Red - 7.5 * Blue) + 1]$	Huete et al. (1999a)
4. EVI2	$2.5 * ((NIR - Red) / (NIR + 2.4 * Red + 1))$	Hunt Jr and Rock (1989), Liu and Huete (1995)
5. GBNDVI	$NIR - (Green + Blue) / NIR + (Green + Blue)$	Wang et al. (2007)
6. GLI	$2 * (Green - Red - Blue) / 2 * (Green + Red + Blue)$	Gobron et al. (2000)
7. GRN/NIR	$(Green - NIR) / (Green + NIR)$	Sripada et al. (2005)
8. GRN/RED	$Green - Red / Green + Red$	Motohk et al. (2010)
9. GRN/SWIR	$(Green - SWIR) / (Green + SWIR)$	Karnieli et al. (2001)
10. GRNDVI	$[NIR - (Green + Red) / NIR + (Green + Red)]$	Wang et al. (2007), Main et al. (2011)
11. MSAVI2	$(2 * NIR + 1 - (SQRT(2 * NIR + 1)^2 - 8 * (NIR - Red))) / 2$	Qi et al. (1994), Rondeaux et al. (1996)
12. MSI	$SWIR / NIR$	Hunt Jr and Rock (1989)
13. MSR705	$((NIR / Red - 1) / (SQRT(NIR / Red)))$	Wu et al. (2008)
14. NBR	$(NIR - SWIR) / (NIR + SWIR)$	Key et al. (2002)
15. NDVI	$(NIR - Red) / (NIR + Red)$	Rouse et al. (1973)
16. NIR/RED	NIR / Red	Birth and McVey (1968)
17. PPR	$(Green - Blue) / (Green + Blue)$	Metternicht (2003)
18. SAVI	$((NIR - Red) / (NIR + Red + 0.5)) * (1 + 0.5)$	Huete (1988)
19. SRI	NIR / Red	Birth and McVey (1968)
20. TNDVI	$SQRT((NIR - RED) / (NIR + RED)) + 0.5$	Tucker (1979)

Traditional field methods for estimating biophysical and biochemical properties of plants provide very accurate information on the response of individual plant species to pollution, but are limited in spatial coverage. Satellite remote sensing allows for monitoring of the

terrestrial vegetation characteristics on a regional, continental and global scale. Vegetation affected by oil pollution experiences changes in the biophysical and biochemical characteristics, which can be detected in changes in reflectance measured using satellite sensors (van der Meer et al., 2002). This is because vegetation spectral reflectance is dependent on the chlorophyll and water absorption in the leaves, which are altered by oil pollution. The relationship between plant pigments and spectral reflectance properties has been demonstrated in (Blackburn, 1999, Blackburn and Steele, 1999). Therefore, vegetation indices derived from satellite data can be used to determine the health of vegetation in areas affected by hydrocarbon pollution. Several researchers (Penuelas et al., 1997, Zarco-Tejada et al., 2005, Li et al., 2005, Khanna et al., 2013) have used vegetation indices as their main method for assessing various biophysical and biochemical properties of plants such as chlorophyll concentration, water content and vegetation structure. Broadband multispectral vegetation indices (BMVIs) are mathematical combinations of reflected energy recorded at various wavelengths (Jensen, 2014, Teillet et al., 1997) and have been used by scientists since the 1960s in terrestrial science applications aimed at monitoring and characterising Earth's vegetation cover from space (Myneni et al., 2002, Saleska et al., 2007).

2.7.3 Factors influencing detection of oil pollution

The influence of some factors, such as volume of oil spill, time period between the oil spill and image date, and spatial distance, on vegetation spectral indices could play a major role in detecting oil pollution in vegetated areas. Once an oil spill has occurred, it releases hydrocarbons into the natural environment. How these hydrocarbons are characterised and weathering (change in composition of hydrocarbons with time) are some of the problems at the polluted sites (Osuji et al., 2006). Wang et al. (2013a), suggested that oil characteristics and weathering may be influenced by the quantity of oil spill in the polluted environment. It is also found that over time hydrocarbon depletion may be dependent on their chemical and biological properties as well as the type of hydrocarbons (Luis, 1993, Osuji et al., 2006, Noomen et al., 2015). Use of appropriate satellite imagery at the earliest date after an oil spill could be very helpful in obtaining the vegetation status using spectral indices from remotely sensed data. Yang et al. (2000); Noomen (2007) and Noomen et al. (2012) have shown that the volume of oil spill in vegetated areas may result in a shortage of oxygen supply to plants and consequently retard their growth. These effects can therefore change the vegetation health of plants and

how they respond to it. The effects on vegetation health may also depend on the volume of the oil spill (Osuji and Opiah, 2007). It is assumed that larger volume oil spills may impact more on the surrounding vegetation and the affected vegetation may also take longer to recover as the oil degrades or evaporates. Small volume oil spills may have a low impact and the recovery of affected vegetation may not take longer compared to large volume spills. However, research and literature on the effect of quantity of spill on vegetation health using broadband indices is limited. Though some of the above assumptions have been shown that larger volume oil spills can have more impact than smaller spills (Masnik et al., 1976, Cushman and Goyert, 1984, Crunkilton and Duchrow, 1990). It is also documented that oil containing heavy insoluble compounds are more persistent compared with light soluble oils that are highly toxic and evaporate faster (Blumer and Sass, 1972, Barton and Wallace, 1979, Rosenberg et al., 1980, Crunkilton and Duchrow, 1990). Osuji et al. (2006), have shown that it is possible to directly monitor the disappearance of hydrocarbon fractions in oil polluted sites. Previous research focused more on large spills relating to natural hydrocarbon leaks' effects on general vegetation health, and thus the effects of the quantity of spills on plant health (BMVIs) were not investigated or emphasised (Noomen, 2007). This section focuses on determining the relationship between the volume of the oil spill and the impact on vegetation health and vigour. Other factors such as time of the image acquisition after the oil spill and scale (spatial distance) will also be assessed. For example we can assume that the quantity of the oil spill can be proportional to the level of impact on vegetation health surrounding the spill point (small size of spill, less impact, large size of spill, high impact). Generally, the area which is most impacted depends on the size of the oil spill, which may also be limited by any form of infiltration and how far it will migrate from the point of source. In Canada the average oil spill size from pipelines was found to be in the range of over 200 barrels and in some extreme cases 2000 barrels (Mackay and Mohtadi, 1975). Based on these figures the spill size within and above this range can be hazardous to the immediate surrounding vegetation. Hypothetical spill scenarios of crude oil showed that infiltration has more influence on spread of oil spill than evaporation (Hussein et al., 2002). Therefore, vegetation roots underground near the leaking pipeline will be most affected while estimation of surface flow of spill could be used to assess the environmental impact (Hussein et al., 2002). BMVIs have shown to be of great potential for the detection of oil pollution impact on vegetation (Zhu et al., 2013).

2.7.4 Importance of determining the flow direction of an oil spill

Determining the source and direction of oil spill flow in a polluted environment is important as it helps in identifying the likely vegetation that could be affected by oil pollution. Garbrecht and Martz (1997), have shown that desired gradients can be obtained by adding an elevation increment without significant alteration to the elevation of the digital landscape, while still producing a sufficient identity of flow direction over a flat surface. It is also reasonable that flat surfaces must have at least one cell at its edge that is at a lower elevation to characterise the downslope drainage off the flat surface. The model has been demonstrated in Douglas (1986), Jenson and Domingue (1988) and Garbrecht and Martz (1997) to track the overland path of pollution from a point of source into the drainage system or lower surfaces. Adopting this model in an oil pollution scenario will help in identifying the flow direction from the point of oil spill towards the steepest downslope into the neighbouring pixels.

Based on the flow direction of the oil spill, it is possible to determine pollution impacts on the vegetation health at varying distances from the point of source (likely impact areas) into the steepest downslope neighbouring areas (less likely impact areas). In a practical implementation of the model in (Garbrecht and Martz, 1997) the elevation increment using vertical DEM resolution, where a small increment does not change the actual size of elevation but numerically is enough to define flow direction, will be used. The analysis is based on the application of the deterministic eight-neighbour (D8) method to simulate flow across a land surface represented by a raster (grid) digital elevation model. The output of the flow direction is defined by the steepest drop, where the direction of the flow is to the left within the current cell, the flow direction is coded as illustrated in Figure 5.1. But where the cell is lower than its eight surrounding neighbours, the value will be assigned the values of its lowest neighbours, and the flow direction is defined towards the cell. Further explanation can be found in (Greenle, 1987). Jenson and Domingue (1988), have demonstrated this approach, which is known as an eight-direction (D8) flow model see Figure 5.1.

2.7.5 Tidal flow model

A tidal flow model, as described in the multiobjective set covering problem (MOSCP) 2016 report, is necessary to determine the type, characteristic, quantity and location of a

spill and to incorporate a number of environmental factors, in order to determine as accurate as possible a prediction on the spill's movement, including changes in characteristics due to weathering, and the prediction of the coastal marine areas potentially at risk. In accurately predicting the direction of movement of an oil spill, knowledge of tides, currents and wind speed and direction is essential. There are processes that influence the spreading of an oil spill on the surface of the land, which are dependent on the chemical and physical properties of the oil and the coastal conditions. Oil spill spread from pipelines can be influenced by currents and turbulent effects between ocean current and the coastal current (Elliott, 1986). A flow model, suitable for modelling contaminant dispersion, is a two-dimensional tidal current that may provide a relatively simple and economic method for accurate simulation of pollutant dispersion (Holly Jr and Usseglio-Polatera, 1984). This model, which has been used for water quality studies in coastal areas, often requires detailed simulation of contaminant dispersion based on mathematical modelling. The model has been demonstrated in (Glass and Rodi, 1981) for determining a finite difference scheme for pollutant transport in river flows. The suitability of this model for the oil spill flow direction is important, as it could help in determining the flow direction of pollutants. The model has been used by many, proves to be reasonable and the results were used to simulate tidal flows around the Portland Bill headland (Blunden and Bahaj, 2006). It has been used for evaluating tidal stream energy resources at Portland Bill to predict the variation of tidal stream in both time and space (Blunden and Bahaj, 2006). Most of the tidal models were applied in a marine environment (offshore) with limited emphasis on land (onshore). Thus, this study focuses on characterizing overland flow of oil spills in the mangrove forest, where fresh and sea water meet to influence the spreading of oil. The period chosen for the study has less influence on oil spill by tidal current from the ocean (this has been described in chapter 3 section 3.4).

2.7.6 Research gap

Few studies focus on the use of spectral vegetation indices derived from terrestrial, airborne and space hyperspectral data for detecting oil impact on vegetation. This study will evaluate and assess the capabilities of vegetation indices derived from broadband multispectral data for detecting the oil impact on vegetation in mangrove forests. Also, there is limited attention from many studies on certain factors (such as volume of oil spill, time gap between oil spill events and image acquisition data and spatial distance)

influencing the detection of oil pollution in vegetated areas using vegetation indices. Thus, this study will focus on these factors and assess how they influence the detection of oil pollution in the vegetated areas using vegetation indices derived from 30m broadband multispectral data. At the end, the technique used in the study will be evaluated on another polluted study site in order to test the validity and transferability of the technique.

2.8 Aim and objectives

The main aim of this research was to identify and detect vegetation affected by oil spills or pollution in the mangrove forest of the Niger Delta using Landsat multispectral data. The study used vegetation indices derived from the Landsat multispectral data for detecting vegetation affected by oil pollution through the assessment of leaf spectral properties. Thus, the three research objectives and research questions to achieve this aim are as follows:

Research questions 1:

- i) Can remote sensing spectral techniques be used to detect changes in leaf pigments of vegetation impacted by oil pollution over the space in mangrove forests?
- ii) Can changes in leaf chlorophyll before and after oil spill be detected using spectral vegetation indices?
- iii) Does vegetation affected by oil spills at polluted and non-polluted sites differ in biochemical and biophysical properties (spectral properties)?

Objective 1:

To apply remote sensing techniques such as broadband multispectral vegetation indices derived from Landsat data to detect and analyse changes in biochemical and physiological properties of vegetation affected by oil pollution.

- This was carried out using statistical analysis (paired t-test) to compare vegetation indices extracted at the polluted and non-polluted sites over time and space, and to assess the capabilities of the indices that can detect changes in reflectance properties of vegetation affected by oil pollution.

Research questions 2:

- i) Can the volume of an oil spill influence the detection of oil spill impact on physiological status of vegetation?
- ii) Does the time gap between oil spill and image acquisition date influence the detection of the oil pollution impact on the biophysical and biochemical changes of vegetation?
- iii) Can the oil pollution impact on vegetation vary with distance from the polluted point?

Objective: 2

To analyse factors influencing the detectability of vegetation affected by oil pollution using spectral vegetation indices.

- This involves determining the relationship between the influential factors identified and vegetation indices using statistical regression analysis.

Research questions 3:

Can the technique adopted in this study be replicated at another study site?

Objective: 3

To assess and validate the remote sensing technique at a new study site.

- This entails identification of new oil spill sites and applying the technique in chapter 4 for analysis at this new study site, as well as validating the results.

Chapter 3 : Study area, data and methodology

3.0 Introduction

To address the research questions developed in chapter one (section 1.2), this chapter provides a description of some environmental and climatic factors. This is important because they could have an influence on the selection of appropriate data and the method of analysis in answering the research questions. The data and methodology sections provide a detailed description of the data, sources and methods used for the analysis, which focuses on data sampling and processing techniques. The chapter describes the general environmental characteristics of the region where the two study sites (SS) are located, but only study site 1 (SS1) was included here. For clarity, the data and its sources used in chapters 4 and 5 (SS1) are described in this chapter, while for the study site 2 (SS2) they are specifically discussed in chapter 6. The method and techniques (image processing and data analysis) for Chapter 4 and 6 are fully described in this chapter and are then validated in chapter 6.

3.1 Study Area

Nigeria lies between longitudes $2^{\circ} 49'E$ and $14^{\circ} 37'E$ and latitudes $4^{\circ} 16'N$ and $13^{\circ} 52'N$, and the Niger Delta consists of 9 states where oil production and transportation activities are carried out. The Niger Delta is located in the southern part of Nigeria bordering the Gulf of Guinea (in the Atlantic Ocean). The study area falls within longitude $5.05^{\circ}E$ and $7.35^{\circ}E$ and latitude $4.15^{\circ}N$ and $6.01^{\circ}N$ near the town of Degema in Rivers State, Nigeria. The region stretches ~240 km from North to South of the country and along the coast for about 320 km. The region covers about 70,000 km² of floodplain out of the 923,768 km² of the country's total land area. The Niger Delta hosts the largest extent of mangroves in Africa, the fifth largest in the world, and is the third largest delta in the world. It has the most extensive fresh water swamp forest in west and central Africa (Ikwegbu, 2007). The uniqueness of the Niger Delta mangroves is a consequence of the geographic pattern of the ecosystem, which is shielded from sea water that differentiates it from that of several other African countries that are directly exposed to sea water. About sixty per cent of the mangroves in Nigeria are found on the coast of the Niger Delta region; Human Rights Watch (HRW, 1999). The River Niger is the principal river in West Africa and the third largest water course in the continent. Originating from the Futa Jallon highlands in Guinea, it flows over 4,184 km, firstly towards the north-east, passing through Mali then

bending to the south east and linking Niger before running into Nigeria where it forms its largest tributary with the River Benue in Central Nigeria. The river continues towards the south of Nigeria for about 400 km to form a fan-shaped delta and finally empties into the Gulf of Guinea.

In Figure 3.0 the Niger Delta is shown in green within the political map of Nigeria. This study focuses on one of two areas with a high concentration of oil facilities; the two areas (both SS1 and SS2) also fit conveniently in a single satellite data frame (Landsat), a fact that is discussed in the subsequent sections of this chapter 3 (SS1) and in chapter six (SS2).

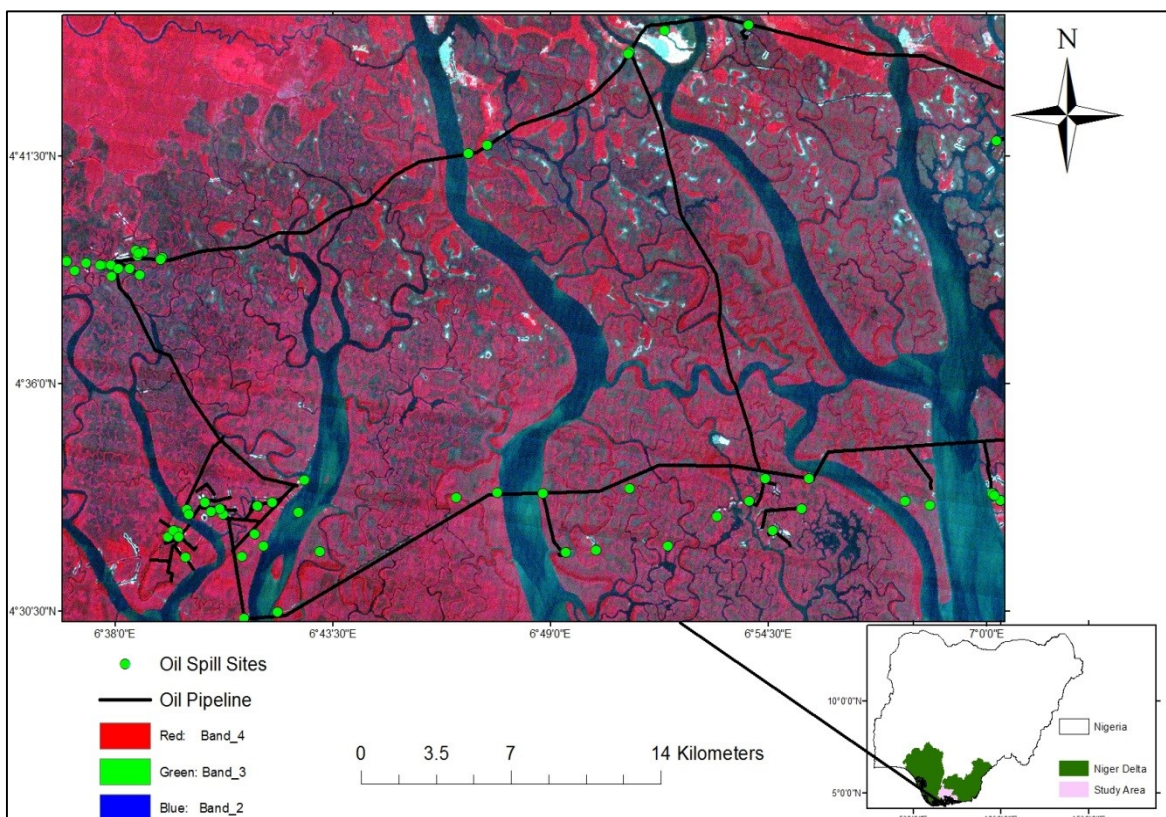


Figure 3.1: Oil pipeline and spill sites distribution within the study area (SS1)

3.1.1 Geology and Soil

The River Niger forms an intricate network of channels which drain into the Gulf of Guinea. It is characterised by rain fed deltaic vegetation in places, with high elevation, and the majority of the region is dominated by low lying landforms. The area is formed of both fluvial and marine sediments built-up over the past 50 million years (since the Upper Cretaceous period). These sediments form a shallow marine and deltaic

environment characterised mainly by the River Niger and its tributaries. They form multiple geological layers of clay, sand, conglomerate, peat and/or lignite with variable thickness and texture covered by soil. The clay beds are discontinuous and groundwater is present in hydraulically interconnected aquifers, which characterise deltaic environments where erosion and deposition of sediments shift the course of channels and tributaries (UNEP, 2011b). The Niger delta coastal mangroves ecosystem is supported by saline soil with a pH value of between 0 and 4 for the freshly deposited soft silt at low tides and 7 for transitional swamps at high tides. An intermediate peat clay soil type forms about 90 per cent of the soil in the ecosystem (Fagbami et al., 1988, Doust, 1990).

The zone of alluvial soils is found in the flood plains of rivers or in deltas, or along coastal flats. This zone extends from the coastal inland and runs along the valleys of the Niger and the Benue rivers, cutting across the vegetation zones. The soils found in this zone do not depend highly on climate and vegetation for their formation. The underlying parent rock is the most important factor in their formation. Soils in this zone are characteristic of freshwater soil of grey to white sand, grey clay and sandy clay with humus topsoil. Another group consists of brownish to black saline mangrove soils, with a mat of rootlets. Additionally, the soils of this region are all of fluvial origin, except for the coastal areas that consist of marine sand overlain with an organic surface layer. The continuous movement of the delta's channels has resulted in a mosaic of soil types. Remnants of old levees consist mostly of water permeable sand and loam. The soil of the depressions behind them (back swamps) consist mostly of water-logged heavy clay covered by peat, while higher lying sections consist of silty loam and clay. The formation of the Niger Delta is as a result of the deposition of sediments brought down by the River Niger and its tributaries along their paths through various countries before reaching the coast (Aregheore, 2005).

3.1.2 Hydrology

The oil spill sites identified were all located in the mangrove swamp areas (Figure 3.1) where there is a presence of both underground and surface water. Therefore, there is a need to describe the hydrological characteristics of the area and how it could influence detection of oil pollution. The hydrology of Nigeria is dominated by two great river systems, the Niger-Benue and the Chad systems. With the exception of a few rivers that

empty directly into the Atlantic Ocean, all other flowing waters ultimately find their way into the Chad Basin or down the lower Niger to the sea (Aregheore, 2005).

The aquifers are a crucial resource upon which the region's entire population depends on for drinking water. They are characteristically very shallow with groundwater levels found anywhere close to the surface within a depth of 10 meters. The community hand-dug wells are usually about 60 cm in diameter (UNEP, 2011a), which in some locations are affected by localised pollution (such as hydrocarbons) of water closer to the surface, though some wells can be up to 50 m deep. In most cases water levels in such areas are highly seasonal. Fresh groundwater is also found in shallow, sandy and unconfined aquifers of the coastal areas, river bars and islands in the mangrove belt, also at varying depth in confined aquifers (Amadi et al., 1989). Most of the drilled wells in the coastal areas produce brackish (salty) water that is not fit for drinking and in some areas were found 200 meters below ground level, which could be due to oil spill/leaks from oil facilities contaminating the groundwater and where fresh and salt water interacts (Kostecki, 1991).

3.1.2.1 Surface Water

Nigeria's major rivers, with an estimated catchment site of about 108,124 km², make up about 11.5 per cent of the total surface area of Nigeria, which is estimated to be approximately 923,768 km² (Scott, 1966). The Niger Delta region is drained by river systems which are mostly associated channels and streams.

The region's freshwater and deltaic estuaries (an area of interaction between fresh and sea water) cover approximately 3,600 km² and 6,170 km² respectively (Scott, 1966). They are mostly from the River Niger and other sources of inflow during the rainy season, and are also influenced by tidal variations. The width and velocity of freshwater channels increase downstream to meandering or braided channels in the delta. As such, hydrocarbon leaks can reach water bodies through the effects of wind, rain, surface or sub-surface flow. Where there are concentrations of hydrocarbons on the surface, water bodies can form a very thin layer as a result of oil slicks that would be distinct enough to be detected aerially or from high resolution satellite images (Fingas and Brown, 1997, Brekke and Solberg, 2005). The concentration of these hydrocarbons in such a swamp area may also influence the detection of oil pollution using vegetation spectral reflectances.

3.1.3 Vegetation

The Niger Delta region generally harbours a wide variety of trees and plants including mangrove trees of all kinds, grasses, herbs and climbers which are attributed to the depositional nature of the shoreline. The *Rhizophora racemosa*, also known as red mangrove, occupies more than 90% of the saline swamps, and dominates the main vegetation of the mangrove swamps in the region. The relative nature of the mangrove vegetation to soils and salt water has made the soil of the region generally acidic, with a pH ranging from 4.6 to 6.7. These soils become more acidic when dried and the pH value drops down to as little as 2.2 (Okoro et al., 2011).

The *Avicennia africana*, also known as white mangrove, is found sparsely distributed amongst the red mangrove and survives in less water-logged areas. The soil under the white mangrove is non-fibrous, less acidic, and on drying exhibits less of a decrease in pH (Egberongbe et al., 2006). There are other common vegetation types where salt water content is not too high, including ferns (e.g. *Acrostichum aureum*), nympa palm (*Nympa fruticans*), and herbs (e.g. *Paspalum vaginatum*). In the mangrove swamp in the eastern flank of the Niger Delta there is a conspicuous presence of *Nympa* palm, an invasive species.

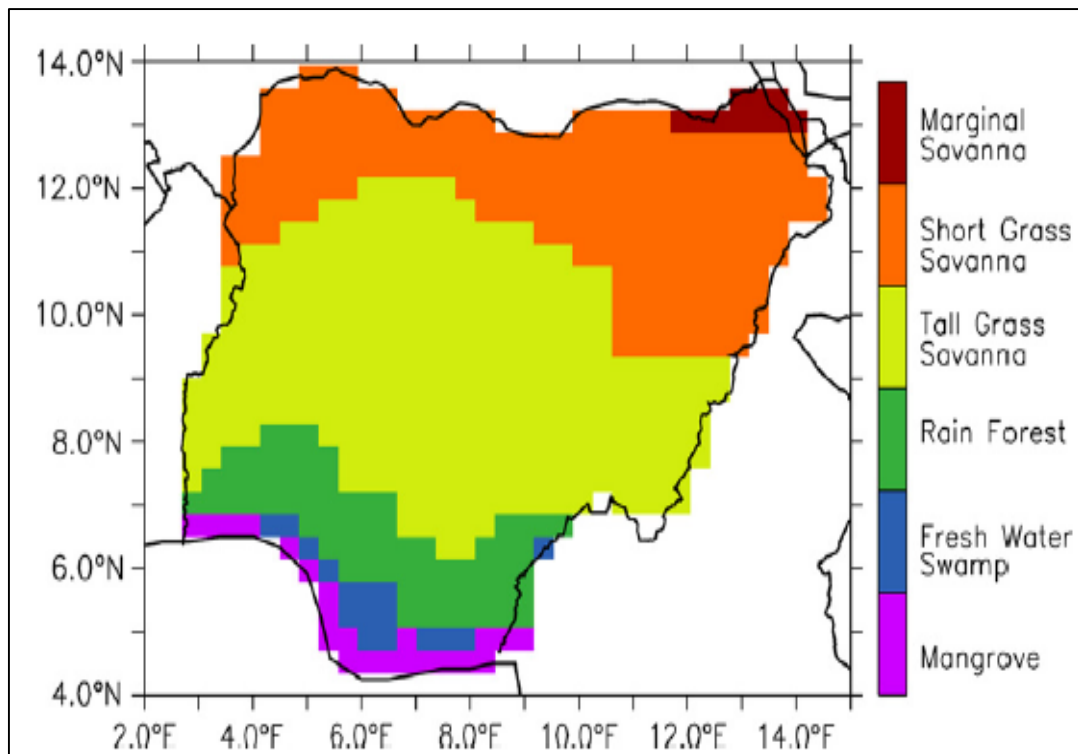


Figure 3.2: Nigeria vegetation zones

Source: (Oguntunde et al., 2011)

In the saltwater zone (*Rhizophora Mangle*) vegetation type is restricted to the coastal strip, which varies in width from less than 1.5 km in the west coast areas to over 50 km in the Niger Delta area. It is pronounced where the fresh water from the rivers meets and mixes with the salt water from the sea, forming brackish swamps. The low-lying nature of the Nigerian coastal zone allows for the influx of saline water through tidal movements into the lagoons, channels and extensive brackish wetlands. This has encouraged the growth of different species of mangrove vegetation, typical in the wetlands of the backshore areas. The mangrove vegetation is a hydromorphic forest type, characterised by an entangled dense growth of stems and aerial roots behind the stretch of coconut palms overlooking the Atlantic Ocean. The freshwater zone vegetation belt and freshwater wetlands occur further inland beyond the reach of tidal waters. Here, there is an enormous supply of fresh water from the inland rivers and run-off from abundant rainfall in the area. The major drainage systems, from west to east, are from neighbouring states which deposit vast quantities of silt, mud and sandy materials into this area. It is a low-lying region, with hardly any parts rising over 30 m above sea level (a.s.l), thus, it facilitates the development of freshwater swamps along the Niger Delta, drowned estuaries, lagoons and channels.

The network of channels and lagoons results in inaccessible swamps of forest vegetation in the southern parts. In the northern part there are floodplains of sandy accumulations, colonised by bush thickets and by tall grasses in the cultivated areas. The most common species of this vegetation type is the raffia palm (*Raffia Hookers*) which dominates the swamps. The better-drained areas support oil palm trees (*Eleais Guineensis*) and large trees like Iroko (*Chlorophora Exceisa*). The development of an oil facility in the mangrove areas is often preceded by dredging and/or vegetation clearance to create navigable accesses. During dredging, the soil, sediment and vegetation along the right of way (ROW) of the proposed site are removed and typically disposed overbank, in most cases infringing upon mangroves, and then abandoned. The impact of these abandoned dredged materials can alter topography and hydrology, and cause acidification and water contamination which may lead to vegetation/mangrove areas being converted to either bare heaps, grassland or freshwater forest after several years of natural weathering (Ohimain, 2004).

3.1.4 Climate

Nigeria's climate is tropical, characterized by high temperatures and humidity as well as marked wet and dry seasons, though there are variations from South to North. Total rainfall decreases from the coast northwards. The South (below Latitude 8°N) has an annual rainfall ranging between 1,500 mm and 4,000 mm and the extreme North between 500 mm and 1000 mm (Odjugo, 2005). The seasonal pattern of climatic conditions over Nigeria gives rise to four seasons in the south and two in the north. This is the result of annual total rainfall occurrence and distribution, which is more predominant in the south than in the north. Therefore they are very important factors to be considered on the suitability and time of the satellite image to be used for the study. These factors can also have influence on detecting oil spills on the water surface because it is associated with tidal movement and wind action which may affect the actual spill point on the satellite imagery.

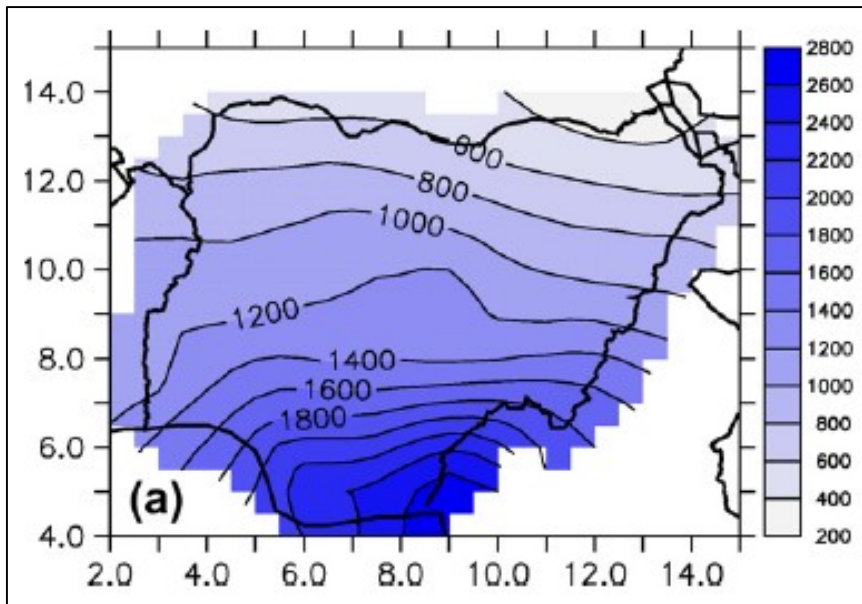


Figure 3.3: Distribution of rainfall in Nigeria (mm/yr) Source: (Oguntunde et al., 2011)

3.1.4.1 Rainfall and Seasonality

The seasonality of the study area is critical in deciding which imagery is to be used for the analysis. It is important to describe rainfall pattern within the year, which will help in identifying appropriate cloud free data. The long wet season starts in March and lasts to the end of July, with a peak period in June over most parts of southern Nigeria (Anyadike, 1993). It is a period of thick clouds and is excessively wet, particularly in the Niger Delta and the coastal lowlands. It is marked by humidity with values hardly below 85 per cent in most parts of the forested south. The short dry season is experienced in August for 3-4 weeks. However, the real dry period known as the "August break" is generally observed in the last two weeks of August in most parts of southern Nigeria. The short wet season follows the "August break" from early September to mid-October, with a peak period at the end of September. The rains are not usually as heavy as those in the long rainy season, although the spatial coverage over southern Nigeria is similar. The two periods of rainfall intensity give the double maxima phenomenon of the wet season characteristic of southern Nigeria. The short dry season in August between these two rainy periods allows for harvesting and planting of fast-growing varieties of grains, such as maize (Anyadike, 1993, Adejuwon, 2012).

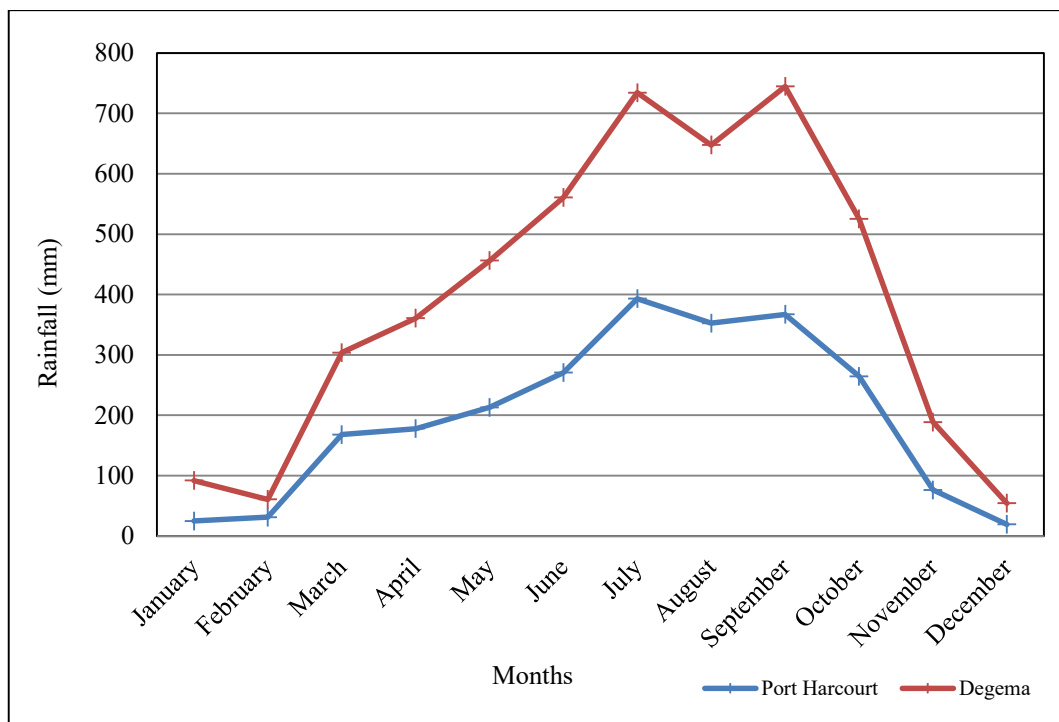


Figure 3.4: Monthly average values of rainfall in the study area (closest towns) from 1931-1997
 Source: (Adejuwon, 2012)

The long dry season period starts from late October and lasts to early March with peak dry conditions between early December and late February (Odjugo, 2005). The period witnesses the prevailing influences of the dry and dusty north-east wind conditions. Vegetation growth is generally hampered, grasses dry and leaves fall from deciduous trees due to reduced moisture. Since cloud cover in the Niger Delta persists for most of the year due to the wet season (from March to October/November), it is appropriate to obtain cloud free data that falls between the months November/December to January/February (long dry season). The preceding assessment or discussion was to provide the researcher with information on areas where there is vegetation growth in contaminated areas that may affect or influence the detection of hydrocarbon leaks from the satellite data.

3.1.4.2 Temperature, Wind, Humidity and Topography

This section describes the characteristics of these climatic elements and how they can influence the distribution, flow direction and dispersion of oil spills. The annual temperature in the Niger Delta ranges between 26 oC and 34oC with the highest during the dry season (November - March) and the lowest between 24. 5oC and 26.9 oC in June,

July and August. The wind in the region is characterised mainly by south westerlies from offshore and generally restricted to azimuths of 215-266 degrees with speeds of 2-5 ms⁻¹ and a force range of 2-3 on the Beaufort scale (a light and gentle breeze). The effects of these winds are curtailed by the effect of local onshore winds from northern Nigeria between January and February when the dust haze concentration reaches the coast. The region has a high surface humidity along the coast with high values recorded in August ranging from 80-100% and low values between 60 to 80% occurring in November and March. The period of low humidity is in January to February with the values between 20 to 40% during the harmattan spell from northern Nigeria (a dry dusty wind that blows along the northwest coast of Africa). Wind can affect the flow direction of oil spills on open surfaces e.g. surface water and bare land (soil). Similarly, high and low temperature or weathering over time could naturally influence the volatility and depletion of spilled hydrocarbons (Osuji and Ezebuio, 2006).

The topography of the Niger Delta or Nigerian coastal areas is also another factor that could influence the analysis of the study. Topography of the region is generally low-lying; in the Niger Delta it is about 2m to 4m above sea level (Allen, 1965) as shown in Figure 3.4. (Ohimain, 2004) reported that physical change in soil topography is linked to the chemical and biological changes in the environment. Ohimain et al. (2010) also suggested that topographic differences between soils supporting healthy mangroves and dredged material heaped within the study area arises from oil exploration, which will help in determining the possible flow direction of an oil spill.

3.2 Data sources

The following datasets were used in this study:

- In chapters 4 and 5 eight (8) Landsat TM & ETM scenes were acquired from the study area on Path/Row 188/57 in Figure 3.0 from the following dates: 17/01/1986, 19/12/1986, 21/02/1987, 29/11/1999, 17/12/2000, 08/01/2003, 26/11/2004 and 19/01/2007. The reasons for the selection of these 8 images for the study are fully explained in the data sampling and analysis section 3.3.
- SRTM data at 30m resolution for the study area was obtained from and was used for modelling flow direction (Figure 3.4).

- Oil spill data from 1985-2007 (Sample Points (SP) =56), consisting of vector layers showing exact location (using GPS) of the 56 sample points (SP) and layers showing the location of oil pipelines obtained from (Shell) Nigeria through Nigeria's oil regulatory agency 'The Department of Petroleum Resources', (DPR) (<https://dpr.gov.ng/>).
- In chapter 6 three (3) Landsat 8 data scenes were acquired in January in years 2013, 2014 and 2015 on Path/Row: 189/57 for the study site 2.
- The new spill sites (9) which occurred in 2014 were identified and obtained from (NOSDRA) [<http://nosdra.gov.ng/>] achieves at [<https://oilspillmonitor.ng/>]. The oil spill data layers contain information on the type of vegetation where the spill occurred, volume of oil spill (barrels) etc.

The accuracy and reliability of these data cannot be independently verified by the researcher thus relying on Nigeria's regulatory laws for oil and gas operations. For the purpose of this study, it is assumed and accepted that the information in the database are accurate and reliable based on Nigerian law on oil and gas operations.

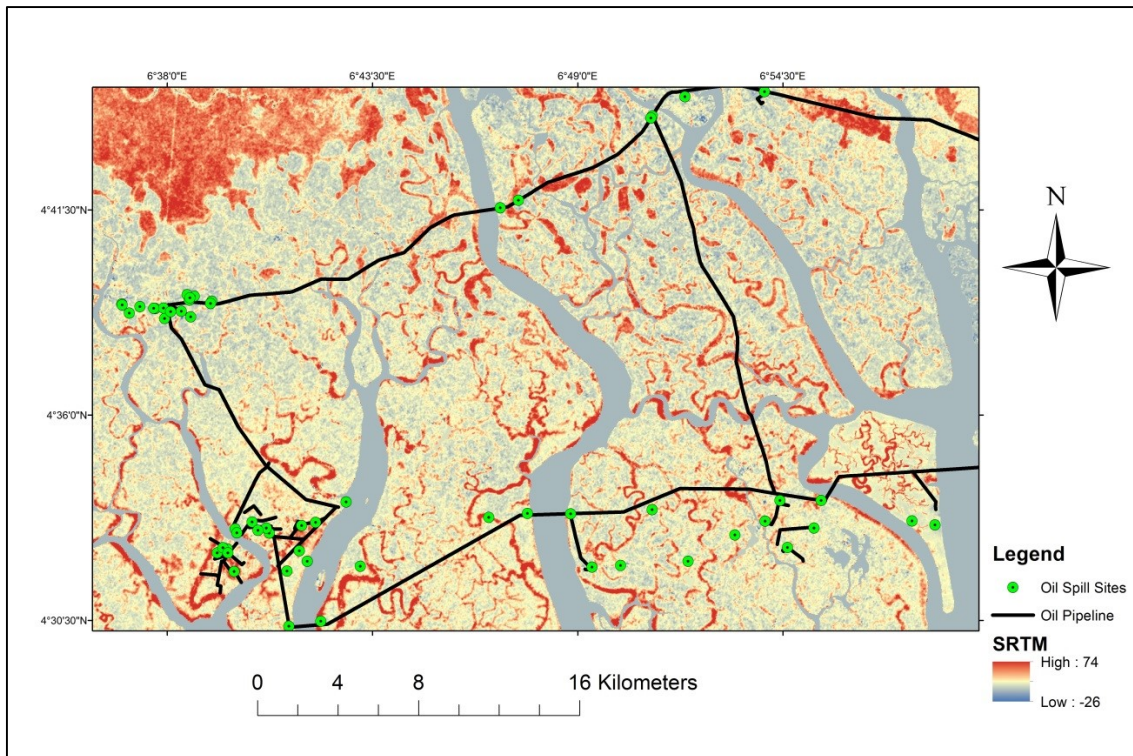


Figure 3.5: SRTM data used for generating flow direction model and oil spill sites

Topography of the region is generally low-lying, in the Niger Delta it is about a minimum of 2m and maximum of 22m (average of 7m) above sea level with average slopes of 0.1% and -0.1% (slope values ranges between 0 – 89 degrees) (Allen, 1965).

3.3 Data sampling and analysis

This section focuses on the selection of both the image and oil spill data based on suitability, which are dependent on some environmental and climatic factors. First, sampling of spill sites that may be possible for identification/observation from available cloud free images of the study area were carried out. Secondly, the climatic windows were taken into account given the persistent cloud cover in the study area, which may cause difficulties in identifying and observing the oil spill sites from satellite data. Therefore only cloud-free images were suitable for the purpose of this study. For this reason the months of November, December, January and February were selected because they fall within the dry season (the climate of the study area was fully discussed in chapter 1). Images acquired during this period are relatively free of cloud cover. Table 3.3 below shows the total number (56) of sample spill sites and available cloud-free data which were used for observing before and after the oil spill events. The total number of oil spills

recorded in the study area was from 1985 - 2007. The challenges faced during these analyses were issues of dense clouds and heavy shadows in images which could not be fixed using atmospheric correction. Some of these problems were solved by exclusion from the analysis of some affected spill sites that were under the cloud, scan-lines and non-vegetated land covers (water, roads, bare surface etc.).

Table 3.1: Oil spills recorded over the years and available image data in spill sites 1.

Year of Spill	Sample Points	Acquisition Date	Sensor
1985	2	17/01/1986	TM5
1986	9	19/12/1986	-
1998	7	21/02/1987	ETM
1999	11	29/11/1999	-
2000	10	17/12/2000	-
2002	6	08/01/2003	-
2004	4	26/11/2004	-
2006	5	19/01/2007	-
2007	1		-
Total	56		Total

In the USGS archives most of the images of the study area between March and November are 40 to 100 per cent covered by cloud. So the critical dates for image acquisition are November to February as they are characterised by relatively cloud-free cover over some spill areas. The number of images were limited by environmental factors as mentioned in sections 3.1 and 3.3 (e.g. seasonality), lack of available data from the USGS archives for the study area from 1992-1998 (as at the time of conducting this research), scan lines on images after April 2003 and available oil spill data (1985-2007). The data was limited to only the period under study, so the available satellite data from 1986-2007 was used for observation of oil spill events from 1985-2007.

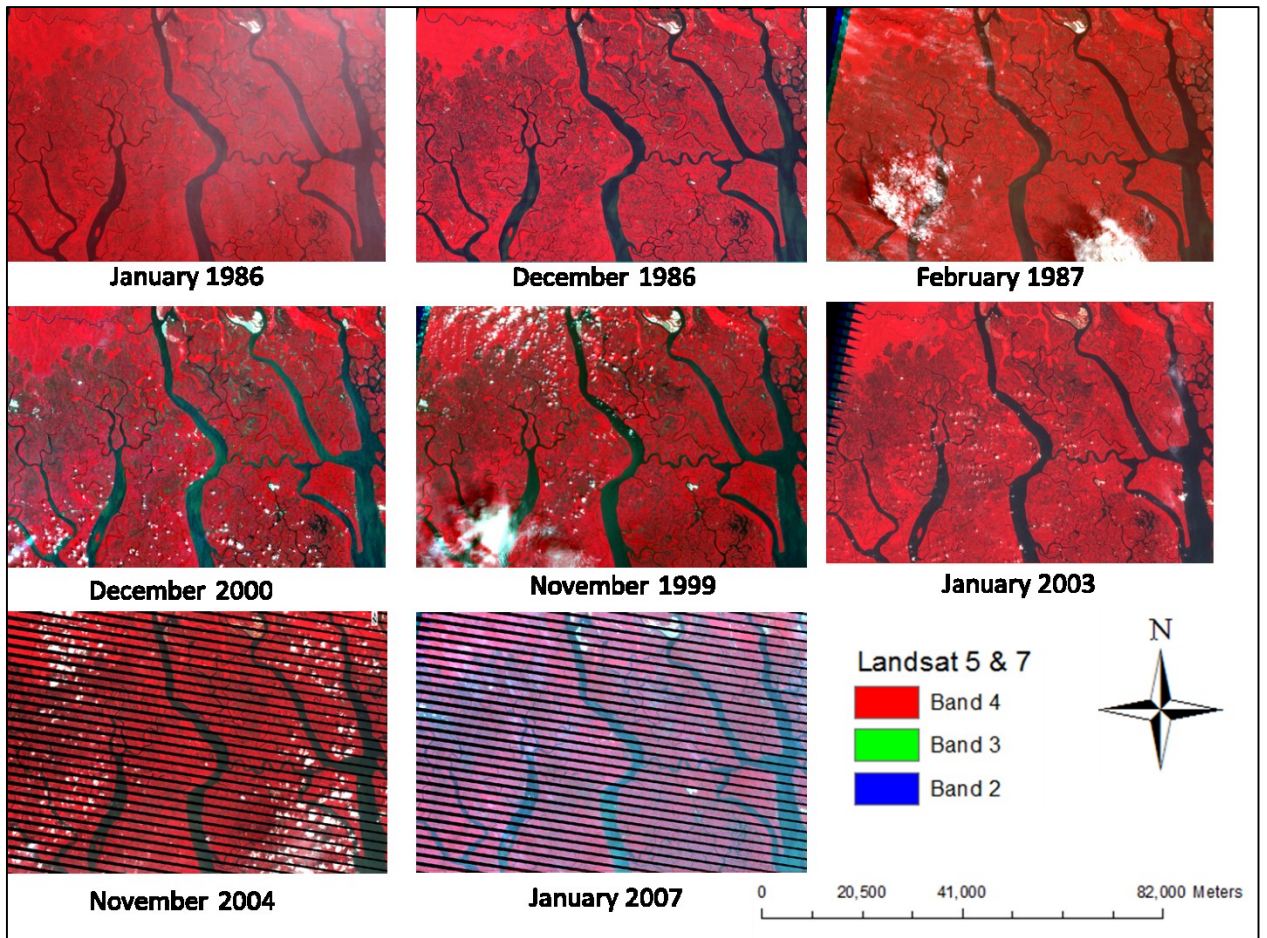


Figure 3.6: Landsat images used for the study site 1

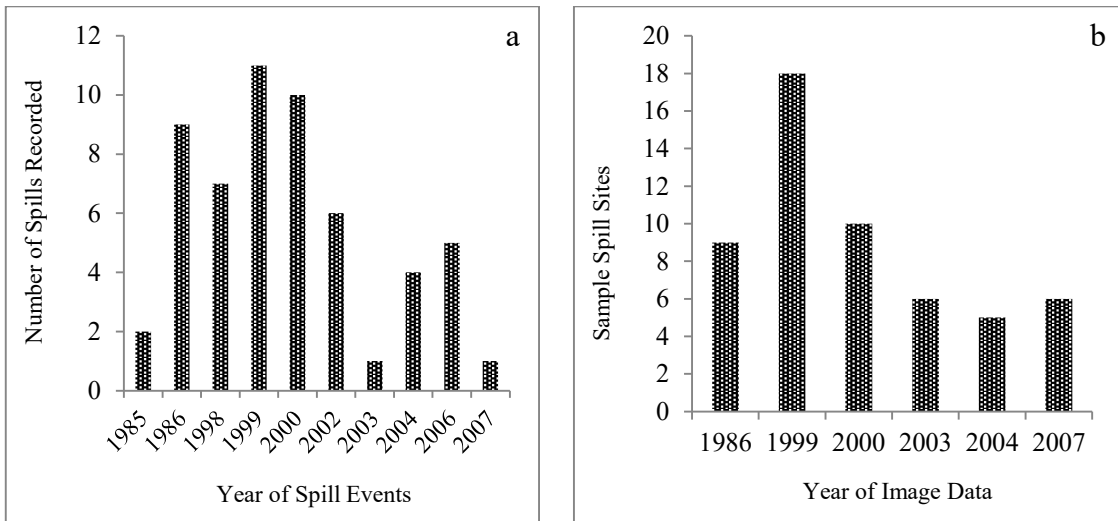


Figure 3.7: (a) Number of spill events recorded over the years and (b) Observable number of sample spill sites by year of image.

Figure 3.6a shows that the highest number of oil spills was recorded in 1999 and the lowest in 2003 and 2007. Figure 3.6b shows that the most sample spill sites were observed

from 1999 image data and the least in 2004. The spills were observed based on availability of data preceding each oil spill event, for example spills that occurred on December 29, 1985 were observed using image data acquired in January 1986; spills recorded after January 1986 were observed using imagery from December 19, 1986 and so on.

3.4 Landsat data

Landsat data have a relatively low temporal resolution, taking 16 days to revisit the last location; it is therefore possible that the period of interest may fall in a rainy season when there is tendency of heavy cloud to decrease the image quality. Hence, local climate and topographical conditions were considered when selecting imagery for the study. The advantages of Landsat data is that the repetitive coverage of an area at 30 metre resolution allows the monitoring and analysis of an environment over a period of time and can be used for mapping at both the local and regional level. There are various factors that influence the choice of sample size for both the ancillary and image data. Some of these factors include cloud cover in image data, availability of data in USGS archives, climatic (e.g. seasonality) and environmental conditions of the study area. The images used in this study were restricted to the months of November, December, January and February (discussed in section 3.1) because they are relatively free of cloud cover.

Table 3.2: Oil spill data points used in the study

Sample Point	Volume	Spill Date	Time Diff (Days)	Sample Point	Latitude	Longitude	Volume	Spill Date	Time Diff (Days)
SP1	2	19/12/2006	32	SP29	4.548372	6.710674	200	09/07/2000	161
SP2	5	12/09/2000	96	SP30	4.556227	6.794154	221	22.07.2004	127
SP3	9	21/08/2000	118	SP31	4.644064	6.643728	232	26.04.1986	237
SP4	10	10/09/1999	363	SP32	4.55289	6.900248	269	27.05.1986	206
SP5	10	22/01/2006	80	SP33	4.538704	6.655578	318	22.10.2004	35
SP6	20	04/01/1985	378	SP34	4.552134	6.699582	346	26.08.2002	135
SP7	27	04/01/1985	378	SP35	4.547682	6.664467	352	18/09/2006	11
SP8	28	17/11/1999	12	SP36	4.534766	6.695854	358	20.09.1998	819
SP9	32	19/08/2004	99	SP37	4.534766	6.695854	379	20/08/1998	46
SP10	39	21/09/1999	69	SP38	4.553049	7.006055	400	01/11/2000	560
SP11	40	04/12/2006	47	SP39	4.550757	6.693101	468	06.06.1999	89
SP12	50	15/11/1999	14	SP40	4.552936	6.965783	500	15/02/2003	650
SP13	54	14/11/2000	33	SP41	4.732953	6.849292	500	19/09/2000	370
SP14	62	08/07/1999	144	SP42	4.549828	6.922278	507	21.12.1998	370
SP15	63	04/11/1986	45	SP43	4.55548	7.002535	558	15/12/2000	300
SP16	63	02/08/2004	116	SP44	4.547457	6.678789	625	21/02/2000	474
SP17	75	13/03/1986	281	SP45	4.530398	6.68668	785	23/07/1998	708
SP18	75	03/10/2000	75	SP46	4.539636	6.692326	807	09.01.1999	3
SP19	96	12/05/1986	221	SP47	4.505723	6.687569	813	16.01.2007	707
SP20	97	18/06/1986	184	SP48	4.539636	6.692326	1000	10.01/1999	158
SP21	117	30/10/2000	48	SP49	4.551067	6.976329	1042	14.08.2006	37
SP22	126	11/05/2006	254	SP50	4.653909	6.642229	1069	02.12.2002	844
SP23	128	16/02/1986	306	SP51	4.532672	6.719641	1505	26.08.1998	163
SP24	150	13/01/2003	169	SP52	4.546667	6.886915	1720	09.07.1986	134
SP25	150	04/08/2006	5	SP53	4.549622	6.677431	1734	07.09.2006	270
SP26	155	11/11/2006	70	SP54	4.561336	6.713058	2578	29.04.1986	234
SP27	180	29/11/2006	52	SP55	4.698156	7.004298	2761	28.12.1985	20
SP28	184	24/08/1999	97	SP56	4.561988	6.906837	3500	24.06.2002	198

Table 3.2 summarizes some of the technical specifications of the data and its applications to this study including more recently launched (February 13, 2013) Landsat 8 Operational Land Imager (OLI), which was used for validation in study site 2.

Table 3.3: Landsat data sensor and band specifications

Satellite	Sensor	Band No's	Spectral Range	Scene Size	Pixel Resolution
L 4-5	TM multi-spectral	1,2,3,4,5,7	0.45 - 2.35 μm		30 meter
L 7	ETM+ multi-spectral	1,2,3,4,5,7	0.450 - 2.35 μm	170	30 meter
L 7	ETM+ thermal	6.1, 6.2	10.40 - 12.50 μm	x	60 meter
L7	ETM+ Panchromatic	8	0.52 - 0.90 μm	185	15 meter
L8	OLI	1,2,3,4,5,6,7,9	0.43 - 2.29 μm	km	30 meter
L8	Thermal Infrared Sensor (TIRS) (1&2)	10, 11	10.60 - 12.51 μm		100 meter
L8	OLI Panchromatic	8	0.50 - 0.68 μm		15

The Landsat 8, originally titled ‘Landsat Data Continuity Mission’ (LDCM) which has 10 bands, compared to the 8 bands of ETM+, collects data with the OLI instrument that has advanced measurement capabilities, with an “ultra-blue” band (Band 1) for coastal and aerosol studies, as well as Band 9, which is useful for cirrus cloud detection. Two thermal bands are also present in the Thermal Infrared Sensor (TIRS) and scene size is comparable to current Landsat scenes (NASA). Landsat 8 has a slight difference in spectral reflectance response and measurements compared with other Landsat data (Flood, 2014). It was expected that some vegetation indices (e.g. NDVI) would be affected by an average of 5% if the systematic differences between the sensors were not adjusted for (Flood, 2014). Thus chapter 4 and 5 in this study utilised only TM and ETM+ data for the temporal analysis in SS1 to avoid the difference in indices values with that of Landsat 8.

3.5 General methodology

The general methodology used for the overall analysis of the Landsat TM and ETM+ for SS1 and OLI data for SS2 for the detection of pollution in oil polluted environments (sample points) is outlined in Figure 3.7. The detailed descriptions of different methods or techniques used in addressing each of the research objectives are discussed at the start of result chapters 4, 5 and 6. Figure 3.7 shows the general methodology employed to achieve the research objectives of this study. The methodology is divided into four sections; the first section (in red) describes the data pre-processing, processing and integration (atmospheric correction, computing flow direction model and spectral transformation). The second section (in black) addresses objectives 1 and 2; objective 3 is separately discussed in chapter 6. Specific methods are fully described in each of the respective chapters.

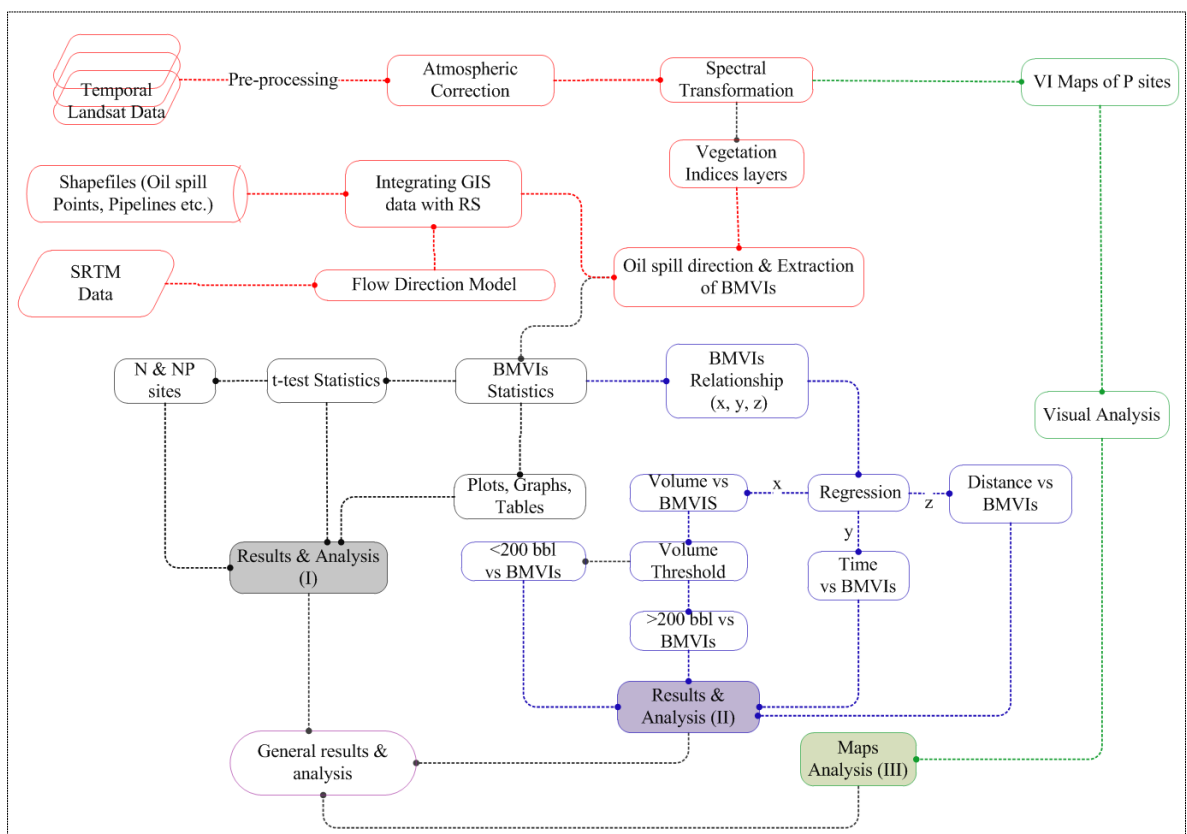


Figure 3.8: General methodology flowchart showing the four stages of analysis used for the study

3.5.1 Data pre-processing

To start any scientific analysis on multiple remote sensors, spectral data must have the same units for radiance before calculating the reflectance. For the purpose of this study necessary information to put Landsat TM and ETM+ into comparable measures of radiance and reflectance has been put together from various sources in order to assist in adjusting the raw sensor data to a common starting point for data processing. The term image pre-processing in remote sensing means correction of radiometric and geometric distortions to improve the quality of the original image. Image data processing and analysis is preceded by various pre-processing techniques in order to provide desirable/appropriate output or operations that are preliminary to the principal analysis (Campbell and Wynne, 2011). In some cases pre-processing is performed by the data provider for the end user. As is the case for this study, Landsat data were downloaded as Level 1 products, which means some of the pre-processing (radiometric and geometric corrections) have been performed by the data provider. Images are characterised by variations in dates of acquisition, errors can occur due to solar angle elevation, which may require radiometric correction (Goslee, 2011). While some errors relating to position of pixels are caused by variation in altitude, attitude and velocity of the sensor platform (Bruce and Hilbert, 2006) other factors include panoramic distortions (change in image shape caused by geometry of a lens movement), Earth curvature, relief displacement and non-linearities in the sweep of a sensor's Instantaneous Field of View (IFOV) (Lillesand et al., 2008).

3.5.1.1 Atmospheric Correction (FLAASH Module)

This procedure was carried out to convert the satellite-recorded digital counts to ground reflectance (Chavez, 1996). Digital sensors record electromagnetic radiation (ER) from each target viewed on the ground surface as digital numbers (DN) for each spectral band; for Landsat TM and ETM+, these are raw DN with integer values from 0-255. In some cases these raw DN values need not be converted to spectral radiance if the actual spectral radiance is not of interest (for example, in the classification of single satellite imagery). In the case of this study which involves analysing changes in spectral signatures from multitemporal data, it became necessary to convert these raw DN values to spectral radiance using parameters provided in image metadata (Duggin, 1990, Goslee, 2011). This was done to provide information on the spectral signature to compare from one

image to another and make effective use of spectral signatures that contain the list of environmental elements and their reflectance. Absolute radiometric correction of multi-temporal satellite imagery requires atmospheric correction associated with the atmospheric properties at the time of the image acquisition. The radiometric correction is necessary for the case of tracking land cover changes and vegetation indices over time (Yang and Lo, 2000). It is also important in reducing error to estimate the surface reflectance in the case of multitemporal datasets and adjust to a common radiometric scale (Song et al., 2001). Absolute atmospheric correction was also carried out in order to correct the electromagnetic radiation signals collected by satellites in the solar spectrum, which are modified by scattering and absorption by gases and aerosols while travelling through the atmosphere from the Earth's surface to the sensor (Song et al., 2001). The images for this study were processed by converting top-of-atmosphere radiance values to surface reflectance following the method proposed by Chander et al. (2009). In this study, the FLAASH routine available on the ENVI software was used to change the digital numbers (DN) values to surface reflectance. Information regarding the processing of these images was contained in the metadata (.txt) file downloaded from the USGS archive.

3.5.1.2 Geometric correction or Image registration

Once the radiometric correction or atmospheric correction process has been concluded, the data will be ready for geometric correction. Geometric corrections are performed in order to avoid geometric distortions from a distorted image, and were achieved by establishing the relationship between the image coordinate system and the geographic coordinate system using calibration data of the sensor, measured data of position and attitude, ground control points and atmospheric condition caused by certain classes of internal and external conditions. External distortions result from the attitude of the sensor or shape of the object, and internal distortion is caused by the geometry of the sensor. The one pre-processing technique that was unavoidable in this work is image registration, since the study intends to carry out temporal analysis of the data. This process is aimed at geometrical alignment of two or more images to match corresponding pixels representing the same object. The 8 year image data used in the study appears to have relatively the same geometric relationship when viewed in the GIS and remote sensing software. To ascertain the geometric relationship of the images, automatic image to image registration was performed. In order to obtain 25 tie points for further filtering, 50

points were chosen to register the images and this process was repeated on all the remaining images. All these processes were conducted to ensure that these images are geometrically aligned into the same coordinate system, so that the corresponding pixels contained the same object. Thus in this study, variability between scenes were normalised for temporal analyses.

3.6 Calculating vegetation indices

This process is an operation that re-expresses images in a more meaningful way and is computed from two or more spectral bands. In this study, the image transformation process used was the generation of vegetation indices (VIs) for the purpose of change detection or temporal analysis and mapping vegetation status at the oil polluted sites. Vegetation indices may provide quantitatively different information on changes that have occurred between two or more dates. Also, the ratio of two or more bands in this work was used to analyse single-date images for differentiating vegetation health or status at the oil polluted and non-polluted sites. The description of vegetation indices used for the study was fully discussed in Chapter Two. The vegetation indices in the study were all derived from Landsat multispectral images, characterised by wide broadband channels, so were termed broadband multispectral vegetation indices (BMVIs) and used in the remaining sections.

The computation of 20 BMVIs in the study was done, using ENVI, on the pre-processed and atmospherically corrected data to improve the quality of the images. This was done to detect the presence, condition and relative abundance of vegetation, and was also dependent on the type of sensor and involved a combination of two or more spectral bands. The product of this computation was a single index value corresponding to the biophysical parameters that have a particular meaning regarding the vegetation. The created vegetation index layers were used to extract values at the polluted (P) and Non-Polluted (NP) sites. The GPS locations of the spill points were obtained as shape files, which are compatible with both GIS and remote sensing software when they are overlaid on the BMVIs layers. The oil pipeline map and information on where spills occurred are contained in the attribute table of spill points that made it easy to identify which vegetation type may have been affected by oil pollution. In the study, land cover types such as built up areas, water bodies, and bare land were considered as non-vegetated and only spill points that fell within the vegetated areas were used for the analysis. Thus data

obtained for this study met the basic requirements because they were already in a digital format and compatible with the remotely sensed data for the study. The study had three objectives, but had some differences in technical approach and method used for the quantitative analysis. The first objective was to perform analysis and temporal evaluation of vegetation indices before and after pollution events to discriminate between vegetation conditions at the polluted and non-polluted sites. The second objective addresses factors that may influence the detectability of oil pollution in vegetated areas using BMVIs in an oil polluted environment. Fifty six (56) oil spill sites were selected based on availability of satellite data and some environmental factors. In the first part of the analysis (chapter 4), 37 sample spill sites were selected for analysis with the satellite data. The samples used for this part of analysis included volumes of oil at spill sites with <200 and >200 bbl. Thus the first part of the analysis was not focused on the volume of oil spill, but rather viewed the time period between image acquisition and spill date and spatial distance as influential factors in detection of oil polluted sites. The second part analysed the 56 sample sites with consideration of the volume of oil spill, the time gap between image acquisition and spill date and spatial distance as influential factors in detection of oil polluted sites. The volume of oil spill used in the study ranged between 2 (minimum) to 3500 (maximum) barrels (bbl) and the time period between the oil spill and image acquisition, ranging from 3 to 840 days, was also calculated for analysis (see Table 3.2). Table 3.2 shows the 56 sample points extracted for analysis in the study, with the thresholds shown containing corresponding information on volume of oil spill (bbl) and calculated time gap between the oil spill and image acquisition date (in days). The information in Table 5.1 was extracted using data from Table 3.2.

Chapter 4 : Investigating BMVIs for detection and analysis of vegetation affected by oil spill over time and space

The work presented in this chapter has been published as:

Adamu, B., Tansey, K. and Ogutu, B. (2015). "Using vegetation spectral indices to detect oil pollution in the Niger Delta." *Remote Sensing Letters* 6(2): 145-154. doi: 10.1080/2150704X.2015.1015656

4.0 Introduction

This chapter investigated and assessed vegetation indices that are capable of detecting vegetation affected by oil pollution and the features which made them suitable for this task. This was done by assessing the temporal changes in the vegetation indices (pre- and post-oil spills) at control sites (where there was no oil spill recorded) and at polluted sites (where oil spills were recorded). Vegetation conditions at the polluted (P) and non-polluted (NP) sites were also assessed to determine if their response differed.

4.1 Data analysis and method

To determine if there are significant differences between vegetation status at the P and NP sites the oil pipeline maps, spill record (1985, 1986, 1998 and 2000) and GPS locations of spill points (Table 3.0) were selected for the first part of the analysis for this objective. The images before and after each (1986, 1987, 1999, 2000 and 2003) of the oil spill events were processed and used for the temporal analysis and comparison of vegetation conditions between the polluted and non-polluted sites. Thirty-seven (37) spill sites during this period that fall along the pipeline routes were considered. 37 out of 56 samples were chosen at this stage to explore the capability of the BMVIs for detecting biophysical and chemical changes in vegetation affected by oil pollution. They were also chosen to identify factors that may influence capability of the BMVIs to detect vegetation affected by oil spills. Only images from 1986-2003 were used at this stage to select the best performing indices before applying them in Chapter 5.

Based on the oil spill database, most of the spill sites were located in different types of vegetation, thus the study selected those spill sites that fell within the mangrove swamp vegetation class as stored in the database. The selection criteria were adopted to ensure that similar vegetation types from the polluted and non-polluted sites were compared. From the sample polluted points 37 samples were selected and an equivalent number of points were also selected in areas which had not experienced any oil spills. These were

located further away from oil facilities (non-polluted) and used as control sites, similar to the method used in field work by (Getter et al., 1981). Both the polluted and non-polluted sites in Figure 4.1 are located in the mangrove swamp vegetated areas, as contained in the oil spill database/records and layers. The areas where oil spills occurred are referred to as polluted sites (P) and the areas where there were no spills were referred to as non-polluted/control sites (NP) for the remainder of this work. Figure 4.1 shows the distribution of samples from P and NP sites over the mangrove swamp vegetation type.

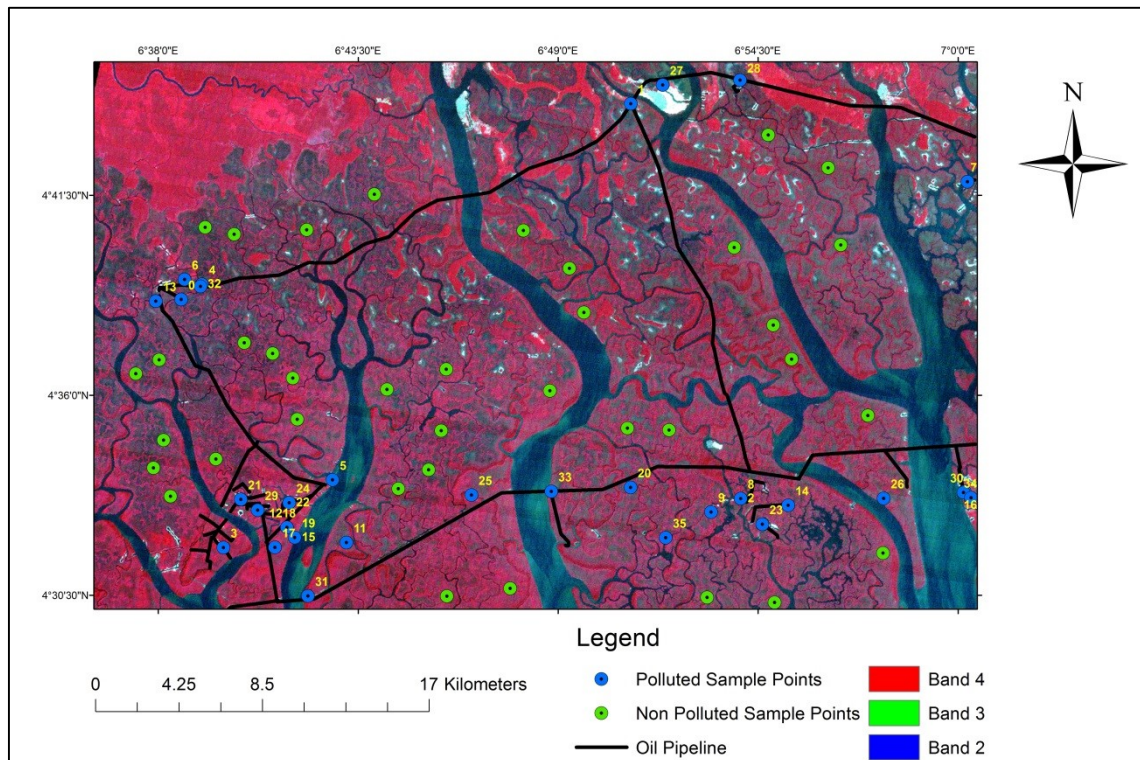


Figure 4.1: Samples from oil polluted (P) and non-polluted (NP) sites

Twenty broadband multispectral vegetation indices (BMVIs) were then extracted from these two groups of sites (i.e. polluted and non-polluted sites) within the mangrove swamp vegetated areas to ensure that the sample sites had the same vegetation properties. At each of the oil spill points, a 3 x 3 pixel window was sampled and vegetation indices (BMVIs) were extracted using ENVI software. The average/mean was calculated in order to have a representation of the surrounding pixels. Because oil spills could migrate beyond the polluted pixel, it may be expected that the impact could reach the neighbouring pixels. This technique was replicated in the selection of samples at the non-polluted sites (i.e. vegetation not affected by pollution) further away from oil facilities. Spatial and temporal values of the 20 BMVIs were computed from the two groups of sites

(P and NP sites) for pre and post oil spill dates. The period between the spill event and image date were considered as the oil spill date for the purpose of this study. Paired t-test statistics for the mean BMVIs values were also calculated to determine whether there is significant difference in vegetation conditions at the P and NP sites and before and after the oil spill. To perform the test, a null ($H_0: \mu_d = \mu_0$) and alternative ($H_0: \mu_d \neq \mu_0$) hypothesis were chosen for the purpose. This analysis was done to provide a view on possible oil pollution effects on biophysical and biochemical characteristics of vegetation before and after the spill at the P sites. A hypothesis was proposed to test (i) whether there is a significant difference between BMVIs at the P and NP sites and (ii) whether there is a significant difference in BMVIs obtained before and after the spills with the ones at the P sites. This was also chosen to determine BMVIs capabilities for detecting oil pollution impact on vegetation and identifying best and least performing indices.

4.2 Results

Vegetation condition before and after the spill both at the P and NP sites were assessed and the potential of BMVIs to detect vegetation affected by oil pollution were also evaluated. The analysis focuses on sensitivity of the BMVIs to vegetation conditions in the oil polluted environment. It is also expected that some factors may have influence the performance of vegetation indices in detection of vegetation stress from oil contamination (to be analysed in chapter 5). The variation in vegetation spectra that reflects biochemical and biophysical characteristics due to oil spill from those images were carried out to assess the vegetation changes. Twenty BMVIs were assessed to determine their capability to detect oil pollution in this study and the best and least performing indices were identified using the calculated statistics.

4.2.1 Analysis of vegetation indices at the (P) and (NP) sites

(a) Testing hypothesis for BMVIs at the P and NP sites:

H0 ($BMVIP = BMVINP$) the mean BMVIs values obtained at P sites are equal to the ones at the NP sites.

H1 ($BMVIP \neq BMVINP$) the mean BMVIs values obtained at P sites are not equal to the ones at the NP sites.

The mean calculated statistics from the total of twenty BMVIs, fifteen (ARVI2, ClGreen, ARVI2, SAVI, EVI2, G/NIR, SRI, GRNDVI, NDVI, MSAVI2, GBNDVI, MSR705, NBR, MSI and GLI) indicate significant difference between the polluted and non-polluted sites with $p < 0.05$ (Table 4.1). Based on the results the low p-values suggest that it is evident to reject null hypothesis and accept the alternative hypothesis for the fifteen BMVIs. The other remaining five VIs (i.e. EVI, G\R, G\SWIR, PPR and TNDVI) show low significant differences between the P and NP sites with high $p > 0.05$ suggest that the null hypothesis be accepted and alternative hypothesis rejected.

From these results it can be interpreted that statistical mean for BMVIs at P and NP sites differs and that these fifteen indices have shown capacity to discriminate vegetation affected by oil pollution and the unaffected vegetation. Thus the five BMVIs are considered potentially less suited for detecting vegetation affected by oil pollution compare to the fifteen BMVIs.

Table 4.1: BMVIs statistics at 95% confidence level from P and NP sites

Indices	Polluted			Non-polluted			Calculated Statistics	
	Mean	Stdev	Std Err	Mean	Stdev	Std Err	t-Test Value	P-Values
CIGreen	0.41	0.33	0.02	1.40	0.59	0.10	8.96	p < 0.05
ARVI2	0.07	0.15	0.01	0.28	0.13	0.02	6.72	p < 0.05
SAVI	0.31	0.19	0.02	0.59	0.16	0.01	6.72	p < 0.05
EVI2	0.50	0.30	0.46	0.94	0.26	0.01	6.71	p < 0.05
GRN NIR	0.14	0.12	0.05	0.31	0.11	0.02	6.35	p < 0.05
SRI	1.64	0.43	0.02	2.40	0.59	0.10	6.33	p < 0.05
GRNDVI	0.15	0.12	1.13	0.03	0.12	0.02	6.27	p < 0.05
NDVI	0.22	0.13	0.07	0.39	0.11	0.02	6.25	p < 0.05
MSAVI2	0.34	0.19	0.05	0.56	0.12	0.01	5.83	p < 0.05
GBNDVI	0.21	0.12	0.02	0.02	0.15	0.02	5.83	p < 0.05
MSR705	0.10	0.13	0.03	0.30	0.17	0.03	5.53	p < 0.05
NIR RED	1.00	0.10	0.01	1.00	0.00	0.01	4.83	p < 0.05
NBR	0.47	0.24	0.02	0.65	0.05	0.01	4.55	p < 0.05
MSI	0.59	0.19	0.03	0.45	0.09	0.01	4.17	p < 0.05
GLI	3.30	6.86	0.01	0.03	0.03	0.01	2.90	p < 0.05
EVI	1.94	2.8	0.01	2.31	1.62	0.27	0.73	p > 0.05
GRN RED	0.07	0.04	0.05	0.09	0.05	0.01	1.99	p > 0.05
GRN	0.33	0.28	0.04	0.41	0.11	0.02	1.59	p > 0.05
SWIR								
PPR	0.05	0.04	0.02	0.01	0.08	0.01	2.25	p > 0.05
TNDVI	0.46	0.14	0.04	0.44	0.06	0.01	1.06	p > 0.05

Note: t-critical value = 1.99 Degree of Freedom = 36.00 Probability Error (α) = 0.05

Table 4.1 showing the best performing vegetation indices computed from P and NP sites. The calculated statistics with $p < 0.05$ indicates significant difference between the two sites and $p > 0.05$ not significant.

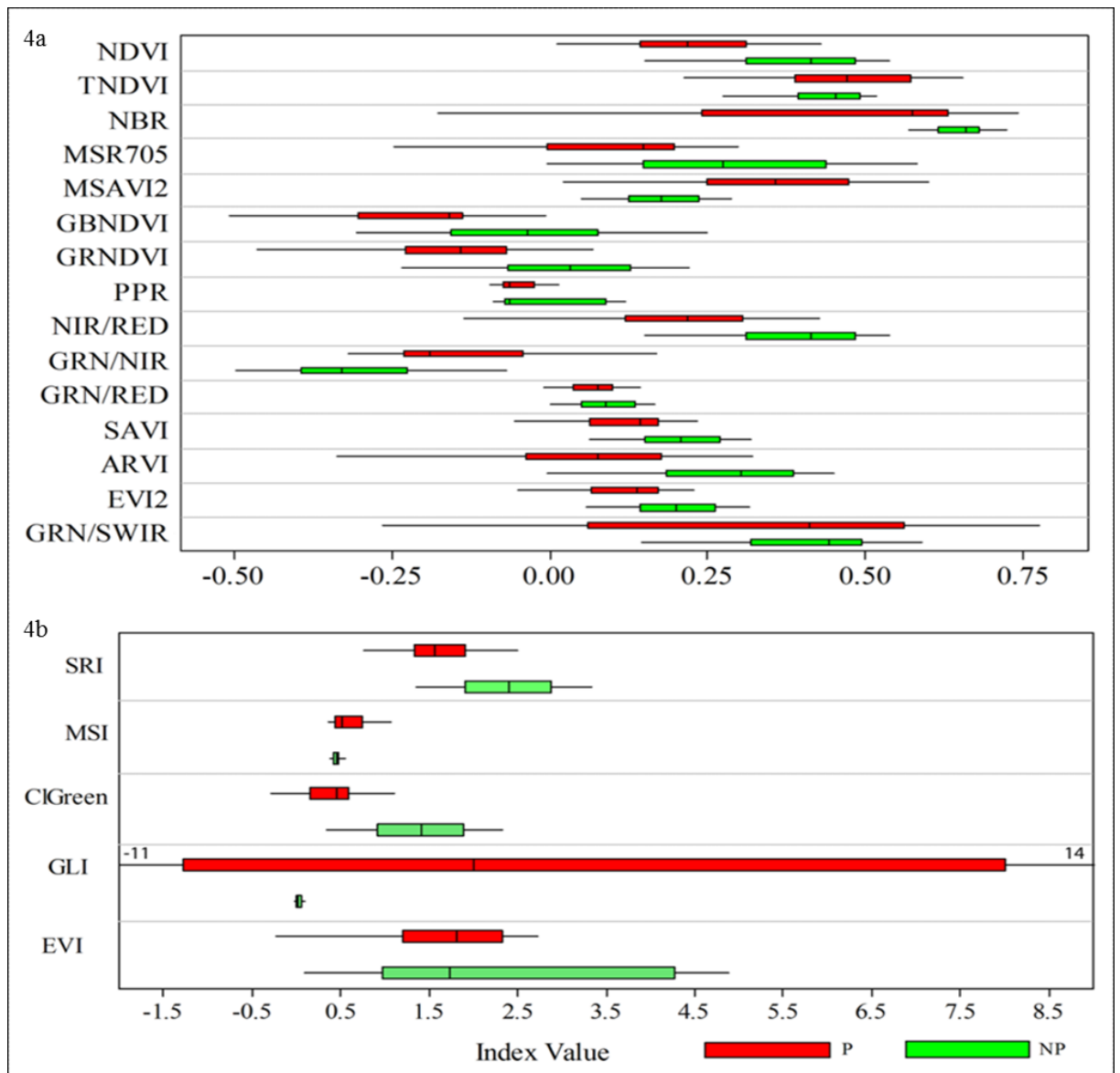


Figure 4.2 : Box plots show the minimum, 25% quartile, median, 75% quartiles and maximum values respectively of BMVIs from P and NP sites. The red color stands for P sites and green for NP sites. Note that the minimum and maximum for the GLI value is -11 and 14 respectively.

4.2.2 Analysis vegetation indices before (*Ppre*), spill date (*Spill Date*) and after (*Ppost*) at the P and NP sites over time

(i) At the P sites

H0 ($BMVIP_{pre} \& P_{post} = BMVIS_{spill\ Date}$) the mean BMVIs values obtained *Ppre* and *Ppost* oil pollution are not different from the ones at the Spill Date.

H1 ($BMVIP_{pre} \& P_{post} \neq BMVIS_{spill\ Date}$) the mean BMVIs values obtained *Ppre* and *Ppost* oil pollution are different from the ones at the Spill Date.

Twelve of the twenty BMVIs (NDVI, SAVI, EVI2, G/NIR, G/SWIR, NIR/R, ARVI2, EVI, MSR705, TNDVI, GLI and PPR) showed significant difference in vegetation condition before and after ($p < 0.05$) (Table 4.2) and 8 less significant ($p > 0.05$). The temporal analysis of the spill sites shows indicated significant difference Pre and Post spill observation. Since the results show that twelve BMVIs before and after oil spill date at the P sites indicated low p-values it suggests that there is evidence to reject the null and accept the alternative hypothesis.

(ii) At the NP sites

H0 ($BMVIP_{pre} \& P_{post} = BMVIS_{spill\ Date}$) the mean BMVIs values obtained *Ppre* and *Ppost* oil pollution are not different from the ones at the Spill Date.

H1 ($BMVIP_{pre} \& P_{post} \neq BMVIS_{spill\ Date}$) the mean BMVIs values obtained *Ppre* and *Ppost* oil pollution are different from the ones at the Spill Date.

At these control (NP) sites (Table 4.3) eleven of the twenty indices (NDVI, SAVI, EVI2, GBNDVI, NBR, G/NIR, G/SWIR, MSAVI2, G/R, ARVI2 and SRI) did not indicate significant change in the index values at Pre and Post spill observation with $p > 0.05$. The results here the show that eleven BMVIs indicated high p which suggests that null hypothesis can be accepted and reject the alternative hypothesis with low p. The results here could be interpreted as statistical means of eleven BMVIs from these NP sites shows that vegetation status remains relatively the same over time compare to ones obtained at the P sites.

Table 4.2: Twelve (12) BMVIs temporal statistics at 95% confidence level from P sites

BMVIs	Ppre			Spill Date			Ppost			p-values	
	Mean	Stdev	Std Error	Mean	Stdev	Std Error	Mean	Stdev	Std Error	Ppre	Ppost
NDVI	0.28	0.18	0.03	0.22	0.12	0.02	0.28	0.17	0.03	$p < 0.05$	$p > 0.05$
SAVI	0.25	0.14	0.02	0.13	0.09	0.01	0.25	0.12	0.02	$p < 0.05$	$p < 0.05$
EVI2	0.41	0.24	0.04	0.13	0.12	0.02	0.4	0.21	0.03	$p < 0.05$	$p < 0.05$
G/NIR	0.71	0.2	0.03	0.14	0.12	0.02	0.73	0.20	0.03	$p < 0.05$	$p < 0.05$
G/SWIR	1.27	0.54	0.09	0.45	0.24	0.04	1.40	0.73	0.12	$p < 0.05$	$p < 0.05$
NIR/R	1.77	0.52	0.09	0.21	0.13	0.02	1.73	0.42	0.07	$p < 0.05$	$p < 0.05$
ARVI2	0.25	0.14	0.02	0.07	0.15	0.02	0.25	0.12	0.02	$p < 0.05$	$p < 0.05$
EVI	1.96	4.07	0.67	1.83	2.82	0.46	0.94	0.66	0.11	$p < 0.05$	$p < 0.05$
MSR705	0.44	0.27	0.04	0.1	0.13	0.02	0.43	0.23	0.04	$p < 0.05$	$p < 0.05$
TNDVI	0.86	0.08	0.01	0.47	0.14	0.02	0.86	0.07	0.01	$p < 0.05$	$p < 0.05$
GLI	5.86	5.50	0.90	3.30	6.86	1.13	1.43	6.69	1.10	$p < 0.05$	$p < 0.05$
PPR	0.11	0.04	0.01	0.05	0.04	0.01	0.15	0.04	0.01	$p < 0.05$	$p < 0.05$

Table 4.3: BMVIs temporal statistics at 0.95confidence level from control or NP sites

BMVIs	Ppre			Spill Date			Ppost			p-values	
	Mean	Stdev	Std Error	Mean	Stdev	Std Error	Ppost	Stdev	Std Error	Ppre	Ppost
NDVI	0.28	0.61	0.10	0.4	0.10	0.02	0.37	0.07	0.01	p > 0.05	p > 0.05
SAVI	0.56	0.12	0.02	0.59	0.16	0.03	0.55	0.11	0.02	p > 0.05	p > 0.05
EVI2	0.90	0.19	0.03	0.94	0.26	0.04	0.88	0.17	0.03	<i>p > 0.05</i>	p > 0.05
GRNDVI	0.10	0.08	0.01	0.03	0.12	0.02	0.01	0.08	0.01	p > 0.05	p > 0.05
NBR	0.62	0.09	0.01	0.65	0.05	0.01	0.61	0.07	0.01	p > 0.05	p > 0.05
G/NIR	0.29	0.07	0.01	0.31	0.11	0.02	0.28	0.07	0.01	p > 0.05	p > 0.05
G/SWIR	0.40	0.12	0.02	0.41	0.11	0.02	0.39	0.11	0.02	p > 0.05	p > 0.05
MSAVI2	0.54	0.09	0.01	0.56	0.12	0.02	0.53	0.08	0.01	p > 0.05	p > 0.05
G/RED	0.10	0.03	0.01	0.09	0.05	0.01	0.10	0.02	0.01	p > 0.05	p > 0.05
ARVI2	0.26	0.09	0.02	0.28	0.13	0.02	0.25	0.08	0.01	p > 0.05	p > 0.05
SRI	2.24	0.37	0.06	2.40	0.59	0.10	2.20	0.34	0.06	p > 0.05	p > 0.05

Note: t-critical value = 1.99 Degree of Freedom = 36.00 Probability Error (α) = 0.05

4.3 Discussion

4.3.1 Spatial analysis of vegetation indices at the P and NP sites

Physiological changes in plants can be related to oil pollution and other environmental stress, which may be responsible for their spectral behaviour. Fifteen of the twenty indices shown in Table 4.1 (CIGreen, ARVI2, SAVI, EVI2, G/NIR, SRI, GRNDVI, NDVI, MSAVI2, GBNDVI, MSR705, NIR/R, NBR, MSI and GLI) indicated significant difference between the vegetation conditions at the P and NP sites when a statistical t-test was computed. The box plot in Figures 4.1 illustrates differences between BMVIs at the P and NP sites. Therefore, these fifteen indices can be said to have the potential of being used to detect vegetation affected by oil pollution. The common feature in these indices is that they include the red (R) and near infrared (NIR) bands in their calculation. The sensitivity shown by these indices to changes in vegetation condition in P areas is likely to be due to the R band being sensitive to chlorophyll in the visible spectrum and NIR being optimal for characterising vegetation varieties and conditions (Ceccato et al., 2001). Thus both the R and NIR band may be capable of indicating changes in chlorophyll content related to changes in vegetation health as NIR decrease in reflectance at 800nm and 1300nm due to oil pollution (Zhu et al., 2013). Evidence of stress in vegetation and changes in plants pigments are commonly noticed in the visual and NIR portions (Rosso et al., 2005). However, it is worth noting that two indices which also use the R and the NIR wavelengths (i.e. the EVI and TNDVI) did not show any significant difference between the polluted and non-polluted sites ($p > 0.05$). The reason for this could be due to the fact that these indices correct explicitly for influence of soil background (Liu and Huete, 1995). This may be assumed to be the reason why it is less efficient in detecting vegetation affected by pollution in such a swampy environments. An interesting observation from this study is that vegetation indices which included wavelengths that are rarely used such as the G and B bands also seemed to perform well in detecting the differences in vegetation condition in P and NP sites. For example, the GBNDVI which is a function of the blue (B) band and NIR showed significant difference between vegetation condition in the P and NP areas. Similarly, BMVIs with green bands (e.g. CIGreen, G/NIR and GRNDVI), showed significant difference between vegetation in P and NP sites.

The results from those vegetation indices calculated using all the three visible bands (i.e. R, G and B bands) was mixed. These indices include the GLI, G/R and PPR. While the GLI detected significant difference between the vegetation condition in the P and NP sites, the G/R and the PPR did not detect this difference. The results of indices that combined SWIR with NIR band performed well because the NIR reflectance can be influenced by water stress due to changes in mesophyll structure (Rosso et al., 2005). The reduction in water content is also responsible for changes in SWIR reflectance (Bowman, 1989). For example, the NBR - which is designed to discriminate burnt areas (López and Caselles 1991) - was capable of discriminating between vegetation in P and NP sites. However, the indices which combined SWIR band with visible band (G) band (e.g. the G/SWIR) did not perform well in detecting the difference between vegetation conditions in two sites. Despite the capabilities of ClGreen and G/SWIR in distinguishing between P and NP sites, they failed to show significant difference in Ppre and Ppost spill with spill event date. In the case of EVI, PPR and TNDVI showed significant differences in Ppre and Ppost spill with poor capacity in differentiating between P and NP sites. Interestingly one index G/R failed in both the analysis to show any capability of differentiating neither P from NP nor Ppre and Ppost spill events.

4.3.2 Temporal analysis of vegetation indices at the P and NP sites

In sections 4.2.1 20 BMVIs were used to discriminate between vegetation affected by oil pollution (P) from unaffected vegetation (NP). This section used the same BMVIs to assess the difference in vegetation index values before and after the pollution. The results show that vegetation at the sample P sites before and after the pollution appears to be unaffected. In Table 4.2, show that twelve BMVIs indicated significant differences between Ppre and Ppost spill events which could be due to their sensitivity in the polluted environment. The twelve BMVIs values at the polluted sites before and after the spill are relatively higher compared to values obtained during the spill event date. However, at the non-polluted control sites, Table 4.3 show that eleven BMVIs values remain relatively the same before and after the spill date. Five BMVIs (NDVI, SAVI, ARVI2, G/NIR and G/SWIR) indicated significant difference before and after the spill at the P sites, whilst showing no significant difference over a similar time period in the control site.

The common features in these five BMVIs which are the most consistent and other similar ones are that they include the red (R) and near infrared (NIR) bands in their calculation. The sensitivity shown by these indices to changes in vegetation condition in polluted areas, before and after the spill, is likely to be due to the R band being sensitive to chlorophyll in the visible spectrum and NIR being optimal for characterising vegetation varieties and conditions. Thus both the R and NIR band may be capable of indicating changes in chlorophyll content related to changes in vegetation health due to oil pollution. However, a small number of indices which also use the R and the NIR wavelengths did not show any significant difference carried study area with ($p > 0.05$). The reason for this could be due to the fact that these indices correct explicitly for influence of soil background (Liu and Huete, 1995). This may be assumed to be a reason why it is less efficient in detecting vegetation affected by pollution in such a swampy environments. An interesting observation from this study is that vegetation indices which included wavelengths that are rarely used - such as the G band - also seemed to perform well in detecting the temporal vegetation condition at both the P and NP (control) sites. For example the BMVIs with green bands (e.g. G/NIR, GRNDVI and G/SWIR), showed that vegetation condition before and after spill events at the polluted sites are significantly different and relatively the same at the non-polluted control sites. It has also been shown that indices using ratios of reflectance from NIR and green regions in both the narrow and broad wavelengths correlated well with chlorophyll (Blackburn, 1999).

Some of these findings support assertions made by other studies such as Yoder and Waring (1994) which showed that the green band is well correlated to vegetation parameters, Leaf Area Index for example, and could be used as a substitute to bands such as the red band. Gitelson et al. (1996), showed that the G band was more sensitive to chlorophyll than the R channel. The results from vegetation indices calculated using all the mixed three visible bands (i.e. R, G and B bands) which includes the GLI and PPR indicated significant difference in vegetation condition before and after the pollution at the polluted sites. But they (indices) performed poorly by indicating significant difference in temporal changes in vegetation conditions at the non-polluted control sites. The results of indices that combined SWIR with NIR band performed well. For example the NBR which is designed to discriminate burnt areas. López and Caselles (1991) was capable of showing vegetation conditions before and after the spill are relatively the same at the non-polluted sites. However, the indices which combined SWIR band with visible band (G)

band (e.g. the G/SWIR) performed well in detecting the difference before and after pollution at the polluted sites. However, the index did not indicate any temporal changes in vegetation conditions at the non-polluted sites (i.e. vegetation condition before and after the pollution at these sites remain relative the same).

4.4 Summary

The twenty investigated BMVIs showed that the best performing indices in detecting vegetation affected by oil pollution were those derived using a combination of reflectance from the visible and NIR wavelengths. Fifteen BMVIs were capable of discriminating between vegetation at P and NP site. Twelve BMVIs indicated significant temporal changes in vegetation at the P sites, but did not indicated significant difference in spectral changes in vegetation at the NP sites. Five BMVIs (NDVI, SAVI, ARVI2, G/NIR and G/SWIR) appear to be most consistent in indicating significant differences in BMVIs before and after pollution and between P and NP sites, and were chosen for further analysis in chapter five. As mentioned at the beginning of this chapter, factors such as volume of oil, time gap between the oil spill and imagery date, and variation in spatial distance may assume to be influential in the performance of BMVIs in detecting impact of oil pollution vegetation. Thus, in chapter five the work focuses on determining how these factors influence the detectability of oil pollution using the five BMVIs.

Chapter 5 : Analysis of factors influencing detectability of oil pollution using BMVIs

The work presented in this chapter has been published as:

Adamu, B., Tansey, K. and Ogutu, B., (2016). “An investigation into the factors influencing the detectability of oil spills using spectral indices in an oil-polluted environment”. *International Journal of Remote Sensing*, 37(10), pp.2166-2185. DOI: 10.1080/01431161.2016.1176271

5.0 Introduction

This chapter focuses on examining factors influencing the detectability of oil pollution using BMVIs, including the volume of oil spilt, the time gap between oil spill and image acquired date and spatial distance. The first step was to determine the relationship between the volume of oil spill and the BMVIs in order to set a threshold using regression analysis. In chapter 4 the capability of BMVIs to detect changes in vegetation spectral reflectance relating to oil pollution was carried out. Five BMVIs (NDVI, SAVI, ARVI2, G/NIR and G/SWIR) show sensitivity in discriminating vegetation affected by oil pollution and the unaffected ones. They show potentials in detection of vegetation affected by oil pollution before and after oil spills as well as at the control sites.

5.1 Method

The second part analysed fifty-six (56) sample sites with consideration of volume of oil spill, time gap between image acquisition and spill date and spatial distance as influential factors in detection of oil polluted sites. Landsat TM and ETM image data used for the second part of this work were acquired in 1986, 1987, 1999, 2000, 2003, 2004 and 2007. The oil spill events for the spill sites were obtained in 1985, 1986, 1998, 1999, 2000, 2004, 2006 and 2007. From the database, the range of spill size that occurred in the study is from the minimum of 5 to maximum of 3500 barrels (bbl).

5.1.1 Volume of oil spill

From the database, the range of volume of oil spill that occurred in the study is from a minimum of 3 to maximum of 3500 bbl and the number of days computed between the oil spill event and image acquisition date range from 2 to 844 days. The relationship between oil spill volume and the level of impact on the vegetation health has been demonstrated in (Mackay and Matsugu, 1973, Mackay and Mohtadi, 1975) in Canada. Hypothetically, a small volume of oil spill over land may occupy little space in a pixel of 30 m resolution. In contrast, the large volume of oil spill could occupy a large space in a

30 m pixel over land. Thus, it is expected smaller volumes of oil spill may have little impact on vegetation, thereby limiting the detectability of these effects using a 30 m spatial resolution sensor such as Landsat. Factors such as land cover types (where the spill occurred), volume of oil spill and time of image acquisition were taken into consideration in this study. To determine if the volume of oil spill and number of days between oil spill events and image acquisition date can have influence on the detection of oil spill over vegetated areas using NDVI and NDWI, a number of assumptions were made. We assumed that index (NDVI and NDWI) values could drop as the volume of oil spill increases and they may remain relatively unchanged or go up at the affected sites as the volume oil spill decreases. Similarly, it is also assumed that as number of days increases between the oil spill event and image date there are high chances of vegetation recovery and that NDVI and NDWI values will go up. Statistical regression was used to determine which volume of oil spill could lead to detectable impacts on vegetation through the use of two indices (NDVI and NDWI). This was done by plotting all the 56 oil spill data at the first stage of analysis to see how a change in volume of oil spill affects the two indices. The second stage of analysis involved determining the minimum amount of oils spill that can effectively fill a 30m by 30m pixel and hence would lead to detectable change in vegetation condition in a single Landsat pixel.

Environmental conditions e.g. water-saturated soil increases the surface pool of oil spill and limits penetration of oil into the ground (Grimaz et al., 2008). When oil spill occurs on a surface, the force balance between the downward pull of gravity caused by density and internal tension of the liquid may allow the oil pool to form a final spill size. A pool is considered to be a large drop of oil with defined amount of oil held to a certain penetration depth in a surface area (Grimaz et al., 2008, Simmons and Keller, 2003). It also depends on the property of the oil (in the case for this study, heavy oils are used as no specific oil type is considered) the spilled oil will eventually stand a certain height or depth above the surface (Simmons et al., 2004). Simmons et al., (2004) proposed that the volume of oil spilled in an area can be calculated using the following equation:

$$V = A \delta \varphi + A h \quad \text{Eq. 1}$$

Where V is the volume of the oil spill, A is the area under consideration, h is the height of liquid standing above the surface, δ is the liquid that has penetrated below a certain depth, and φ is the substrate porosity. To calculate height they used the following equation:

$$(1 - \cos(\theta)) \times \sigma = \rho \times g \times h^2 \quad \text{Eq. 2}$$

where h = spill height (cm)

ρ = density (gm/ml)

g = gravity acceleration

σ = surface tension (dyne/cm)

θ = contact angle

Based on various scenarios (e.g. contact angles, gravity acceleration, surface tension) and types of spills (e.g. liquid density and adhesion properties), Simmons et al., (2004) calculated that the height of spills on concrete and asphalt to range from 0.01- 0.5cm. However, in the present study the oils spills occurred in a natural setting where some oil is expected to percolate into the soil. Furthermore, the oil type in the present study is heavy oil, which would accumulate at greater heights due to its high surface tension, density and viscosity. In a subsequent study, Simmons and Keller (2005) showed that that the front heading height of corn syrup (which may be similar to heavy oil in the present study) ranged from 1.65 – 5 cm in sandy soil. Therefore, we assumed in the present study that the heavy oil heading height would be around 0.04 m (which includes the percolated portion). The following calculation was used to predict expected volume of oil spill to fill a 30 by 30m pixel:

$$1\text{m}^3 = 1000 \text{ litres}$$

$$1 \text{ barrel of oil} = 160 \text{ litres}$$

$$\text{Volume of oil spill (V}_{spill}) = (l \times b) \times (h \times 1000) / 160 \text{ litres}$$

$$V_{spill} = A \times (h \times 1000) / 160 \quad \text{Eq.1}$$

where:

$$V_{spill} = \text{Volume of oil spill expected to fill a pixel area (m}^2\text{)?}$$

$$A \text{ (Pixel area): length} = 30\text{m, breadth} = 30\text{m [l} \times \text{b]}$$

$$h = \text{Assumed height of oil spill} = 0.04\text{m}$$

Therefore:

$$V_{spill} \text{ (bbl)} = (30 \times 30) \times (0.04 \times 1000) / 160 \text{ litres} = 225 \text{ bbl.} \quad \text{Eq.2}$$

Consequently, in further analysis, a ‘minimum value’ of approximately 200 barrels was used to assess where impacts of oil pollution on vegetation can be detected.

5.1.2 Spatial distance

This part of the analysis was to determine if variation in spatial distance has any influence on the vegetation indices; for example, it is expected that polluted point (pixel) may be more likely to be affected compared to pixels further away. In this analysis the most likely impacted pixel by the oil spill is referred to as “First pixel” denoted by (P1), the immediate pixel “Second pixel” (P2) and third pixel further away from the polluted “Third pixel” (P3). The vegetation indices were extracted along the oil spill possible-flow direction Figure 5.1. The oil spill flow direction is important in assessing how far the neighbouring pixels or surrounding vegetation may have been affected by the oil spill. There is an assumption that oil spill over land may tend to flow from the point of source, therefore determining the flow direction is essential for example if there is a variation in topography or terrain. The flow direction model of oil spill for this study area where the terrain is relatively flat is adopted from (Garbrechta and Martzb, 1997), where DEM elevations of a flat surface was modified with one away from higher terrain and the other towards the lower terrain. Even though, this model was used to produce drainage patterns over flat surfaces with consistent topographical properties this study will attempt to apply it in the area oil spill over vegetated sites.

A 30 m SRTM was used for the calculation of 8 Flow direction model to determine the likely flow direction of the oil spill and how far the oil might have migrated. From Figure 5.1 the flow direction model can be used to determine the potential flow of the spill from the cell value. For example, if the oil sample point occurred on a cell with a value of 128, meaning the largest compared to surrounding cells (pixels), it suggests the likely and potential cell whose flow passes through the cell. The potential flow direction in Figure 5.1 will pass through a cell with smaller value of 2 and then to the smallest value (1) (down slope). Thus values of the vegetation indices were extracted based on the possible flow direction from the source of pollution as illustrated in Figure 5.1, even though the flat terrain nature of the study area could make the application of this model less effective.

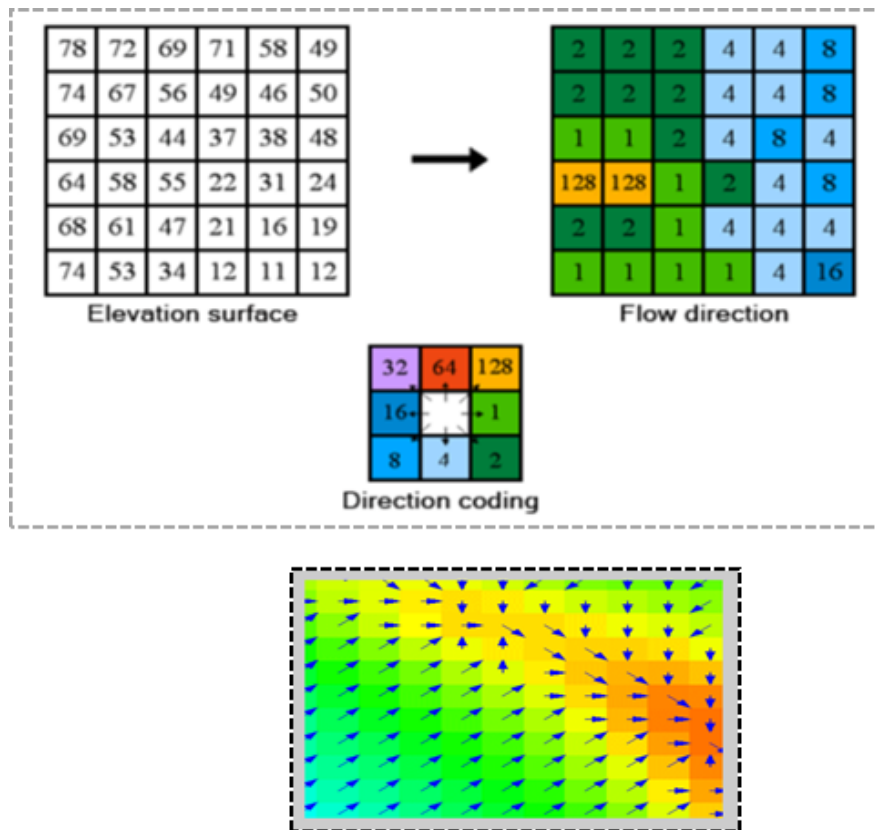


Figure 5.1: Illustrates coding of flow direction

To determine the steepest direction of descent from each cell the following equation can be used to compute the flow direction.

$$\text{Maximum Drop} = \text{Change in Z-Value} / \text{Distance} * 100$$

Flow grid can be generated using the equation above which could be used to determine the flow direction. Here the number of cells contributes to each cell in grid to determine which cell whose flow path passes through the cell. A cell with potential flow network is assigned with larger value and cells where overland flow dominates will have low value.

5.1.3 Time gap between spill and image acquisition date

Time between the oil spill and image acquisition date were also considered as one of the factors that could influence the detectability of oil polluted sites over vegetated areas using the BMVIs. In theory it can be assumed that the wider the time gap between the oil spill and image acquisition may influence the detection of oil pollution over vegetated sites using BMVIs. For example, it is possible that during these wider intervals between the two events (oil spill and image date), there would be a higher chance of climatic conditions favouring the recovery of the vegetation at the P sites. Also it is possible oil

spilled concentration may reduce at these P sites thereby providing a likely chance for vegetation recovery through natural attenuation over time (Astm, 2003, Wiedemeier, 1999, Weston and Gibson Jr, 1993). The difference in time gap (days) between the oil spill and image date were calculated for each spill sites. Regression statistics between the number of days and the vegetation indices extracted at each polluted sites were carried out.

5.2 Results

Table 5.1 indicates the 5 best-performing vegetation indices (NDVI, SAVI, ARVI2, G/NIR and G/SWIR) identified in Chapter 4 against volume of oil spilt. The vegetation indices are plotted against volume of oil spill at sample sites with threshold at 1-3500 bbl, 1- 201 bbl and 201-3500 bbl. This was done in order to choose which threshold would have significant relationship between the two variables (volume of oil spill and the BMVIs).

5.2.1 Influence of volume of oil spill on the selected BMVIs from 56 sample sites

The five BMVIs that indicated capability to detect impact of oil pollution on vegetation in Chapter 4 were selected to determine if they relate with the volume of oil spill at these thresholds in Table 5.2.

Table 5.1: The mean of BMVIs and volume of oil from 56 spill sites

Sample Point	Volume (bbl)	Oil Spill Date	NDVI	SAVI	ARVI2	G/NIR	G/SWI R	Sample Point	Volume (bbl)	Oil Spill Date	NDVI	SAVI	ARVI2	G/NIR	G/SWIR
SP1	2	19/12/2006	0.18	0.28	0.04	0.16	0.08	SP29	200	09/07/2000	0.33	0.50	0.21	0.23	0.02
SP2	5	12/09/2000	0.22	0.34	0.08	0.25	0.32	SP30	221	22.07.2004	0.11	0.16	0.05	0.07	0.17
SP3	9	21/08/2000	0.24	0.36	0.10	0.20	0.12	SP31	232	26.04.1986	0.22	0.33	0.08	0.20	0.04
SP4	10	10/09/1999	0.06	0.09	0.11	0.06	0.48	SP32	269	27.05.1986	0.04	0.06	0.23	0.14	0.54
SP5	10	22/01/2006	0.06	0.09	0.11	0.04	0.15	SP33	318	22.10.2004	0.14	0.21	0.01	0.12	0.12
SP6	20	04/01/1985	0.32	0.48	0.20	0.25	0.20	SP34	346	26.08.2002	0.32	0.47	0.19	0.25	0.08
SP7	27	04/01/1985	0.42	0.62	0.31	0.32	0.13	SP35	352	18/09/2006	0.18	0.28	0.04	0.15	0.07
SP8	28	17/11/1999	0.19	0.29	0.04	0.05	0.20	SP36	358	20.09.1998	0.22	0.32	0.07	0.16	0.01
SP9	32	19/08/2004	0.34	0.51	0.22	0.30	0.35	SP37	400	20/08/1998	0.42	0.63	0.31	0.32	0.08
SP10	39	21/09/1999	0.20	0.29	0.05	0.18	0.10	SP38	468	01/11/2000	0.45	0.67	0.34	0.33	0.10
SP11	40	04/12/2006	0.11	0.17	0.05	0.12	0.04	SP39	500	06.06.1999	0.35	0.52	0.23	0.26	0.10
SP12	50	15/11/1999	0.09	0.14	0.29	0.15	0.46	SP40	500	15/02/2003	0.37	0.56	0.25	0.28	0.06
SP13	54	14/11/2000	0.17	0.26	0.02	0.10	0.33	SP41	507	19/09/2000	0.37	0.55	0.25	0.26	0.13
SP14	62	08/07/1999	0.32	0.48	0.19	0.20	0.15	SP42	558	21.12.1998	0.27	0.41	0.14	0.25	0.27
SP15	63	04/11/1986	0.27	0.4	0.13	0.20	0.17	SP43	625	15/12/2000	0.13	0.20	0.03	0.03	0.42
SP16	63	02/08/2004	0.15	0.23	0.10	0.12	0.14	SP44	785	21/02/2000	0.23	0.34	0.09	0.20	0.06
SP17	75	13/03/1986	0.51	0.77	0.42	0.39	0.04	SP45	807	23/07/1998	0.20	0.29	0.05	0.19	0.07
SP18	75	03/10/2000	0.31	0.46	0.18	0.25	0.03	SP46	813	09.01.1999	0.25	0.37	0.11	0.20	0.06
SP19	96	12/05/1986	0.32	0.48	0.19	0.23	0.14	SP47	1000	16.01.2007	0.20	0.29	0.05	0.20	0.13
SP20	97	18/06/1986	0.45	0.68	0.35	0.36	0.04	SP48	1042	10.01/1999	0.27	0.40	0.13	0.21	0.09
SP21	117	30/10/2000	0.03	0.04	0.15	0.06	0.42	SP49	1069	14.08.2006	0.39	0.58	0.27	0.33	0.22
SP22	126	11/05/2006	0.06	0.08	0.11	0.03	0.19	SP50	1505	02.12.2002	0.20	0.29	0.05	0.13	0.10
SP23	128	16/02/1986	0.35	0.52	0.23	0.26	0.10	SP51	1720	26.08.1998	0.15	0.23	0.10	0.19	0.30
SP24	150	13/01/2003	0.17	0.26	0.02	0.10	0.33	SP52	1734	09.07.1986	0.02	0.03	0.16	0.03	0.28
SP25	150	04/08/2006	0.09	0.13	0.08	0.06	0.13	SP53	2573	07.09.2006	0.13	0.19	0.03	0.01	0.35
SP26	155	11/11/2006	0.17	0.25	0.02	0.15	0.04	SP54	2578	29.04.1986	0.29	0.43	0.16	0.18	0.15
SP27	180	29/11/2006	0.12	0.18	0.04	0.13	0.04	SP55	2761	28.12.1985	0.25	0.38	0.12	0.22	0.06
SP28	184	24/08/1999	0.37	0.55	0.25	0.30	0.01	SP56	3500	24.06.2002	0.23	0.35	0.09	0.17	0.00

Table 5.2: Coefficient of determination (R^2) and between BMVIs response and volume of oil spill (statistics at 0.95 confidence level with p at 0.05).

Volume of Oil (bbl)	NDVI		SAVI		G/NIR		ARVI2		G/SWIR	
	R^2	p-value	R^2	p-value	R^2	p-value	R^2	p-value	R^2	p-value
1 - 3500	0.009	n.s	0.02	n.s	0.001	n.s	0.01	n.s	0.001	n.s
1 - 200	0.008	n.s	0.008	n.s	0.001	n.s	0.008	n.s	0.1	0.001***
201 - 3500	0.230	0.002***	0.093	n.s	0.224	0.002***	0.231	0.001***	0.002	n.s

*** p -value < 0.0001, ** p -value < 0.005, ** p -value < 0.05, * p -value < 0.01, ^{ns} p -value \geq 0.05

***Highly significant, **Highly significant, **Very significant, *Significant, ^{ns}Not significant

As shown in the results within Table 5.2, five BMVIs (NDVI, SAVI, G/NIR, ARVI2 and G/SWIR) did not show any significant relationship between the BMVIs and volume of oil spill 1 – 3500 bbl from the 56 sample polluted sites. The first part of the analysis is to establish relationship between the volume of oil spill and the BMVIs from the 56 sites without considering quantity of oil spill and image date (time) at this stage. At the threshold 1-200 bbl four BMVIs (NDVI, SAVI, G/NIR and ARVI2) show no significant (n.s.) relationship with the volume of oil spill (Table 5.2 and Figure 5.2). The only threshold that indicated a weak relationship between the BMVIs (NDVI, SAVI, G/NIR and ARVI2) and the volume of oil spill is at threshold 201 – 3500 bbl compared to (<200 bbl and 1 - 3500 bbl). The relationship between the BMVIs from oil spill sites with volume of oil at threshold < 200 bbl appear not significant. These results may suggest that the volume of oil spilt is below that which the sensor (with 30m resolution) may resolve, and can be related to detection of changes in vegetation index values as a result of oil pollution.

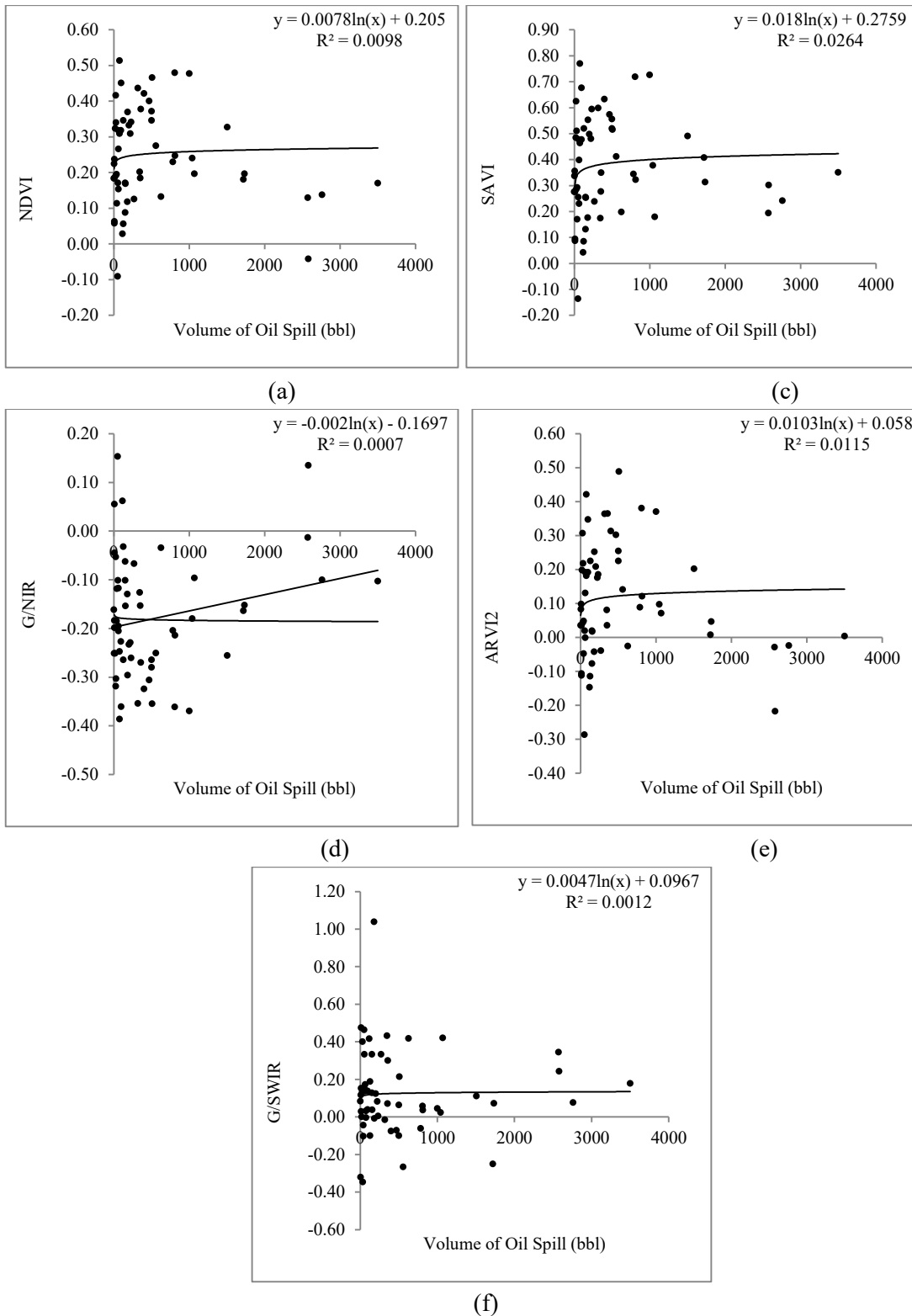


Figure 5.2: Regression between BMVIs response and volume of oil spill between 1 – 3500 bbl

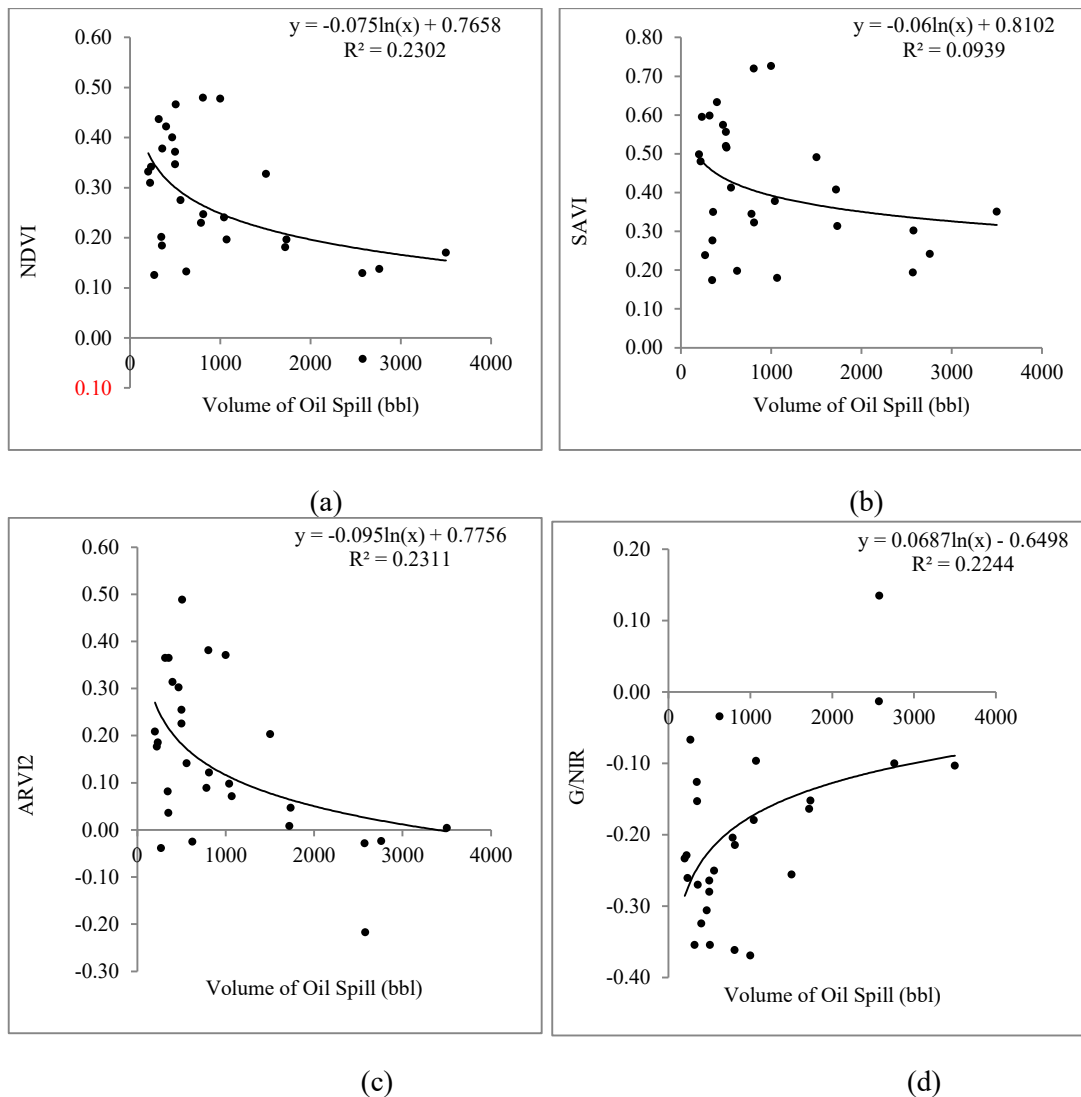


Figure 5.3: Regression between BMVIs response and volume of oil spill threshold between 201 – 3500 bbl

At this threshold spill sites where the volume of oil > 200 bbl indicated a significant relationship between NDVI ($R^2 = 0.2$), SAVI ($R^2 = 0.1$), G/NIR ($R^2 = 0.2$) and ARVI2 ($R^2 = 0.2$) with volume of oil spill with a *p-value* 0.05 in Table 5.2 and Figure 5.3. This could also suggest that there is a possibility that increase in the volume of oil spill may be related to changes in biophysical and biochemical changes of the vegetation. G/SWIR indicated a very weak relationship with volume of spill threshold < 200 bbl $p < 0.05$ and no significant relationship at threshold > 200 bbl $p > 0.05$.

From these analyses there are indications that volume of oil spill < 200 bbl may be difficult to detect using the BMVIs as there is no any significant relationship found. It may also be argued that the scale of impact may be limited by the volume size and the choice of

image/sensor resolution could be influential in this case. Thus, the study focuses on the analysing the volume of oil spill > 200 bbl which have indicated weak but significant relationship with the BMVIs. The relationship indicated between the BMVIs and volume of spill from the sample sites threshold between 201 -3500 bbl were further used for analysing time gap between the oil spill and imagery date Table 5.4 and Figure 5.5 and to determine the oil flow direction Figure 4.

5.2.2 Spatial analysis of oil spill on the BMVIs

In Figure 5.2 the aim is to establish a relationship between the oil spill direction and vegetation indices. A 30m SRTM was used for calculation 8 Flow direction model to determine the likely flow direction of the oil spill and how far the oil might migrate and the influence on the detection of impact on vegetation using the indices. In Figure 5.3 the calculation of potential flow direction of the oil spill from the polluted pixel. For example oil sample point occurred on a pixel with value of 128 meaning (the largest) compare to surrounding cells (pixels), which means that the likely and potential cell whose flow passes through the cell. The potential flow direction in Figure 5.3 will pass through a cell with the smallest value 1 (down slope pixel). The 8 flow direction model was used to obtain the vegetation indices from the first polluted pixel, to the second and then to the third neighbour pixels respectively based on the flow direction calculated.

In Table 5.3, vegetation indices were obtained at the various spill points using the flow direction model. The “pixel 1” (P₁) denotes polluted pixel, “pixel 2” (P₂) and “pixel 3” (P₃) as neighbouring pixels. The vegetation index values were extracted based on the flow direction of oil spill using the model. The volume of oil threshold at spill sites with >200 bbl were used in establishing the relationship between the vegetation indices with the variation spatial distance of pixels from the polluted point.

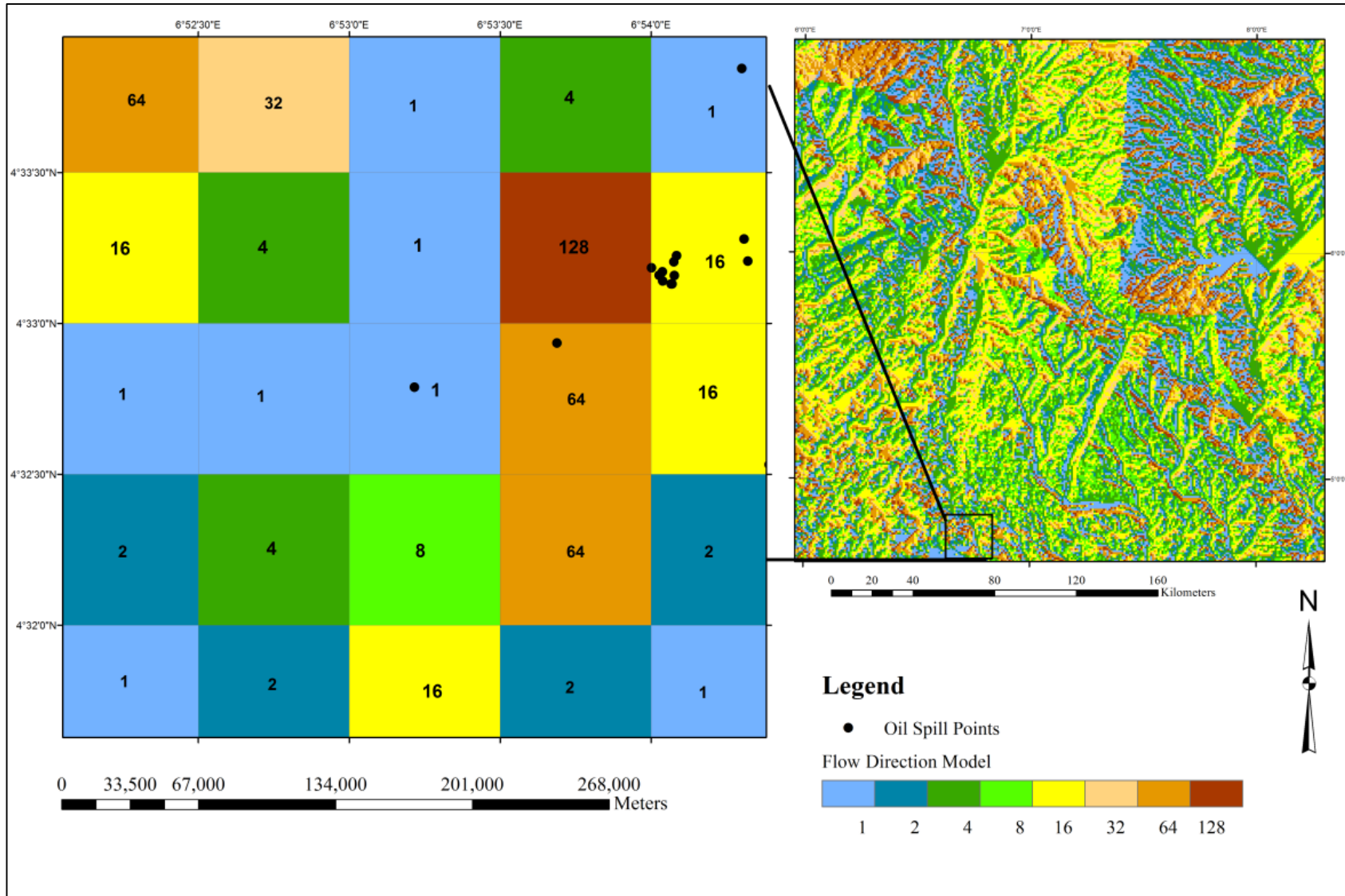


Figure 5.4: Calculated direction flow model from SRTM data

Table 5.3: BMVIs obtained at spatial distance from polluted and neighbouring pixels

Sample Points	Volume	Time (D)	NDVI			SAVI			ARVI2			G/NIR			G/SWIR		
			P ₁	P ₂	P ₃	P1	P2	P3	P1	P2	P3	P1	P2	P3	P1	P2	P3
SP46	813	3	0.25	0.23	0.29	0.32	0.42	1.5	0.12	0.07	0.77	0.21	0.19	0.25	0.04	0.01	1
SP55	2761	20	0.14	0.17	0.18	0.24	0.28	0.16	0.02	0.02	0.06	0.1	0.12	0.15	0.08	0.09	0.37
SP33	318	35	0.44	0.4	0.45	0.6	0.62	0.53	0.36	0.27	0.45	0.35	0.33	0.36	0.01	0	0.03
SP49	1069	37	0.2	0.12	0.18	0.18	0.27	0.31	0.07	0.05	0.02	0.1	0.03	0.09	0.42	0.24	0.27
SP30	221	127	0.31	0.31	0.5	0.48	0.67	0.72	0.18	0.11	0.42	0.23	0.23	0.39	0.08	0.05	0.08
SP52	1734	134	0.2	0.21	0.18	0.31	0.3	1.5	0.05	0.07	0.35	0.15	0.16	0.15	0.07	0.07	1
SP34	346	135	0.2	0.12	0.32	0.17	0.45	1.36	0.08	0.07	0.13	0.13	0.04	0.23	0.43	0.14	0.79
SP48	1042	158	0.24	0.23	0.18	0.38	0.27	0.28	0.1	0.1	0.03	0.18	0.19	0.14	0.02	0.07	0.07
SP51	1720	163	0.18	0.18	0.15	0.41	0.23	0.31	0.01	0.04	0.02	0.16	0.19	0.14	0.25	0.05	0.3
SP56	3500	198	0.17	0.3	0.15	0.35	0.28	0.35	0	0.23	0.02	0.1	0.15	0.05	0.18	0.31	0.32
SP32	269	206	0.13	0.17	0.11	0.24	0.19	0.44	0.04	0.03	0.08	0.07	0.1	0.05	0.33	0.29	0.17
SP54	2578	234	0.04	0.2	0.46	0.3	0.63	0.26	0.22	0.01	0.63	0.14	0.14	0.39	0.24	0.1	0.27
SP31	232	237	0.34	0.36	0.22	0.59	0.31	0.06	0.19	0.34	0.17	0.26	0.32	0.15	0.01	0.13	0.53
SP41	507	370	0.47	0.36	0.19	0.52	0.27	1.41	0.49	0.35	0.16	0.35	0.23	0.05	0.21	0.41	0.83
SP38	468	560	0.4	0.36	0.41	0.57	0.56	0.7	0.3	0.24	0.25	0.31	0.3	0.31	0.07	0.06	0.03
SP47	1000	707	0.48	0.48	0.46	0.73	0.72	0.55	0.37	0.39	0.45	0.37	0.38	0.38	0.05	0.03	0.13
SP45	807	708	0.48	0.47	0.48	0.72	0.72	1.12	0.38	0.36	1.68	0.36	0.36	0.38	0.06	0.06	0.91
SP36	358	819	0.38	0.21	0.43	0.35	0.57	0.56	0.36	0.02	0.37	0.27	0.12	0.28	0.3	0.11	0.13
SP50	1505	844	0.33	0.35	0.36	0.49	0.54	0.92	0.2	0.22	0.88	0.26	0.24	0.27	0.11	0.13	0.84

Table 5.4: Coefficient of determination (R^2) of BMVIs and spatial distance.

BMVIs	Regression Equation	Pixel 1 (P1)		Pixel 2 (P2)		Pixel 3 (P3)	
		R^2	p-value	R^2	p-value	R^2	p-value
NDVI	$y = -0.077\ln(x) + 0.7884$	0.2268	$p < 0.05$	n.s.	n.s.	n.s.	n.s.
ARVI2	$y = -0.102\ln(x) + 0.8372$	0.2401	$p < 0.05$	n.s.	n.s.	n.s.	n.s.
G/NIR	$y = 0.0657\ln(x) - 0.6392$	0.203	$p < 0.05$	n.s.	n.s.	n.s.	n.s.

Probability Error (α) = 0.05

Table 5.4 Coefficient of determination (R^2) and p-values of BMVIs and volume of oil at spatial distance (P1, P2 and P3), show no significant relationship at P2 and P3.

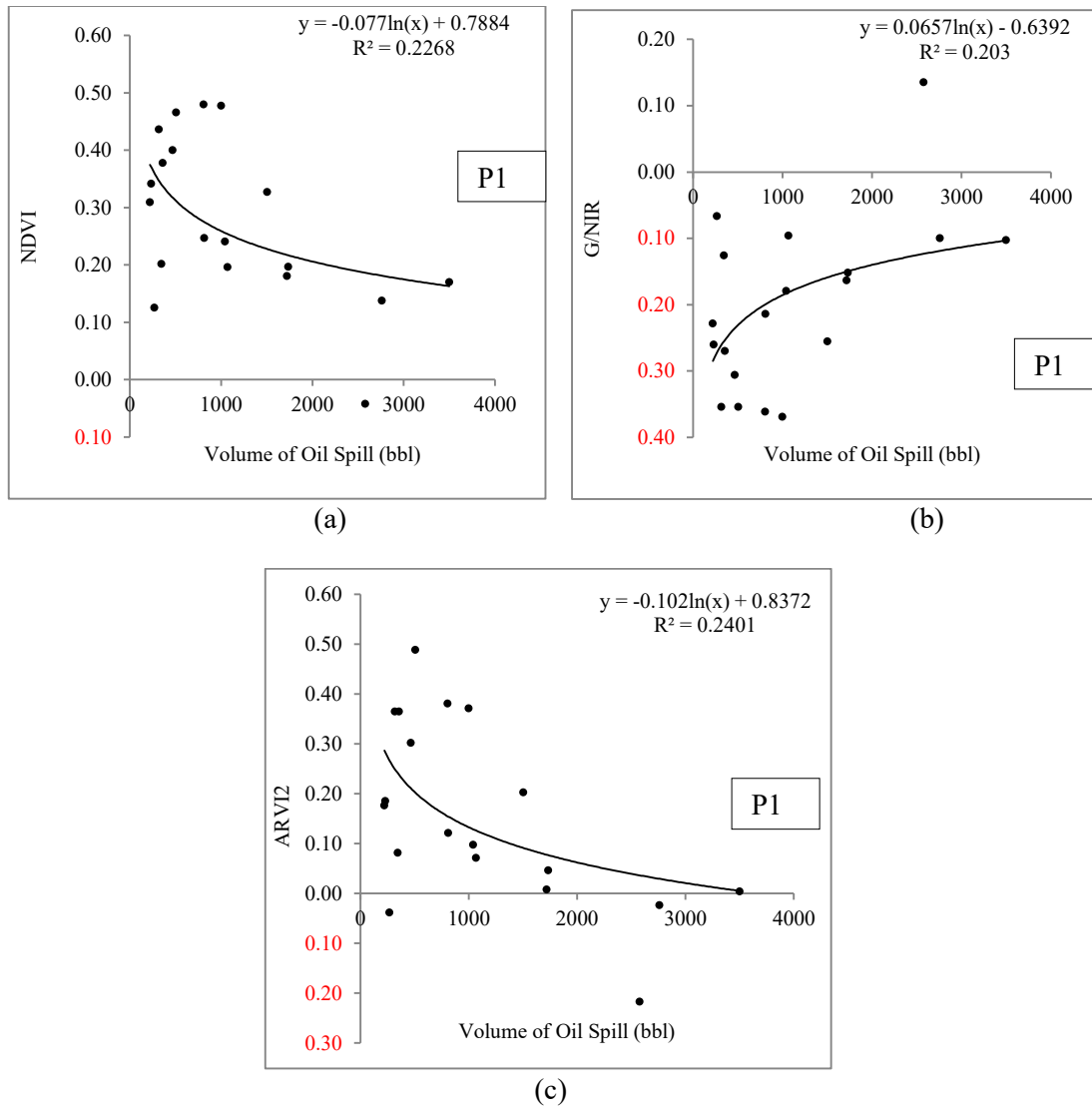


Figure 5.5: Regression plot for volume of oil spill on BMVIs based on spatial distance.

In Figure 5.4 only 3 out of the 5 BMVIs (NDVI, SAVI and ARVI2) indicated significant relationship with the volume of oil spill at pixel (P1) and the remaining 2 did not. The result did not indicate any significant relationship found at the P2 and P3 with the BMVIs. This result suggests that since only P1 indicated significant relationship with volume of oil spill at this point, it can be assumed that oil spill did not migrate from the point of spill. It is a possibility that the neighbouring pixel P2 and P3 were not affected by the oil spill as shown in Figure 5.4. Thus the implication of the results of this model suggest it may only be applicable in a study area which is characterised by relatively flat terrain.

5.2.3 Influence of time gap between spill and observation on BMVIs

Further analysis include calculating the difference between the time of oil spill event and image dates then compared with the volume of oil spill in Table 5.1.

Table 5.5: Coefficient (R^2) time gap between oil spill and image date on BMVIs

BMVIs	Regression Line	R^2	p-value
NDVI	$y = 0.0351\ln(x) + 0.0994$	0.13	$p < 0.05$
SAVI	$y = 0.0545\ln(x) + 0.1422$	0.21	$p < 0.05$
ARVI2	$y = 0.0447\ln(x) - 0.0697$	0.12	$p < 0.05$
G/NIR	$y = -0.024\ln(x) - 0.0806$	0.07	$p < 0.05$
G/SWIR	$y = 0.0036\ln(x) + 0.1025$	0.07	n.s.

Probability Error (α) = 0.05

In Table 5.5 four BMVIs indicated significant relationship with number of days between oil spill event and image acquisition data with $p < 0.05$ and G/SWIR non-significant. Similarly in Figure 5.5 the regression line showed a direct proportion between number of days and the BMVIs.

Table 5.6: Time gap (days) between oil spill and image date and selected BMVIs.

Sample Points	Volume of Oil (bbl)	Time (Days)	NDVI	SAVI	ARVI2	G/NIR	G/SWIR
SP46	813	3	0.25	0.32	0.12	0.21	0.04
SP55	2761	20	0.14	0.24	0.02	0.10	0.08
SP33	318	35	0.44	0.60	0.36	0.35	0.01
SP49	1069	37	0.20	0.18	0.07	0.10	0.42
SP30	221	127	0.31	0.48	0.18	0.23	0.08
SP52	1734	134	0.20	0.31	0.05	0.15	0.07
SP34	346	135	0.20	0.17	0.08	0.13	0.43
SP48	1042	158	0.24	0.38	0.10	0.18	0.02
SP51	1720	163	0.18	0.41	0.01	0.16	0.25
SP56	3500	198	0.17	0.35	0.00	0.10	0.18
SP32	269	206	0.13	0.24	0.04	0.07	0.33
SP54	2578	234	0.04	0.30	0.22	0.14	0.24
SP31	232	237	0.34	0.59	0.19	0.26	0.01
SP41	507	370	0.47	0.52	0.49	0.35	0.21
SP38	468	560	0.40	0.57	0.30	0.31	0.07
SP47	1000	707	0.48	0.73	0.37	0.37	0.05
SP45	807	708	0.48	0.72	0.38	0.36	0.06
SP36	358	819	0.38	0.35	0.36	0.27	0.30
SP50	1505	844	0.33	0.49	0.20	0.26	0.11

Table 5.6: the number of days calculated between oil spill and image acquisition date in the study area. The average number of days obtained for observing the spill sites is 130 days (20 weeks) to detect and average volume of oil spill at 1277 bbl.

Table 5.5 and Figures 5.5 shows that the number of days between spill and detection indicates a significant relationship with BMVI values. This could be argued that as the number of days increases the BMVIs also increases. It may also suggest that oil spill impact on vegetation may have reduced allowing possibility for vegetation recovery at the spill sites. It is also likely that imagery acquired closed to the spill event were not available - or contain cloud cover - so cloud-free images from another year for these sites were used, with a consequential increase in temporal separation relating to high BMVI values. The BMVIs with low values were influenced by substantially-lesser time separation between the spill event and image acquisition free of issues associated with

cloud cover. This can be interpreted in terms of increases in volume of oil spill as BMVI values decreases. This contrasts with those in Figure 5.3.

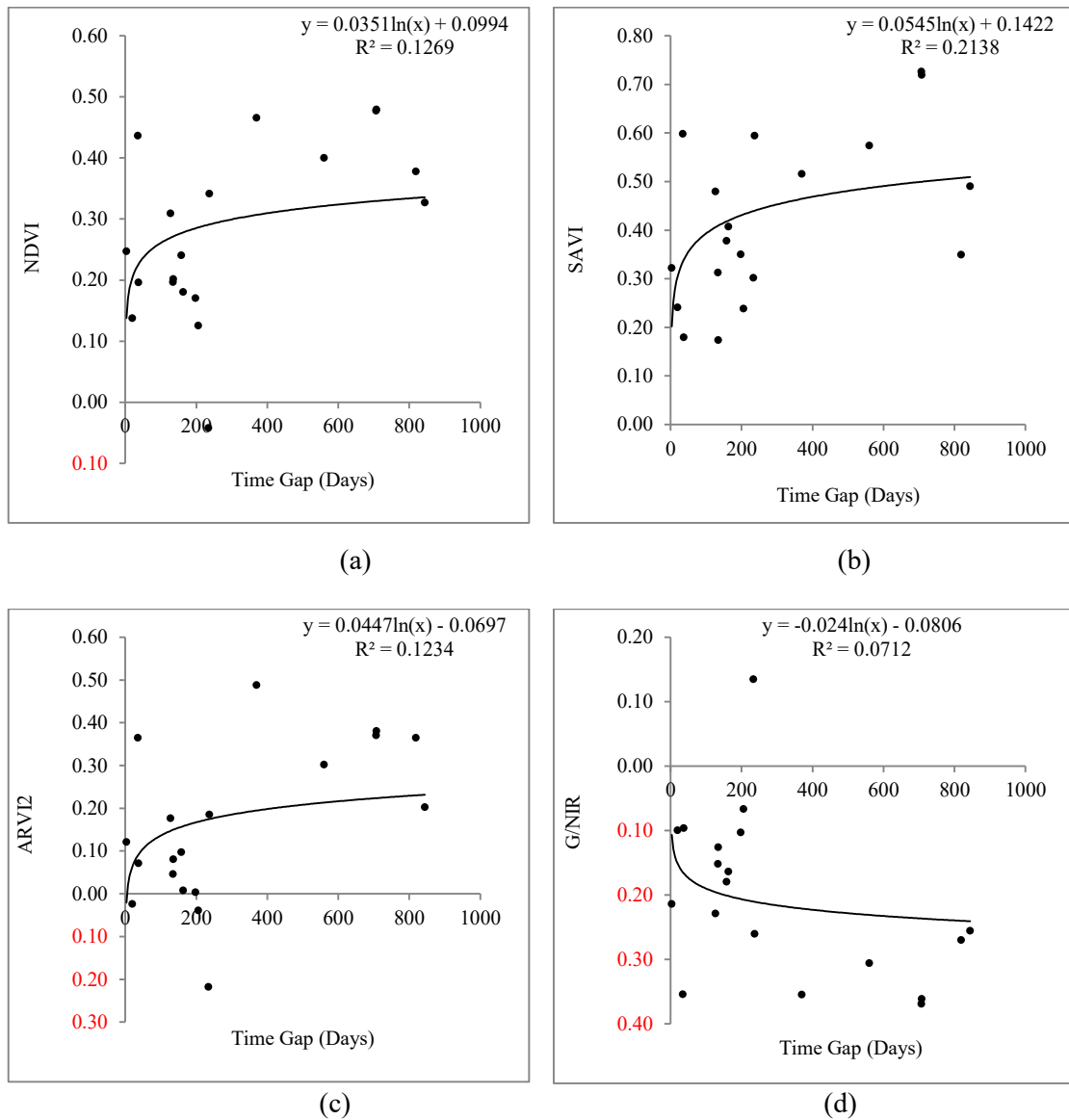


Figure 5.6: Regression between the time gap between spill and observation date and selected BMVIs at the polluted sites.

Table 5.6 and Figures 5.5 Logarithm plot of time gap (number of days) between oil spill and the BMVIs. Four indices (NDVI, SAVI, ARVI2 and G/NIR) have indicated weak relationship but showed a significant correlation between number of days and the BMVIs with the exception of G/SWIR.

5.3 Discussion

5.3.1 Influence of volume of oil spill on the selected BMVIs

Changes in vegetation spectral reflectance are associated with leaf chlorophyll content and structure that can be detected in visible and NIR wavelengths (Purkis and Klemas, 2011, Mather and Koch, 2011b). Thus changes in vegetation health in oil polluted sites may depend on the volume of a given oil spill (Osuji and Opiah, 2007). It is assumed that larger-volume oil spills may have a greater impact on the surrounding vegetation and the affected vegetation may then take a longer period to recover as the oil degrades or evaporates. In this study it has been shown that volume of oil e.g. above 200 bbl is related to vegetation indices obtained at the sample polluted sites. In Noomen (2007), it was argued that larger oil spills lower oxygen concentrations in soil due to methanotrophic bacteria. These are responsible for methane oxidation and are the main cause of changes possibly related to vegetation reflectance at the polluted sites. It has also been documented that soil oxygen shortage leads to reduced root and shoot growth in plants (Drew, 1992, Huang et al., 1997). It was also found that there is a strong relationship between hydrocarbon gas and oxygen concentration (Noomen, 2007).

The result from the plotted regression line indicates a weak R^2 with a significant relationship at $p < 0.05$ between the volume of oil spill and the 4 BMVIs in Table 5.2 and Figure 5.3 with the exception of G/SWIR. This can be interpreted as the volume of oil spill increases the value of BMVIs decreases. Thus the weak relationship between the variables could also be due to some environmental factors that may be responsible, although it is not very clear to conclude that oil pollution may be a solitary cause factor. It could also be that the impacted vegetation at some spill sites may have recovered due to the time gap between the oil spill and image acquisition date, since the spill sites are located in swampy, mangrove areas where the climatic condition (e.g. rainy season) may influence the vegetation recovery. These factors could also influence the vegetation signals as well as the value of vegetation indices, thus could be other reasons for the weak relationship between the volume of oil spill and the BMVIs. The influence of sensor spectral bands used in the derivation of the BMVIs could be responsible due to their characteristics. The 4 BMVIs that indicated vegetation response to oil pollution as seen in the Figure 5.2 uses both visible and NIR channels that can characterise chlorophyll

contents in leaves and high reflectance of vegetation canopies. Meanwhile the G/SWIR is a function of Green and SWIR1 located at 0.550 μm and 1.24 μm channels, and used for estimating vegetation liquid water from space (Gao, 1996). The suitability of these 4 BMVIs indicates a significant relationship with the volume of spill in Figures 5.2. However, the advantage of G/SWIR is the ability to sense changes in liquid water content of vegetation canopies that may be affected by oil pollution. These could be some of the reasons why the indices were explored for analysing volume of oil spill impact on vegetation health. It should be noted that the satellite sensors used for the study can also contribute to the performance of the BMVIs as some of the oil spill sites may not be detected through vegetation signals alone due to small-volume oil spill incidences.

5.3.2 Spatial analysis of oil spill on the BMVIs

The relationship between BMVIs and spatial distance in Table 5.4 and Figure 5.4 is represented by “pixel 1” (P1), “pixel 2” (P2) and “pixel 3” (P3). The Pixel 1 (P1) is represented by the pixel that is the most likely to be polluted where the spill occurred, the second pixel 2 (P2) is the likely to be affected and the third pixel 3 (P3) is the less likely affected by oil pollution. In 5.4 and Figure 5.4 the relationship between 3 BMVIs and the points of oil spill (polluted pixel) and the neighbouring pixel where migration is expected to have been affected by oil spill were only significant at P1. These can also observed in the correlation between the first pixel (P1) regression between which has a significant relationship with 3 BMVIs, while other two neighbouring pixels with non-significant. For example, the relationship between the 3 BMVIs and the volume of oil spill indicated weak relationship at polluted pixels with NDVI ($R^2 = 0.23$), SAVI ($R^2 = 0.010$) and ARVI2 ($R^2 = 0.24$) but significant relationship at $p < 0.05$. Conversely, the relationship at the second (P2) and third (P3) (Table 5.4) pixels indicate a weak relationship, suggesting that volume of oil spill has relatively less - or no - influence on vegetation health further away from the polluted pixel. It is a possibility that the oil spill size may have not migrated further away from the polluted pixel and it may be the less impacted vegetation recovers in between spill event and image acquisition data. Two indices, SAVI and G/SWIR, have not shown any significant relationship with the volume of oil spill even at the first point of spill P1 in Table 5.4. It is interesting that SAVI and G/SWIR performed relatively well in differentiating between the polluted and non-polluted sites and before and after oil spill but did not perform well in this study chapter. It is not very clear why SAVI and G/SWIR

were not able to show significant relationship with volume of oil spill at these points. It is worth also considering the effect of tidal flow model since the study is located in a brackish coastal region.

5.3.3 Influence of time gap between spill and observation on BMVIs

In Table 5.4 and Figures 5.5 the regression indicates a relatively weak, yet significant, positive relationship between number of days and BMVIs with (NDVI, $R^2 = 0.013$, SAVI, $R^2 = 0.21$, ARVI2, $R^2 = 0.012$ and G/NIR, $R^2 = 0.007$) i.e. as the number of days increases, the BMVIs values increases. This is also an indication that affected vegetation at oil spill sites may have recovered with time (Luis, 1993, Osuji and Ezebuoro, 2006, Noomen et al., 2015). On the average volume of oil spill that may impact on vegetation health in this study, the average number of days was calculated and then compare with the BMVIs. In Table 5.3 the average volume of oil spill 1277 bbl that could have impact on vegetation health within this average number of days 130 days (i.e. about 20 weeks). In a study Wang et al. (2013), suggested that oil chemical properties and weathering (change in composition of hydrocarbons with time) characteristics may be influenced by quantity of oil spill in the polluted environment. This result could also mean that some factors such as time between oil spill event and image acquisition date may have influential in the detection of vegetation stress related to oil pollution.

5.4 Summary

Five BMVIs (NDVI, SAVI, ARVI2, G/NIR and G/SWIR) were used for determining the volume of oil spill in the polluted sites. It was found that Four (4) indices (NDVI, SAVI, ARVI2 and G/NIR) indicated a correlation that could be term as relatively weak with the volume of oil spill but $p < 0.05$ show a significant relationship between the two variables. The result also showed that time between the imagery and spill dates have weak correlation but with a significant relationship with the BMVIs. The spatial variation of the oil impact on vegetation with the BMVIs from the three pixels did not show any significant variation between (P1, P2 and P3) despite applying direction flow model to determining the likely flow direction of the oil pollution. In summary, the result indicated significant relationship between volume of spill and vegetation indices (BMVIs). This study also demonstrated that time gap (between spill and image date) and volume of oil

spill are important and could be an influential factor for detecting the impact of oil pollution on vegetation.

Chapter 6 : Validation of vegetation spectral techniques for detection of oil pollution on vegetation

The work presented in this chapter is in preparation for publication as:

Adamu, B., Tansey, K. and Ogutu, B., (2016). Remote sensing for detection and monitoring of vegetation affected by oil spills. *Remote Sensing* (Manuscript submitted 09.06.2016 under review).

6.1 Introduction

The objective of any analytical measurement is to obtain consistent, reliable and accurate data. Validated analytical methods play a major role in achieving this goal. The validation of methods can be used to judge the quality, reliability and consistency of analytical results, which is an integral part of any good analytical practice. In chapter 4, vegetation indices have shown to be capable of detecting oil pollution impact on vegetation spectral signature. The techniques using the indices have also indicated the potential to monitor temporal changes in the vegetation affected by oil pollution in a mangrove forest in the Niger Delta (study site 1 – SS1 in chapter 4). In SS1 these indices were also used to determine factors influencing their capacity in the detection oil spill impact on vegetation. The results in the chapter 4 have shown that there are significant relationships between these factors (volume of oil spill, time gap between oil spill and image acquisition date) in addition to the vegetation indices.

The objective of this chapter is to assess and validate these techniques in a different study area (study site 2- SS2) with similar climatic and environmental conditions using new oil spill data from 2014. Thus an assumption that vegetation affected by oil spill at P sites will statistically differ in mean index values with the ones obtained at the NP sites (with no oil spill). Also that temporal vegetation conditions before (2013) and after (2015) the oil spill at the P site may be relatively different with the one at spill sites (2014). The analysis will also statistically test if there are temporal variations in vegetation biophysical and biochemical properties at the NP sites.

6.2 Study area

The study site (SS2) is located in the north-western part of the study site (SS1) in the Niger Delta region in Figure 6.1. The SS1 is located within (4°33'27.77"N, 6°52'34.43" E), in the other part of the Niger Delta region of Nigeria. It shares common environmental and climatic conditions with the SS2 that have been described in chapter 3. The part of

this region experiences moderate rainfall and moderate humidity for most of the year. The study area 1 (SS1) is characterised with features similar to the SS2 area, which is a tropical monsoon climate with lengthy and heavy rainy seasons and very short dry seasons. Only the months of December and January truly qualify as dry season months in the region. The dry and dusty winds, which climatically influences many regions in West Africa, is less pronounced in the area. The heaviest precipitation occurs during September with an average of 367 mm of rain. The month of December on average is the driest month of the year, with an average rainfall of 20 mm. Temperatures throughout the year in the region (SS1 and SS2) are relatively constant, showing little variation throughout the course of the year. Average temperatures are typically between 25 °C-28 °C in SS2. The relative difference between the SS1 and SS2 in terms of climatic elements such as rainfall, temperature and seasonality might present some variation in the analysis of results. This is because in the vegetation is highly influenced by some climatic conditions which has two active months of dry season (December and January) but in SS2 the active dry months occur between (November – April). In terms of vegetation cover SS1 is generally characterised by swamp mangrove, compared to SS2 which is rainforest with less swamp mangrove forest. They two sites also differ locally in terms of significant atmospheric haze or dust “harmattan” in the atmosphere. For example SS2 is most affected by atmospheric haze than SS1. These characteristics can affect the image quality in the study areas, for example in SS1 cloud cover is more persistent because of the long wet season (February to November). In SS2 which is characterised by short dry season and less cloud cover (December and January) with obvious presence of atmospheric dust and haze.

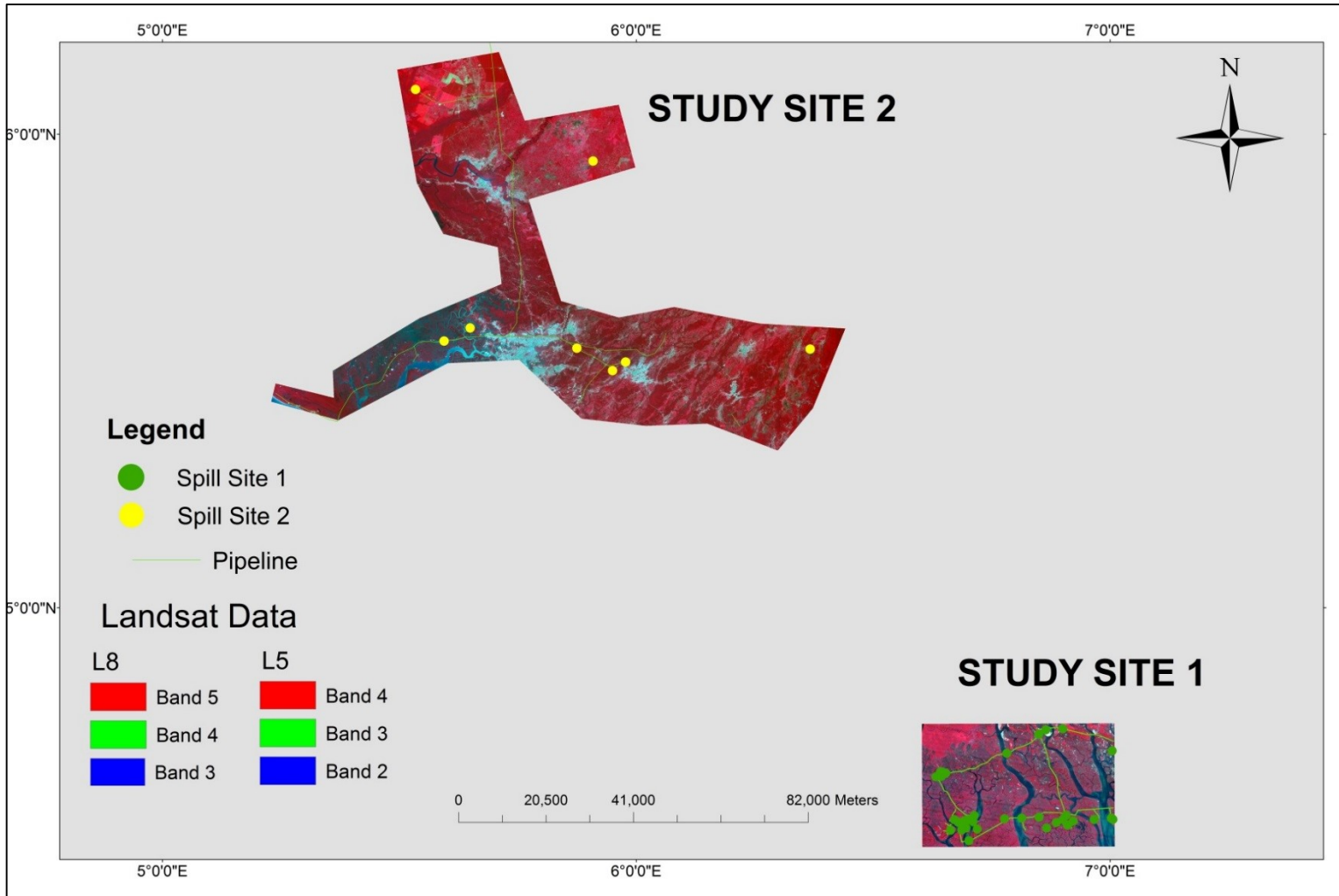


Figure 6.1: Location of the two study sites on Landsat 5 (SS1) and 8 (SS2)

6.3 Sources of data and method

6.3.1 Source of oil spill data

Nine new oil spill sites (Table 6.1) were identified which occurred in 2014 obtained from the National Oil Spill Detection and Response Agency (NOSDRA) <https://oilspillmonit.or.ng/> an agency of Nigeria Government. NOSDRA was established in 2006 by the Federal Government of Nigeria as institutional framework to create, nurture and sustain a zero tolerance for oil spill incident in the Nigerian Environment. NOSDRA an institutional framework to co-ordinate the implementation of the National Oil Spill Contingency Plan (NOSCP) for Nigeria in accordance with the International Convention on Oil Pollution Preparedness, Response and Cooperation (OPRC 90) to which Nigeria is a signatory. The Agency embarks on Joint Investigation Visits, ensures the remediation of impacted sites and monitors oil spill drill exercises and facilities inspection. Thus oil spill sites reported on their website may be considered valid as mandated by the law of Nigeria. Nine oil spill sites in 2014 were obtained from the agency website. Information such as date of spill, GPS points, location name, quantity of oil spill and vegetation land cover type is shown in Table 6.1.

Table 6.1: Oil spill data for the new study site 2 (SS2)

Sample Point	Latitude	Longitude	Date of Spill	Image Date	Time Period (Days)	Quantity of Oil Spill (bbl)
SP1	6.0945278	5.534583	29/12/2014	08/01/2015	10	108
SP2	5.56325	5.5948056	25/11/2014	23/12/2014	28	5000
SP3	5.5191111	5.9779444	08/09/2014	23/12/2014	106	na
SP4	5.5633056	5.5948333	06/09/2014	23/12/2014	108	60
SP5	5.9433889	5.9090556	01/09/2014	23/12/2014	113	1000
SP6	5.5009722	5.9501667	20/08/2014	23/12/2014	125	3
SP7	5.54825	5.8749722	n/a	23/12/2014	na	na
SP8	5.5464722	6.3670833	05/08/2014	23/12/2014	140	7.7
SP9	5.5908889	5.6496667	18/07/2014	23/12/2014	158	60

6.3.2 Image Data

Landsat 8 images Level 1 terrain corrected products for 20/12/2013 (pre-spill), 23/12/2014 (oil spill date) and 08/01/2015 (post spill) were used in the study on path 189 row 57. The images were collected during dry season (December and January) with a

minimal cloud cover <26% at the scenes centre (does not affected study sites). The 9 spill sites in 2014 were analysed using pre-spill image from 20/12/2013 and post-spill image from 08/01/2015. The image from 23/12/2014 were used as the spill date data to observe the oil spill sites in 2014. Landsat 8 differs with other Landsat data e.g. TM and ETM+, for example L8 signal to noise ratio (data quality) and radiometric quantization has 12-bits which is higher than TM and ETM+ with 8-bit. Thus L8 provides significant improvement in the ability to detect changes in the earth's surface. The Landsat 8 Operational Land Imager (OLI) and Thermal Infrared Sensor (TIRS) has two additional spectral bands band 1 (deep blue visible channel) and band 9 for detection of cirrus clouds. Also the OLI has a new Quality Assurance band included in each data product which provides information on the presence of features such as clouds, water and snow. As expected OLI's narrower panchromatic band provides better spectral contrast over land surfaces. The push-broom sensor's higher signal-to-noise ratio makes it possible to narrow the spectral bands and move them away from atmospheric absorption features, thereby reducing the sensitivity of the changes in the atmosphere. The biggest change is in the near infrared (band 5 in OLI). That band is substantially narrower and will be less sensitive to atmospheric conditions than Landsat 5 and 7. The satellite is required to return 400 scenes per day to the USGS data archive (150 more than Landsat 7 is required to capture). Landsat 8 has been regularly acquiring 725 scenes per day (and Landsat 7 is acquiring 438 scenes per day). This increases the probability of capturing cloud-free scenes for the global landmass. The spectral response of vegetated areas can present a complex mixture of vegetation, soil brightness, environmental effects, shadow, soil colour and moisture (Bannari et al., 1995). The images used in the study were atmospherically corrected in order to obtain a surface reflectance image free from noise. In Figure 6.2 pre-processed L8 data used for the study.

6.3.3 Landsat 8 image processing

In chapter 3 image processing were described based on the Landsat data 5 and 7, in the case for this study the Landsat 8 sensor used is new and its calibration is not supported by some ENVI products such as the FLAASH module for atmospheric correction. Nevertheless, in ENVI 5.3 new radiometric calibration can be used to convert any Landsat 8 data to radiance or TOA reflectance as contained in other ENVI versions. Landsat 8 spectral radiance data can also be converted to TOA planetary reflectance using reflectance rescaling coefficients provided in the Landsat 8 OLI metadata file. The

following equation is used to convert DN values to TOA reflectance for OLI image. Therefore, since ENVI can convert Landsat data easily from the USGS in the “USGS GeoTIFF with metadata” format in a single step, the optical data can be converted to TOA reflectance values when opened with “_MTL.TXT”. The method was used to convert the data into surface reflectance using the calibration parameters. The first step is the conversion of DN to radiance; the image was calibrated using gains and offsets for each band which are read from metadata file from the image folder. The radiance values from Landsat 8 can be computed from DN values using band math or the built-in function within ENVI 5.0 Service Pack 3. Radiance is computed using

$$L_{\lambda} = Gain * Pixelvalue + Offset \quad \text{Eq. 1}$$

In ENVI gains and offsets are in the units as ($\mu\text{W}/(\text{cm}^2 * \text{sr} * \text{nm})$) and radiance units will be in $\text{W}/(\text{m}^2 * \text{sr} * \mu\text{m})$.

$$\rho_{\lambda} = \pi * L_{\lambda} * d^2 / ESUN_{\lambda} * \cos\theta_s \quad \text{Eq. 2}$$

Where:

- ρ_{λ} = Unitless planetary reflectance
- L_{λ} = spectral radiance (from earlier step)
- d = Earth-Sun distance in astronomical units
- $ESUN_{\lambda}$ = mean solar exoatmospheric irradiances
- θ_s = solar zenith angle

The second step is the conversion of TOA to surface reflectance. Surface reflectance, i.e., TOA reflectance corrected for atmospheric effects, is needed because atmospheric gases and aerosols are variable in space and time and may have significant impacts on Landsat data (Roy et al., 2015). The OLI band data can also be converted to TOA planetary reflectance using reflectance rescaling coefficients provided in the product metadata file (MTL file). The following equation is used to convert DN values to TOA reflectance for OLI data as follows:

$$\rho_{\lambda} = M\rho_{cal} + A\rho \quad \text{Eq. 3}$$

where:

ρ_{λ} = TOA planetary reflectance, without correction for solar angle. Note that ρ_{λ} does not contain a correction for the sun angle.

M_p = Band-specific multiplicative rescaling factor from the metadata (REFLECTANCE_MULT_BAND_x, where x is the band number)

A_p = Band-specific additive rescaling factor from the metadata (REFLECTANCE_ADD_BAND_x, where x is the band number)

Q_{cal} = Quantized and calibrated standard product pixel values (DN)

In Figure 6.2 pre-processed L8 data used for the study.

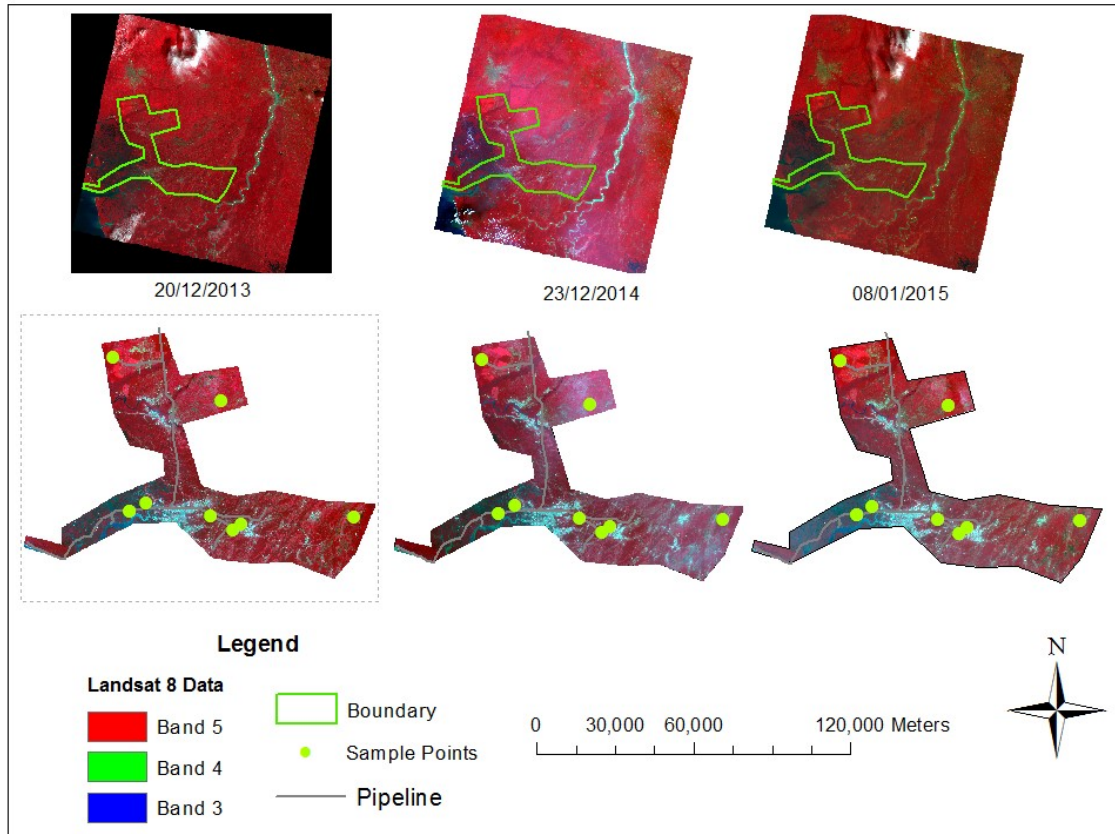


Figure 6.2: Landsat 8 and oil spill data used for the study site 2

From the reflectance images of 2013, 2014 and 2015 in bands 5, 4 and 3 appears have a bit visual variation despite applying the atmospheric correction. Images 2014 and 2015 seem to contain effect of atmospheric dust and haze in some part of the study sites.

6.3 Method and data analysis

From Table 6.1 only 9 spill sites in 2014 can be observed using the image obtained on the 23rd December 2014. Pre-spill data (data before spill event) is taken from the 20/12/2013 image and post-spill data (data after oil spill) from the 08/01/2015 image. Information on the volume of oil spill, vegetation type, date of oil spill, location (GPS) etc is included in

the oil spill database. The method of analysis in the new spill sites will replicate the techniques used in chapter 4. The reflectance data was used in the calculation of the 5 vegetation indices from the P and NP in 2013, 2014 and 2015 for statistical analysis. NDVI derived from Landsat 8 will be altered by looking at the earth through this “sub-visible” cirrus band. It has been reported that due to the flat Mie scattering (Otterman and Fraser, 1979) from cirrus, cirrus will increase the apparent NDVI for water and decrease the apparent NDVI for vegetation. Rajitha et al. (2015), shown that NDVI values obtained after cirrus correction is found to be significantly more than that of NDVI values without cirrus correction. Empirically derived vegetation indices products seem to be unstable due to soil color and moisture, and bidirectional reflectance distribution function (BRDF) effects on atmospheric conditions (Qi et al., 1995). For these reason it is expected that other values of vegetation indices could be affected by BDRF effects. In Figure 6.3 vegetation indices map of 2014 showing sample polluted (P) and non-polluted points (NP), oil pipeline and spill point’s data for the analysis.

At each of the oil spill point vegetation indices were extracted and NP sample points were taken from areas with no oil spill as control points. The NP samples were taken where there are no oil facilities and also ensuring that the vegetation is of similar characteristics.

Figure 6.4 illustration few of the sample points on the Google Earth image on how it was conducted.

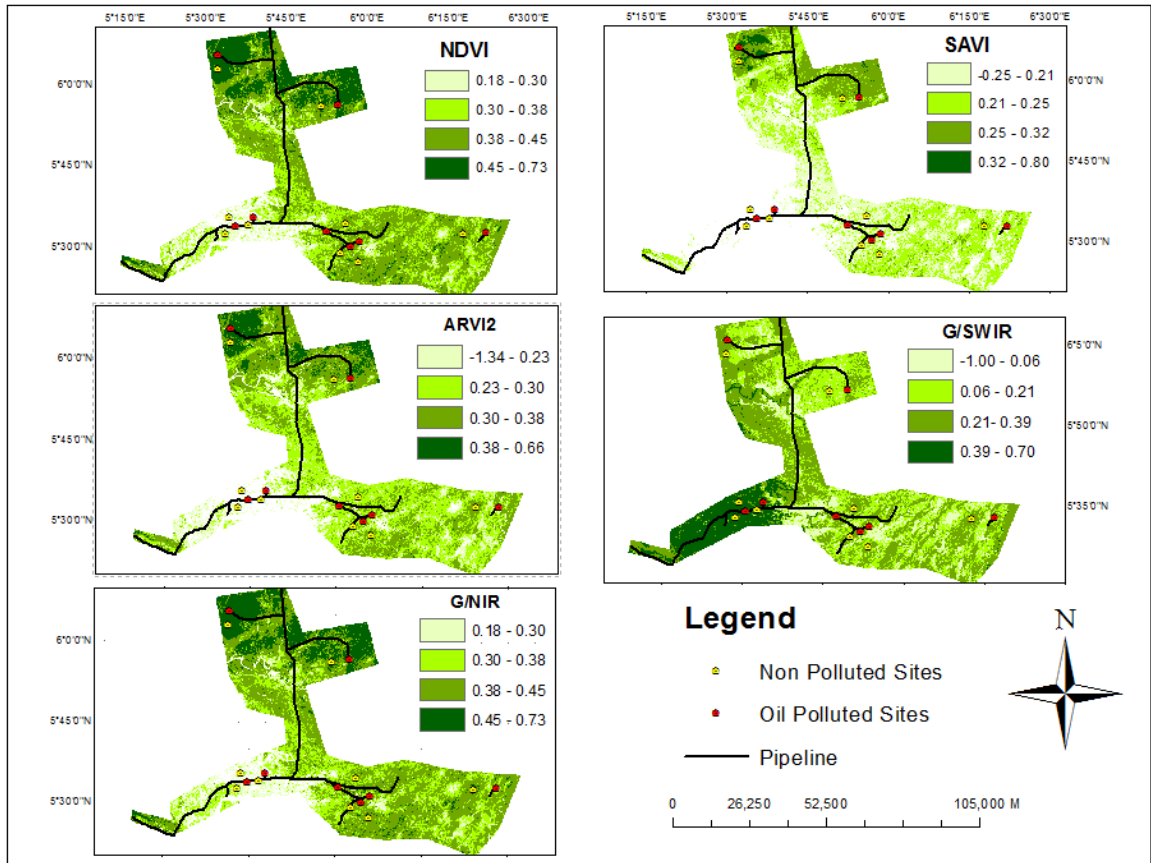


Figure 6.3: Sample P and NP points on vegetation indices maps in 2014.



Figure 6.4: Few sample sites illustrating on Google Earth maps how P and NP points were obtained from Landsat data

6.4 Results

The aim of this analysis is to present a result that may be used to validate the techniques in chapter 4. It is expected that the results from this study area will provide relatively similar results as in chapter 4.

6.4.1 Impact of oil spill on vegetation in the image of 2014

To assess whether there is an effect of oil pollution on vegetation at the spill sites, vegetation indices at both the polluted sites and non-polluted sites were extracted from the SS2. The extracted indices are expected to indicate if there is any statistical significant difference in the levels of pollution impact on the vegetation at the P sites and the ones at the NP sites. This statistical difference will be used to determine spectral changes in the vegetation affected by oil at the two sites. Figure 6.5 is the difference between vegetation indices obtained at the polluted and non-polluted sites.

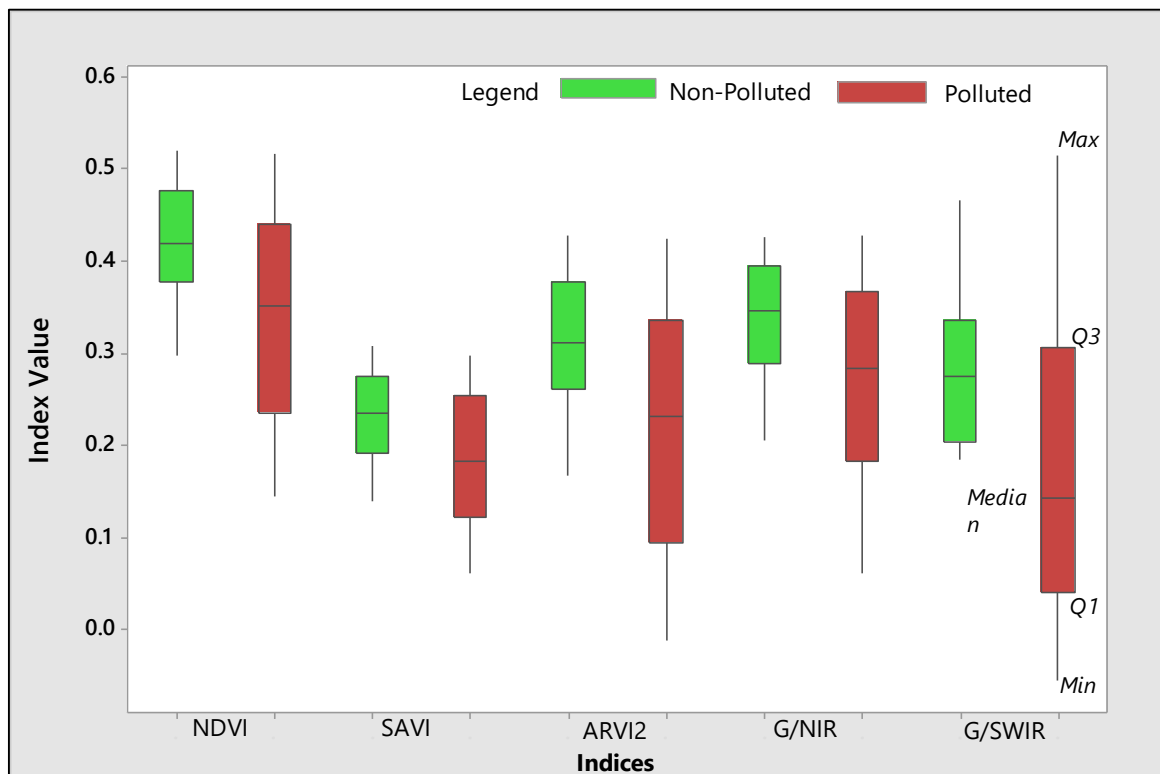


Figure 6.5: Box plot for the calculated mean of the 5 vegetation indices from polluted (P) and non-polluted (NP) sites in 2014

Figure 6.5 is the mean values of the vegetation indices extracted from the P and NP sites, the “green” colour indicates non-polluted sites where oil spills were not recorded while

the “red” represents P sites with record of oil spills. The box plot shows the maximum whiskers, Q3, median, Q1 and minimum whiskers respectively. The vegetation indices from NP sites show high vegetation values and P with low mean values.

Table 6.2 is the generated statistics for the vegetation indices extracted from 9 oil spill sites which occurred during the year 2014. In the table the P sites were extracted where the spill occurred and the NP sites where no oil spill was recorded. These were used for the analysis of paired t-test at 0.05 for samples from P and NP in Table 3. It is assumed that vegetation indices obtained at the P and NP sites differs in response to oil impacts. This was done in order to determine if there is any significant differences between vegetation affected by oil spill (P) and the unaffected vegetation at the non-spill sites (NP).

Table 6.2: A comparison of p-values from paired t-test analysis for the study sites (P and NP sites) in 2014

	<i>Indices</i>	NDVI	SAVI	ARVI2	G/NIR	G/SWIR
P Sites vs NP sites	<i>P-values</i>	0.01	0.02	0.01	0.03	n.s

n.s. = not significant

Table 6.3 demonstrates the result of the t-test analysis to determine if there are significant differences between the vegetation affected by oil spill (P) and the unaffected at the NP sites. The results show 4 vegetation indices (NDVI, SAVI, ARVI2 and G/NIR) with significant difference at $p < 0.05$, between vegetation at the P and the NP sites. Similar results were also found in Chapter 4, which showed that vegetation affected by oil pollution indicated significant differences between the vegetation at the polluted and non-polluted sites.

6.4.2 Change detection of vegetation at the oil spill sites

In chapter 4 results confirmed that vegetation health at P and NP sites before and after oil spill remain relatively unchanged but differs at the spill date (year of spill) based on the statistical analysis conducted at both the P sites. Thus this section attempt to validate if the results obtained in chapter 4. This section will determine if the level of significant differences in vegetation biophysical and biochemical properties at the P and NP sites in 2013 (before spill) and 2015 (after spill) then compared to 2014 (oil spill date). Table 6.4 is the statistical analysis of change detection between P and NP.

Table 6.3: Statistics of extracted vegetation indices from 9 P and NP sample oil spill sites in 2014

	NDVI			SAVI			ARVI2			G/NIR			G/SWIR		
Sample	NP	P	Change	NP	P	Change	NP	P	Change	NP	P	Change	NP	P	Change
Points			(Δ)			(Δ)			(Δ)			(Δ)			(Δ)
SP1	0.46	0.52	0.05	0.26	0.30	0.04	0.36	0.42	0.06	0.38	0.43	0.05	0.24	0.24	0.00
SP2	0.52	0.25	-0.07	0.29	0.25	-0.04	0.43	0.35	-0.08	0.43	0.37	-0.05	0.32	0.12	-0.20
SP3	0.49	0.43	-0.06	0.31	0.26	-0.05	0.39	0.32	-0.07	0.41	0.36	-0.05	0.19	0.08	-0.10
SP4	0.34	0.14	-0.20	0.17	0.06	-0.11	0.22	-0.01	-0.23	0.25	0.06	-0.19	0.35	0.52	0.16
SP5	0.30	0.16	-0.14	0.14	0.07	-0.07	0.17	0.01	-0.16	0.21	0.09	-0.12	0.47	0.37	-0.09
SP6	0.41	0.42	0.01	0.22	0.23	0.01	0.30	0.31	0.01	0.32	0.34	0.02	0.22	0.15	-0.07
SP7	0.42	0.33	-0.09	0.23	0.18	-0.05	0.31	0.20	-0.11	0.34	0.28	-0.06	0.31	0.00	-0.31
SP8	0.41	0.31	-0.11	0.23	0.18	-0.06	0.30	0.18	-0.12	0.35	0.28	-0.07	0.00	-0.05	-0.06
SP9	0.44	0.35	-0.09	0.24	0.18	-0.06	0.34	0.23	-0.11	0.36	0.28	-0.07	0.27	0.14	-0.13
Mean	0.42	0.35	-0.08	0.23	0.19	-0.04	0.31	0.22	-0.09	0.34	0.28	-0.06	0.26	0.17	-0.09
Std Dev	0.07	0.13	0.06	0.05	0.08	0.03	0.08	0.15	0.07	0.07	0.13	0.06	0.13	0.18	0.05
Std error	0.02	0.04	0.02	0.02	0.03	0.01	0.03	0.05	0.02	0.02	0.04	0.02	0.04	0.06	0.02
Max	0.52	0.52	0.00	0.31	0.30	-0.01	0.43	0.42	0.00	0.43	0.43	0.00	0.47	0.52	0.05
Median	0.42	0.35	-0.07	0.23	0.18	-0.05	0.31	0.23	-0.08	0.35	0.28	-0.06	0.27	0.14	-0.13
Min	0.30	0.14	-0.15	0.14	0.06	-0.08	0.17	-0.01	-0.18	0.21	0.06	-0.14	0.00	-0.05	-0.06

Table 6.4: Statistics of extracted vegetation indices from 9 P and NP sample oil spill sites in 2013 (pre-spill not polluted)

Sample	NDVI			SAVI			ARVI			G/NIR			G/SWIR		
	NP	P	Change (Δ)	NP	P	Change (Δ)	NP	P	Change (Δ)	NP	P	Change (Δ)	NP	P	Change (Δ)
Points															
SP1	0.56	0.60	0.04	0.29	0.33	0.05	0.47	0.52	0.05	0.46	0.51	0.05	0.23	0.07	-0.16
SP2	0.62	0.34	-0.08	0.33	0.28	-0.05	0.54	0.45	-0.10	0.51	0.44	-0.06	0.29	0.03	-0.26
SP3	0.56	0.49	-0.07	0.30	0.25	-0.05	0.48	0.40	-0.08	0.46	0.41	-0.05	0.13	-0.02	-0.15
SP4	0.46	0.15	-0.31	0.21	0.05	-0.16	0.35	-0.01	-0.36	0.34	0.05	-0.30	0.34	0.57	0.23
SP5	0.42	0.33	-0.09	0.19	0.13	-0.05	0.31	0.21	-0.10	0.30	0.22	-0.09	0.50	0.45	-0.05
SP6	0.47	0.46	-0.01	0.22	0.23	0.00	0.37	0.36	-0.01	0.37	0.37	0.01	0.18	0.08	-0.10
SP7	0.56	0.40	-0.16	0.28	0.20	-0.08	0.48	0.29	-0.19	0.45	0.36	-0.09	0.31	-0.13	-0.43
SP8	0.50	0.33	-0.17	0.26	0.17	-0.09	0.41	0.21	-0.20	0.41	0.29	-0.12	-0.03	-0.15	-0.12
SP9	0.52	0.42	-0.10	0.26	0.20	-0.06	0.43	0.31	-0.12	0.42	0.34	-0.08	0.30	0.09	-0.21
Mean	0.52	0.41	-0.11	0.26	0.20	-0.05	0.43	0.30	-0.12	0.41	0.33	-0.08	0.25	0.11	-0.14
Std Dev	0.06	0.13	0.07	0.04	0.08	0.04	0.07	0.16	0.08	0.06	0.14	0.07	0.15	0.24	0.10
Std error	0.02	0.04	0.02	0.01	0.03	0.01	0.02	0.05	0.03	0.02	0.04	0.02	0.05	0.08	0.03
Max	0.62	0.60	0.04	0.33	0.33	0.05	0.54	0.52	0.05	0.51	0.51	0.05	0.50	0.57	0.23
Median	0.52	0.42	-0.09	0.26	0.20	-0.05	0.43	0.31	-0.10	0.42	0.36	-0.08	0.29	0.07	-0.15
Min	0.42	0.15	-0.31	0.19	0.05	-0.16	0.31	-0.01	-0.36	0.30	0.05	-0.30	-0.03	-0.15	-0.43

Table 6.5: Statistics of extracted vegetation indices from 9 P and NP sample oil spill sites in 2015 (post-spill not polluted)

Sample	NDVI			SAVI			ARVI			G/NIR			G/SWIR		
	NP	P	Change (Δ)	NP	P	Change (Δ)	NP	P	Change (Δ)	NP	P	Change (Δ)	NP	P	Change (Δ)
Points															
SP1	0.46	0.54	0.07	0.25	0.30	0.05	0.36	0.45	0.09	0.39	0.45	0.06	0.19	0.20	0.01
SP2	0.55	0.44	-0.11	0.31	0.24	-0.07	0.46	0.34	-0.13	0.46	0.38	-0.08	0.29	0.04	-0.25
SP3	0.49	0.38	-0.11	0.28	0.20	-0.08	0.40	0.27	-0.13	0.41	0.33	-0.08	0.13	0.00	-0.12
SP4	0.30	0.12	-0.18	0.14	0.05	-0.09	0.17	-0.04	-0.21	0.22	0.04	-0.17	0.35	0.49	0.14
SP5	0.23	0.12	-0.11	0.11	0.05	-0.05	0.09	-0.04	-0.13	0.15	0.05	-0.10	0.46	0.36	-0.10
SP6	0.36	0.34	-0.01	0.18	0.18	0.00	0.24	0.22	-0.01	0.28	0.28	0.00	0.20	0.11	-0.09
SP7	0.40	0.30	-0.10	0.21	0.15	-0.06	0.29	0.17	-0.12	0.33	0.26	-0.07	0.27	-0.04	-0.31
SP8	0.35	0.24	-0.11	0.19	0.13	-0.06	0.23	0.10	-0.12	0.30	0.22	-0.08	0.05	-0.09	-0.14
SP9	0.40	0.32	-0.08	0.21	0.16	-0.05	0.29	0.19	-0.09	0.32	0.26	-0.06	0.25	0.11	-0.14
Mean	0.39	0.31	-0.08	0.21	0.16	-0.05	0.28	0.18	-0.10	0.32	0.25	-0.06	0.24	0.13	-0.11
Std Dev	0.10	0.14	0.04	0.06	0.08	0.02	0.12	0.16	0.05	0.10	0.14	0.04	0.12	0.19	0.07
Std error	0.03	0.04	0.01	0.02	0.03	0.01	0.04	0.05	0.01	0.03	0.04	0.01	0.04	0.06	0.02
Max	0.55	0.54	0.07	0.31	0.30	0.05	0.46	0.45	0.09	0.46	0.45	0.06	0.46	0.49	0.14
Median	0.40	0.32	-0.11	0.21	0.16	-0.06	0.29	0.19	-0.12	0.32	0.26	-0.08	0.25	0.11	-0.12
Min	0.23	0.12	-0.18	0.11	0.05	-0.09	0.09	-0.04	-0.21	0.15	0.04	-0.17	0.05	-0.09	-0.31

Tables 6.4 and 6.5 are the statistics of the vegetation indices extracted from P and NP sites for temporal analysis. Table 6.2 was used to analyse vegetation condition before the oil spills in 2013 and Table 6.5 for post spill analysis in 2015. Changes in vegetation spectral characteristics were assessed before and after oil spill for comparisons with the ones in 23/12/2014 (as spill date). It is assumed that vegetation spectral reflectance before (20/12/2013) and after (08/01/2015) the spill may differ with the ones at the P sites in 23/12/2014, depending on the time and volume of oil spill (discussed in Chapter 5). The time gap between oil spill event and image acquisition date could also influence the record of the vegetation signals by the sensor (discussed in Chapter 5). The result of temporal paired t-test analysis of means of vegetation indices from P and NP sites in 20/12/2013 (pre-spill), 23/12/2014 (spill date) and 08/01/2015 (post spill) is presented in Table 6.6.

Table 6.6: Analysis of change detection using paired t-test statistics of means of vegetation indices at the P and NP in 2013, 2014 and 2015.

<i>Indices</i>	2013 (Pre-Spill Not Polluted)		2014 (Spill Date - Polluted)		2015 (Post-Spill-Not Polluted)	
	<i>Change (Δ)</i>	<i>P-values</i>	<i>Change (Δ)</i>	<i>P-values</i>	<i>Change (Δ)</i>	<i>P-values</i>
	P Sites vs NP sites		P Sites vs NP sites		P Sites vs NP sites	
NDVI	-0.11	*	-0.08	***	-0.08	***
SAVI	-0.05	*	-0.04	***	-0.05	**
ARVI2	-0.12	*	-0.09	***	-0.10	***
G/NIR	-0.08	*	-0.06	**	-0.06	**
G/SWIR	-0.14	*	-0.09	*	-0.11	*

*** p -value < 0.0001 , ** p -value < 0.005 , ** p -value < 0.05 , * p -value < 0.01 , ^{ns} p -value ≥ 0.05

Key: ****Highly significant, ***Highly significant, **Very significant, *Significant, ^{ns}Not significant

In Table 6.6 vegetation indices extracted from the 20/12/2013 image at the both P and NP sites were statistically compared. This was done to determine whether biophysical characteristics of vegetation at the P and NP sites before the oil spill differs. The results show that the 5 vegetation indices indicated less significant difference in 20/12/2013 at ($p < 0.05$) but in 2014 three indices (NDVI, SAVI and ARVI2) indicated highly significant difference between the vegetation at P and NP sites with ($p < 0.005$). G/NIR shows a very significant

difference in 2014 while G/SWIR remains relatively the same (no change). In post spill image in 2015 which has a small time difference with the image 23/12/2014 showed almost the same results with the exception of G/NIR and G/SWIR with a significant difference. The similarity in the results found in image (23/12/2014) used for the observation of the oil spill and the post spill (08/01/2015) have a relative difference in acquisition date (16 days). The result suggests that the small difference in the image acquisition date could be that the vegetation status between the two dates (images) and may have not changed within this period. This could also mean that the changes in biochemical and biophysical properties of vegetation due to oil spill at these P sites remain relatively unchanged before the acquisition of post spill data. There is also a possibility that few days between the spill date and image date the surface changes are less likely to occur within such a short period, although atmospheric conditions may change. Thus the satellite sensor may just have recorded a small changes that occurred in the vegetation signals though it does not suggest the technique and results are not valid. It is will ideal to use an available image with appropriate time difference with that of spill date to improve the detection of changes in the vegetation affected by oil spill.

Temporal analysis was done to justify the spatial analysis conducted in section 6.4.1 and 6.5.1. Table 6.6 showed that in the year 20/12/2013 data before the oil spill events, vegetation at the P and NP sites exhibits similar characteristics. The 5 indices indicated less significant difference between vegetation at supposed polluted points and the ones at NP sites, this result suggests that vegetation biochemical and biophysical properties at these two sites are not significantly different with $p < 0.01$. At the same sites in 23/12/2014 (the year of spill events) there is a significant difference with $p < 0.005$ for (NDVI, SAVI and ARVI2) and G/NIR and G/SWIR with $p < 0.01$. The three indices were capable of providing some evidence of plant biochemical alterations in vegetation affected by oil pollution. These 3 indices were capable of discriminating changes vegetation biochemical and biophysical properties before spill and the spill event data and the remaining two were not in SS2. To also confirm if the vegetation indices at these sites in 23/12/2014 vary with the ones obtained after the oil spill in 08/01/2015, the result in Table 6.6 showed that only two indices (NDVI and ARVI2)

indicated highly significant difference between the P and the NP sites with $p < 0.005$, SAVI and G/NIR with $p < 0.05$ and only G/SWIR with $p < 0.01$. Based on the results it is proposed that there is not much difference in the vegetation conditions in 23/12/2014 (as oil spill events year) and 08/01/2015 (post oil spill year) at the P and NP sites. As previously stated, some vegetation affected by oil pollution in 23/12/2014 may still be under stress at the post spill data date (08/01/2015) as the time difference may be too short for a sensor to record any difference in the changes of the affected vegetation but this does not invalidate the result and the technique. The post spill data for 08/01/2015 may be appropriate for the assessment of oil affected vegetated sites as the sensor may be able to record changes in the vegetation signal at these sites. It is also expected that at these affected sites vegetation could also recover, but that may depend on the level of impact (volume of oil spill, type of oil etc.) and environmental conditions that could influence the vegetation recovery. The results in this section for SS2 appear to be slightly different with the ones obtained in SS1 because of the post spill data used 08/01/2015. In the analysis of data in SS1 (Chapter 4) significant differences in vegetation conditions before and after oil spill at the P and NP sites were observed. This is because the images used for analysis of post oil spill have relative time difference between the oil spill event and the post spill data.

6.4.3 Changes in vegetation affected by oil pollution at the P sites (2013, 2014 and 2015)

Table 6.7: shows the statistical analysis of the mean values for indices of vegetation affected by oil spill at the P sites.

Indices	Change (Δ) 2013 vs 2014	Change (Δ) 2014 vs 2015
	<i>p-values</i>	<i>p-values</i>
NDVI	***	*
SAVI	ns	***
ARVI2	***	*
G/NIR	***	**
G/SWIR	ns	****

*****p-value* < 0.0001, *** *p-value* < 0.005, ** *p-value* < 0.05, * *p-value* < 0.01, ^{ns} *p-value* \geq 0.05
Key: ****Highly significant, ***Highly significant, **Very significant, *Significant, ^{ns}Not significant

Table 6.7 shows the temporal difference in the mean of vegetation indices at the P sites in 2013 (when there was no oil spill has occurred) and the oil spill date in 2014 (when the oil spill has occurred). In 2013 the vegetation at the P sites shows that three indices (NDVI, ARVI2 and G/NIR) indicated significant difference with the same vegetation in 2014 and not significant (ns) for SAVI and G/SWIR. The post-spill results showed that there are significant difference between P sites in 2014 and 2015 (after oil spill has occurred) with at least a $p < 0.01$ for NDVI and ARVI2, $p < 0.05$ for G/NIR, $p < 0.005$ for SAVI and $p < 0.0001$ for G/SWIR.

The analysis of vegetation condition before the spill was statistically assessed in relation to the ones at the oil spill date (2014). This is to confirm the assumption that vegetation index values before (2013) and after (2015) the oil spill impact may differ to the ones at P sites on the spill date (2014). The results show that some indices (SAVI and G/SWIR) indicated no significant difference between vegetation at the P sites in 2014 and the one before the oil spill in 2013. Three indices (NDVI, ARVI2 and G/NIR) indicated significant differences between the vegetation at the P sites in 2013 and the ones at the same sites in 2014 with $p < 0.005$. In this result 3 (ARVI2, G/NIR and NDVI) indices were able to detect changes in biochemical and biophysical characteristics of vegetation affected by oil pollution and the unaffected ones and two (SAVI and G/SWIR) did not. As found in chapter 4 the best performing indices are ones that combine the elements of red and NIR spectral bands which are capable of detecting changes in the chlorophyll contents in plants (leaf) in red channel and leaf structure in NIR (Hongliang et al., 2005) but SAVI which also belong this group did not in this SS2. This result showed that the 3 BMVI (NDVI, ARVI2 and G/NIR) at the vegetation at the polluted sites before the spill significantly differs ($p < 0.005$) as obtained during the spill event date and SAVI and G/SWIR not significant ($p \geq 0.05$) during 2013 and 2014. While in the post spill analysis it appears that the 2 indices (SAVI and G/SWIR) indicated significant difference with p-values between ($p < 0.0001$ to 0.005) compared to NDVI, ARVI2 and G/NIR with ($p < 0.01$ to 0.05). The result suggested that some indices (NDVI, ARVI2 and G/NIR) were better in discriminating vegetation affected by oil spill before and during the

spill year (2013 and 2014), but not effective during post spill (2014 and 2015) where SAVI and G/SWIR were better. It is not clear if the result in this study has been influenced by local physical environmental variation. It could also be related to characteristics of spectral bands combined to derive the indices for the detection of vegetation in oil polluted sites. Although, in chapter 4 the indices which combined the SWIR band with the visible (G) band (e.g. the G/SWIR band) performed well in detecting the difference before and after pollution at the polluted sites.

6.4.4 Analysis of vegetation condition at the NP sites (2013, 2014 and 2015)

Table 6.8: Temporal comparison of means of indices using a paired t-test of vegetation indices at the NP sites.

Indices	Change (Δ) 2013 vs 2014	Change (Δ) 2014 vs 2015
	<i>p-values</i>	<i>p-values</i>
NDVI	****	**
SAVI	***	***
ARVI2	****	*
G/NIR	****	ns
G/SWIR	ns	ns

*****p-value* < 0.0001, ****p-value* < 0.005, ***p-value* < 0.05, **p-value* < 0.01, ^{ns}*p-value* \geq 0.05

Key: ****Highly significant, ***Highly significant, **Very significant, *Significant, ^{ns}Not significant

Table 6.8 demonstrates the analysis of temporal vegetation condition at the sites to confirm whether there are changes in the biochemical and biophysical status of the vegetation at the NP sites. This will help to compare with the ones at the P sites. It is expected that the vegetation characteristics at NP sites may remain unaffected (as control sites) by oil spill, since no spill effects were observed over the sites. It is also assumed that there was no influence of climatic and environmental conditions, spatial and temporal variations of the atmosphere (Bannari et al., 1995, Baret and Guyot, 1991) at the spill sites. Since the study used image data of the same period of the year to avoid changes in vegetation phenology, it is assumed that vegetation at the NP sites may not change much over the period of time (i.e. January and December months). Though, it is expected that some local physical and environmental factors may cause changes in the vegetation cover that could be related to

vegetation stress. Another change that may result in the variation of the vegetation signals is the image data with noise such as haze, dust, cloud etc. may affect the quality of the image and subsequently the output of the results. From the Table 6.2.6 NDVI, SAVI, ARVI2 and G/NIR indicated a highly significant difference in vegetation characteristics between before the spill in 2013 and the oil spill date in 2014 with $p < 0.0001$ to 0.005 . These results suggest there are differences between vegetation at the NP site before and on the spill date even though no spill impact on vegetation is expected at these sites as they are further away from oil facilities. Therefore it may be assumed that the difference in the vegetation status at the sites could not be related to only oil pollution. Also there is a possibility that image quality (such as effect of haze, dust etc.) and environmental factors, vegetation phenology of the area might have contributed to these differences. The only index (G/SWIR) with no difference between in the vegetation in 2013 and 2014 suggests that vegetation during the period remained relatively the same over time. The result of this index may have been influenced by the function of SWIR which has the potential to detect changes in water contents in leaves (plants). In the post spill analysis the G/SWIR remain consistent by indicating no significant difference in vegetation at spill date (2014) and post spill (2015) and G/NIR showing similar result. NDVI, SAVI and ARVI2 indicated significant difference with $p < 0.005$ and < 0.01 for vegetation condition in 2014 and 2015. The performance of these indices for example NDVI and SAVI may have been affected by the effects of background as demonstrated in (Díaz and Blackburn, 2003) in this study site. In the overall performance of vegetation indices in this study NDVI and ARVI2 are found to be effective and consistent in the results. The performance of these two indices could be related to their combination spectral wavelength bands (NIR and red channels) in their calculation.

6.4.5 Mapping likely stressed vegetation affected by oil pollution

In the previous sections NDVI demonstrated as the most useful in discriminating between vegetation at P and NP sites, and before and after oil spills and that was also discussed in chapter 4. The index has shown consistent sensitivity in terms of discriminating vegetation affected by oil spill and the non-affected ones. The index has shown the ability to separate or distinguish between vegetation affected by oil pollution from NP. The NDVI has also

exhibited clearly the capability to detect a change in vegetation pigments before and after oil spills are the reason that was selected to map the likely polluted sample points in 2014.

Table 6.9: NDVI values and oil spill data used for mapping likely SP in 2013 and 2014

Sample Point	Time Period (Days)	Quantity of Oil Spill (bbl)	NDVI 2014	NDVI 2013	NDVI (Δ) (2014 -2013)
SP1	10	108	0.52	0.60	-0.08
SP2	28	5000	0.25	0.34	-0.09
SP3	106	na	0.43	0.49	-0.06
SP4	108	60	0.14	0.15	-0.01
SP5	113	1000	0.16	0.33	-0.17
SP6	125	3	0.42	0.46	-0.04
SP7	na	na	0.33	0.4	-0.07
SP8	140	7.7	0.31	0.33	-0.02
SP9	158	60	0.35	0.42	-0.07

From Table 6.9 shows the changes in NDVI between 2013 and 2014 has indicated a dropped at some polluted sites. The minimum drop in the NDVI between the two periods is recorded at SP4 (-0.1) and maximum at SP5 (-0.17). As observed in the NDVI map in Figure 6.5 the SP4 appears to show a sign of more stress compared to SP5. It cannot be conclusive to suggest that the stress could only be related to oil pollution as the NDVI for the both years did not show much difference. The average values of NDVI were calculated for the likely polluted sites and used for mapping the likely polluted areas. The average NDVI value computed is 0.32 and the standard deviation of 0.12 and the minimum is 0.14 thus the likely polluted areas map ranges between NDVI values 0.12 to 0.32, the 0.14 used as minimum and 0.32 as the maximum likely polluted areas from the sample spill sites.

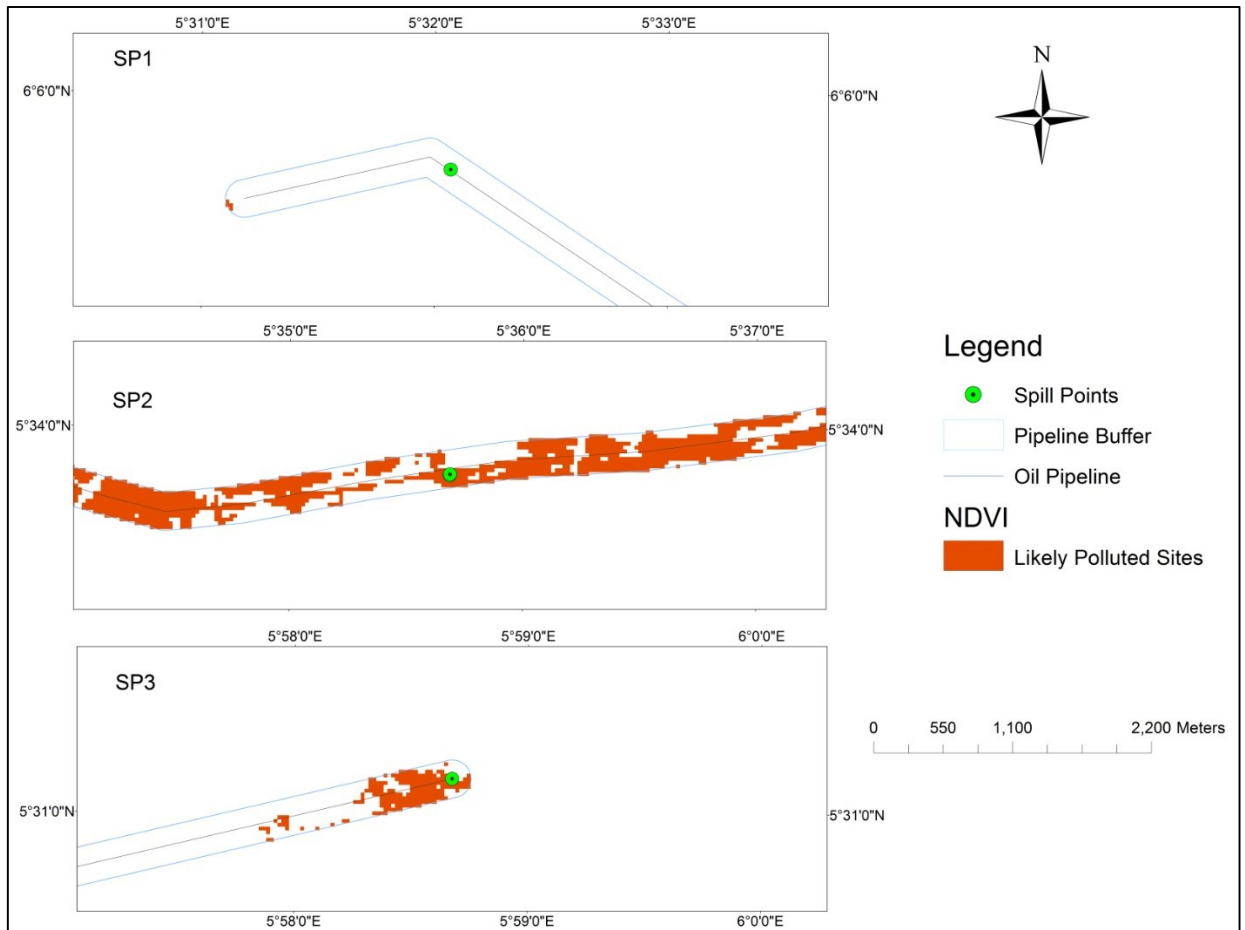


Figure 6a: Areas identified as likely vegetation stress based on the NDVI in 2014

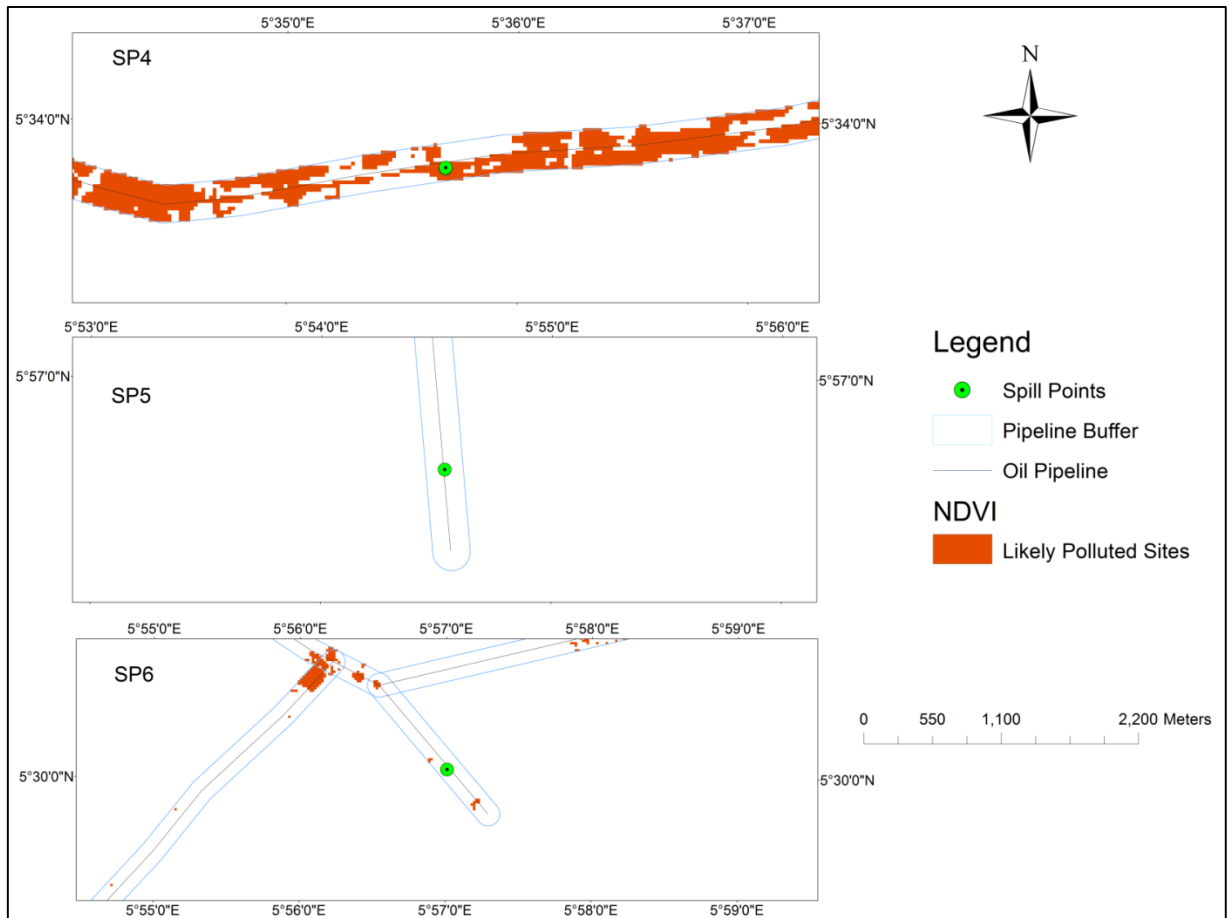


Figure 6b: Areas identified as likely vegetation stress based on the NDVI in 2014

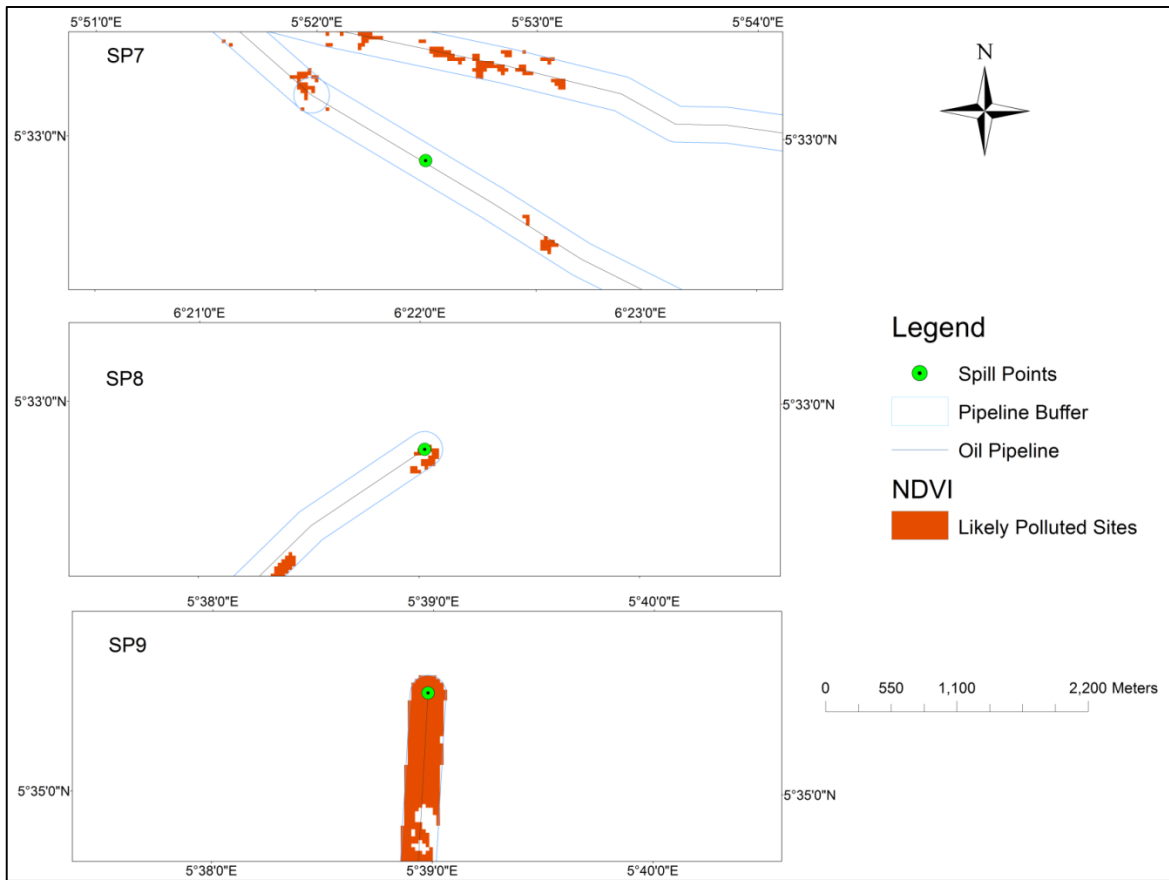


Figure 6c: Areas identified as likely vegetation stress based on the NDVI in 2014

6.5 Discussion

The main objective of this analysis is to test the applicability of techniques from Chapter 4 in a different study sites with relatively similar physical environmental conditions. The technique was replicated in this study site and appears to present a relatively similar result to the ones obtained in chapter 4. The variations in some of the results may have been influenced by relative differences in the physical environmental conditions, satellite sensor characteristics, volume of oil spill, and time gap between oil spill event and image acquisition date etc. Notwithstanding, the best performed indices used in Chapter 4 were applied in the SS2 and showed a potential of replication in this study site (SS2). For example in Figure 6.4 the box plot show that the five indices (NDVI, SAVI, ARVI2, G/NIR and G/SWIR) were capable of detection of changes in vegetation chlorophyll content, leaf internal structure and

water contents in leaf that relates stress. In the box plot the indices show potential in discriminating between stress in vegetation resulting in vegetation biochemical alterations at the P sites and the ones at the NP sites. Researches have attributed these biochemical alterations in forest areas (Arellano et al., 2015, van der Meer et al., 2000, Zhu et al., 2013, Noomen et al., 2012) to oil pollution. This analysis aimed to assess the capacity of these indices to detect changes in the vegetation affected by oil spill and the unaffected ones. The assumptions that were stated at the beginning of the chapter include the statistical testing of these indices to differentiate between vegetation affected by oil at the P and NP sites in 2014. The results from Table 6.2.1 showed that there are significant difference between vegetation at the P and NP sites with $p < 0.01$ (NDVI, SAVI, ARVI2 and G/NIR) while G/SWIR with no significance difference. It is not clear if the lack of sensitivity at these sites could be as a result of the new sensor (Landsat 8) which has relatively narrow spectral bands compared to the previous sensors (Landsat 5 and 7) used in chapter 4. In the case of G/SWIR index for example in Landsat 8 data the spectral wavelengths is between (0.53 - 0.59 nm) for green band and (1.57 - 1.65 nm) for SWIR 1 compared to L7 with (0.52-0.60 nm) for green and (1.55-1.75 nm) for SWIR 1 respectively. Though, it is expected that specific band designations will differ from Landsat 1-3 to Landsat 4-5, Landsat 7 to Landsat 8. In Chapter 4 (SS1) the 5 best performing indices were the ones derived from red and NIR channels which appear to be sensitive in this analysis of vegetation at P and NP sites in SS2 with the exception of G/SWIR and G/NIR. The consistency of the indices derived from red and NIR channels could be because of their sensitivity to changes in leaf chlorophyll content and internal structure. These features make them capable of detecting stress symptoms of vegetation resulting from oil pollution since the effect of the oil spill can cause biochemical changes that is recorded in the red and NIR channels. Stress levels may vary dependent on the volume of oil spill, vegetation type, oil type, other environmental conditions (e.g. soil type and soil organic matter) (Pezeshki et al., 2000), sensitivity of the index derived from broadband channels, and sensor resolution etc. In this study site (SS2) the three indices (NDVI, SAVI and ARVI2) were able to detect changes in pigment concentration and leaf structure from red and NIR channels respectively of vegetation affected by oil pollution at the P sites. The low levels of chlorophyll recorded can result in vegetation stress as it may

reduce photosynthetic activity in vegetation affected by oil pollution at the investigated sites. At the NP sites the indices were not able to detect much of the change in vegetation biochemical and biophysical properties where no oil spills were recorded. It is expected that the observations in the vegetation biochemical and biophysical properties at these sites could be used to affirm that vegetation at P sites may have been exhibiting symptoms of stress due to oil pollution compare to the ones at NP sites.

It also worth assessing the general vegetation conditions in the study area before and after oil spill to justify if they differ with ones found at the P and NP sites over time. The results in Table 6.2.4 show that vegetation condition in 2013 between the P and the NP sites were significant with $p < 0.01$ for all the 5 indices. Similar approach was applied for 2014 (year of oil spill) the results indicated 3 indices (NDVI, SAVI and ARVI2) with a highly significant difference of $p < 0.005$ between vegetation conditions at the P and NP sites. G/NIR and G/SWIR indicated significance of $p < 0.01$ between the vegetation at P and NP sites. In 2015, which was used as the post spill year, significant difference was observed between vegetation at the P and NP and only G/SWIR maintaining consistency over the period (2013, 2014 and 2015). Green (G) band in Landsat 8 emphasizes on peak of vegetation, which is useful for assessing plant vigour. This result may suggest that vegetation biochemical status in 2013 between N and NP sites was relatively similar, though there could be alterations but these may be relative between the two sites. In 2014 vegetation status at the P and NP sites appears to differ which could be as a result of changes in vegetation affected by oil pollution with the ones at the NP sites. The post spill analysis which did not presented much difference with the ones in 2014 could suggest that vegetation conditions in 2015 are similar with no significant changes. The assumption that the vegetation condition at the same polluted point in 2013 (pre-spill) and 2014 (spill date) could differ was also statistically tested. The results show that only two indices SAVI and G/SWIR did not detect any significant difference between vegetation at the P sites in 2013 and 2014. For example, SAVI which is a modification of NDVI to adjust the influence of soil has been found to be less sensitive to changes in vegetation but more sensitive to atmospheric differences (Huete, 1988). But NDVI, ARVI2 and G/NIR indicated a significant difference during the same period and

sample points. In the post spill there are highly significant differences between vegetation condition in 2014 and 2015 indicated by SAVI ($p < 0.005$), NDVI ($p < 0.05$) and ARVI2 ($p < 0.01$) while the G/NIR and G/SWIR with no significance difference. It can be argued that the significant difference indicated by SAVI, NDVI and ARVI2 were poor and inconsistent in their sensitivity in the post spill vegetation at the NP sites. The only consistent index is the G/SWIR at pre (2013 vs 2014) and post (2014 vs 2015) spill at the NP sites indicating no significance difference in this study sites compare to the results in chapter 4 where all the 5 indices were consistent. The performance of this index could be influenced by spectral band combination (from Landsat 8) for example G (green) at 0.53 - 0.59 nm which is capable of sensing peak vegetation and useful for assessing plant vigour. Also SWIR at 1.57 - 1.65 nm has capacity to discriminate moisture content of soil and vegetation and penetrates thin clouds. These wavelength bands in L8 are narrower compare to the ones obtained in L5 and 7 (e.g. Green - L8: 0.53 - 0.59 nm and L7 - 0.52 - 0.60 nm while SWIR L8: 1.57 - 1.65 nm and L7 - 1.55 - 1.75). It has been shown that spectral narrow bands are sensitive to distinct biophysical and biochemical characteristics of vegetation (Marshall et al., 2016) though with reference to hyperspectral data.

From the NDVI map of likely polluted sites there was no certainty that the alterations in vegetation biochemical and biophysical properties could be as a result of either oil pollution or other local environmental conditions with a drop in NDVI value from 0.33 in 20013 to 0.16 in 2014. However, for example location of SP5 near built up areas, there are possibilities that built up land cover signals mixed up with the vegetated polluted pixels as appear in the map Figure 6.6. There are also noticeable drop in NDVI at SP2 (-0.09) and SP1 (-0.08), but despite the drop in the index value did not really match with the one in the image e.g. SP1 show that vegetation at this site may have not been impacted by the oil pollution. Although, at SP2 the volume of oil spill (5000 bbl.) involved and time (28 days) the image was acquired after oil spill may have influenced the detection of spectral changes in vegetation in Figure 6.5. It can also be argued that the vegetation near the oil pipelines could be stressed vegetation related to oil pollution.

6.6 Summary

In conclusion, the findings revealed that the SS2 with shows statistical results from vegetation indices are not significant compared to the one in SS1. The performance of these indices in both SS1 and SS2 could be influenced by variation between different vegetation types and between individual pigments between the same vegetation type (Blackburn, 2007). These variations could also be attributed to some factors such as difference in physical environment, climatic conditions, volume of oil spill, image and spill date etc. The data used in the two study sites are of the same sensor type but with relative differences in their characteristics for example in SS1 used (Landsat 5 and 7) and SS2 Landsat 8. The difference in spectral band properties may influence the output of reflectance image for example aerosol band (band1) in most cases the model uses radiance values for this band which is not found in other Landsat data. Thus techniques in Chapter 4 can be successfully replicated or used in another environment with a relatively similar climatic condition and physical environmental characteristics using vegetation indices derived from other sensors e.g. Landsat 8 these has been demonstrated in (Rajitha et al., 2015). Other factors not fully assessed and validated in SS2 are volume of oil spill and time gap between oil spill and image acquisition dates. However, time gap between oil spill and image date in SS2 could be influential in detection of impact of oil pollution on vegetation. For example number of days between the oil spill and image is 1 day minimum and the maximum is 6 months. Thus, in SS2 it might be possible that sensor may have not recorded spectral changes in vegetation properties due to low volume of oil spill at some spill sites. Further study will require considering other factors such as variations in local physical environment, climatic conditions, satellite sensor characteristics (spectral bands) etc.

Chapter 7 : Discussion, conclusion and future work

7.1 Discussion

The aim of this thesis was to contribute knowledge towards the identification and detection of the impact of oil pollution on vegetation health from oil pipelines using BMVIs derived from satellite data in the Niger Delta. The three results chapters (4, 5 and 6) addressed the following research questions as follows:

7.1.1 Are the BMVIs capable of detecting changes in the leaf pigments of vegetation affected by oil pollution in mangrove forests?

In recent times there have been developments in the monitoring of vegetation stress in an oil polluted environment. Remote sensing has been demonstrated to be a capable and effective technique for detection, monitoring and quantification of vegetation stress levels impacted by oil spills from pipelines (van der Werff et al., 2008, Li et al., 2005). Changes in vegetation health can be related to different environmental stressors, thus detecting the causes of stress in vegetation can be challenging. This study intended to detect vegetation stress relating to oil pollution impact from oil pipelines in a mangrove forest where oil operations are carried out. Stress in vegetation could be as a result of alterations in biochemical and biophysical properties (Noomen et al., 2008). For example a gradual loss of photosynthetic pigments in plants and collapse in a cell wall structure of a leaf, are good influential factors and indicators for assessing vegetation health (Jensen, 2014, Mather and Koch, 2011a). These alterations or changes in vegetation pigments can reflect in spectral reflectance in visible and NIR wavelengths from the satellite data (Sims, 2002). Guyot et al., (1992), Noomen et al., (2012) have also shown that change in the colour of leaves, stems and trunks are very good indications of a plant's response to oil concentration or stress. Studies have focused on using handheld to satellite borne hyperspectral data to detect vegetation affected by oil pollution in a pipeline environment (van der Meer et al., 2000, Noomen et al., 2015). Thus, this study focused on assessing the capabilities of BMVIs derived from multispectral data from Landsat for the detection of oil impact on vegetation in the Niger Delta mangrove forest.

Twenty vegetation indices, derived from multispectral satellite data (Landsat), were used to test their capabilities and see what made them unique for detecting the impact of oil pollution on the biochemical and biophysical characteristics of vegetation. Statistical tests were carried out on the entire sample of polluted and non-polluted sites, in order to assess the indices that are sensitive to changes in vegetation at the two sites. Statistical analysis was used to determine whether vegetation status has changed before and after oil pollution due to pollution impact. The best performing indices in detecting the impact of pollution on vegetation affected by oil spills were those derived from a combination of spectral reflectance from the visible and NIR wavelengths. Both the visible and NIR band were found to be capable of indicating changes in chlorophyll content and leaf structure related to changes in vegetation health, as NIR decreases in reflectance at 800 nm and 1300 nm due to oil pollution (Zhu et al., 2013). It has also been shown that evidence of stress in vegetation and changes in plant pigments are commonly noticed in the visual and NIR portions (Rosso et al., 2005). It is known that the reflectance signatures of vegetation in these bands are sensitive to any changes in vegetation condition. Therefore, any changes in vegetation's biophysical and biochemical characteristics induced by oil pollution would affect the reflectance signature of vegetation. In this study the indices derived using these bands (visual and NIR) have the potential to detect alterations in chlorophyll content and leaf structure of vegetation due to oil pollution, similar to findings in (Arellano et al., 2015). The vegetation indices which included all the three bands in the visible spectra (i.e. B, G and R bands) showed mixed results in their ability to detect changes in vegetation induced by oil pollution. Only the GLI (Green Leaf Index), which combines all the visible bands, has indicated significant difference between the vegetation condition in the P and NP sites, whilst the G/R and the PPR indices did not detect any difference between the two sites. The indices which combined the SWIR band with the NIR performed well in discriminating vegetation affected by pollution, while the index where the SWIR was combined with the green band did not. Vegetation indices which included bands not often used in deriving indices (i.e. blue and the green bands), were found to be relatively effective in detecting vegetation affected by oil pollution. These indices include the GBNDVI, ClGreen, GRNDVI and G/NIR. The ability of these existing indices to differentiate between the P and NP sites could be influenced by the spectral band

combination, characteristics, sensitivity or suitability of the index to vegetation and the nature of land cover at the affected sites. The temporal evaluation carried out on the 20 BMVIs revealed the differences in vegetation index values before and after pollution (with higher values) compared to the spill event date (with lower values). Twelve BMVI values showed significant temporal changes at the polluted sites, which were not detected in the non-polluted sites (Table 4.2). The temporal changes of the BMVIs at the spill sites could be attributed to biophysical and biochemical alteration in the vegetation due to the effects of oil pollution. Five BMVIs; NDVI, SAVI, ARVI2, G/NIR and G/SWIR were found to be consistently sensitive to oil pollution effects as shown by their significant temporal changes between pre and post spill events.

From the evaluation carried out on the 20 BMVIs, this study showed that some indices have shown capabilities. However, the best performing indices capable of detecting vegetation affected by oil pollution were those derived using a combination of reflectance from the visible and NIR wavelengths. Based on the results from this study, it can be concluded that these indices have demonstrated the capacity to detect changes in vegetation (chlorophyll contents, leaf structure, water contents etc) affected by oil pollution and can be used to monitor pollution in forest areas. However, results from this study can be improved upon significantly if high resolution data (of at least less than 5m) is available, since 30 m resolution may not be able to accurately capture vegetation signals affected by small volumes of oil spill.

7.1.2 How do the identified factors influence detectability of vegetation affected by oil spills using spectral vegetation indices?

A number of factors were identified that were assumed to be influential in the detection of oil pollution using spectral vegetation indices. This objective is aimed at determining the statistical relationship between these factors and the five selected vegetation indices. Below are summaries of the factors (volume of oil spill, variation in spatial distance from spill point and time gap between oil spill and image acquisition date).

How can the volume of oil spill influence detection of vegetation affected by oil pollution?

When hydrocarbons are released into the natural environment, characterising how the environment is affected could depend on the weathering processes of the sites (Osuji and Ezebuio, 2006). It has been shown that oil characteristics and weathering (i.e. change in composition of the oil) can reduce the quantity of oil released into the environment (Wang et al., 2013b). It is well understood that the volume of oil spilled into the environment can deplete over time and reduce the quantity spilled, depending on the chemical and biological properties as well as type of oil involved (Luis, 1993, Osuji and Ezebuio, 2006, Noomen et al., 2012). Thus, the impact of oil pollution on vegetation can be influenced by the quantity of oil released into the environment. Studies on the effect of time on the influence of volume of spill on detectability of oil impact on vegetation using BMVIs is limited. Thus, this study had assumed and tested how the volume of oil spill could impact on vegetation health and be related to a drop in the values of vegetation indices.

In order to establish whether the volume of oil spill could influence detectability of oil impact on vegetation health, the assumption that a certain volume of oil spill would impact vegetation was statistically tested. This was done to determine what quantity of oil spill would indicate a relationship with a change in the vegetation indices. Based on the performance of the 5 BMVIs (NDVI, SAVI, ARVI2, G/NIR and G/SWIR) that were chosen and used to test the effect of volume of oil spill on impact on vegetation. It has been shown that the impact of pollution on vegetation health and vigour depends on the oil spilled in the environment, and it is assumed that a larger volume may impact more severely on vegetation compared to a smaller volume. It has been suggested that a larger oil spill lowers oxygen concentration in soil, which may affect plant health in a polluted environment. These effects can be attributed to changes in vegetation chemical contents and structure as well as spectral reflectance. Noomen (2007), found that there are strong relationships between hydrocarbon and oxygen concentration that may be responsible for changes in the biochemical and biophysical status of vegetation. In this study it was found that four (4) indices (NDVI, SAVI, ARVI2 and G/NIR) indicated a relationship with volume of oil, that could be termed as

relatively negative because the regression line tends to approach 0 (downward slope). Though the BMVIs relationship with the volume of oil spill is not strong enough to justify their performances, they show the potential for further study. Where there is a weak relationship, it could be as result of factors such as the time gap between the oil spill event and imagery date, local physical environmental factors, sensor resolution etc. Thus, the relationship between volume of oil and the vegetation indices was improved by further refining the time gap between oil spill and imagery date. Refining the number of days to less than 365 days (in Table 5.3) has improved the relationship between the volume of oil spill and the BMVIs. This result is similar to (Zhu et al., 2013) where BMVIs were used in estimating Total Petroleum Hydrocarbon (TPH), but for the case of this study, volume of oil spill was used instead of TPH. This result showed that volume of oil spill is related to changes in BMVI values and could be one of the influential factors in the detection of oil pollution impact on vegetation in the study area.

Can variation in spatial distance from the polluted point influence detection of oil pollution?

The variation in spatial distance was assessed to determine the impact of oil pollution on values of vegetation indices. The result showed that the relationship between the BMVIs from the three neighbouring pixels “pixel 1” (P1), “pixel 2” (P2) and “pixel 3” (P3) did not show significant variation in index values. This analysis was carried out after applying flow direction modelling to determine the likely flow direction of the oil pollution. The result found here could be linked to factors such as volume of oil spill and the extent of area coverage. Therefore, this factor is dependent on the volume of oil and ability of the oil spilled to migrate from the point of source.

Can the time gap between oil spill and image acquisition date have an influence on the detection of vegetation affected by oil spills?

It is assumed that oil characteristics change in composition and that over time, the spilled oil may deplete depending on the chemical and biological properties of the oil. This study assumed that the time gap between the oil spill date and image acquisition date can be an

influential factor in detecting oil pollution over vegetated areas. For example, as the number of days increases, there is a chance that the oil concentration may deplete and it may be difficult to detect the pollution as the vegetation at the sites may have recovered. The result here showed that there is a relatively better correlation between the number of days and the BMVIs, signifying that as the number of days increase, the BMVIs increase. Thus, it shows that time between the imagery and spill dates is crucial in detecting oil pollution and could be appropriate as from 20 to 237 days, but could also be dependent on the volume of oil spill. This may be interpreted as the vegetation at these sites recovering (as indicated by an increase in the values of BMVIs). This result may also be dependent on the volume of oil spilled, as the impact of larger spills may last longer at the polluted sites and there is a greater possibility of detecting the vegetation stress relating to the spill from satellite data. Sensor characteristics, such as temporal and spatial resolution, can improve the detectability of oil impact on vegetation, for example, the revisit time of satellite sensors with high resolution in order to capture possible cloud-free areas in the polluted environment. This can be helpful in capturing early symptoms in vegetation stress resulting from oil spills. Spatial resolution of sensors is also an important factor, as highlighted earlier that a 30m pixel may not be capable of detecting a small volume of oil spill that did not occupy a 30m pixel. Other local and physical environmental factors can also be considered when embarking on research of this nature.

7.1.3 Can the method developed be implemented in a different part of the wider study area?

The main aim of this chapter is to present an extension and replication of the method used in this part of the study site 1 (SS1) to test its potential replication in study site 2 (SS2). Replication of analytical techniques is carried out to judge the quality, reliability and consistency of results, and can be considered as good practice in analytical research. In chapter 4, vegetation indices were used to determine their capability for detecting oil pollution impact on vegetation health. The indices have shown the potential to detect and monitor changes in biochemical and biophysical properties of vegetation affected by oil pollution. The findings revealed that the statistical results in SS2 show that differences in the results are not very significant with to the ones found in SS1. The likely variations in the

results could be as a result of the influence in the variations in local physical environment between the two study sites (SS1 and SS2). Also, the sensors (Landsat 5, 7 and 8) have small variations in wavelength properties that could influence the calculation of vegetation indices used for the analysis (Rajitha et al., 2015).

7.2 Conclusion

All the vegetation indices derived from the multispectral data (Landsat 30m resolution) have demonstrated certain levels of capabilities and potential for detecting and monitoring oil pollution in a vegetated environment of this nature (mangrove forest). The results also showed that some BMVIs did not perform well in the detection of oil pollution. Their performance could be related to the size of oil spill and time factors analysed in chapter five. Characteristics of the spectral bands used for deriving these BMVIs can also influence their sensitivity to vegetation impacted by oil spills.

Two factors (i.e. volume of oil spill and time gap between spill event and image acquisition date) were identified to be influential factors in detecting vegetation affected by oil pollution using vegetation indices. These factors should be considered when carrying out similar studies. The variation in spatial distance on the detection of impact of oil polluted sites can be influential in areas with high topography, as the large oil spill can tend to migrate from the source. Thus, this factor can be applied in such areas with high topography, using the flow direction model to determine the flow direction of the oil spill. The variation in spatial distance of oil spill in this study did not indicate much influence on the detectability of oil spill using vegetation indices, due to the low topography of the area studied. However, this factor can also be dependent on the first two factors (volume and time) highlighted above.

From the validation of the technique in chapter six, there is the potential of replicating the technique in wider study areas with similar physical environmental characteristics. It is possible to conclude that the technique can be replicated in other study sites, whilst considering variations in environmental factors between study sites and data to be used.

7.3 Future work

- Most of the uncertainties and shortcomings of this study have already been highlighted in previous chapters. The proposals for direction of future work are based on the results, uncertainties and challenges from this research.
- The opportunity to consider the development of a hybrid vegetation index that combines the elements of the best vegetation indices evaluated in this study to optimize the method for detecting vegetation affected by oil pollution, could be explored. This can be done by evaluating the combination of spectral bands used in the calculation of the indices, in order to develop an improved algorithm from these BMVIs for oil pollution impact on vegetation.
- Some of the challenges the study had to deal with included the non-accessibility and cost implication of airborne and high resolution satellite data. Thus the study resorted to using vegetation indices derived from satellite sensors with medium resolution (Landsat data 30m resolution) for detecting oil pollution. This means that it was not possible to detect and map the volume of oil spill at some polluted sites using a 30m pixel resolution. But it has shown the capability of detecting a large volume of spill beyond a 30m pixel. This problem can further be addressed using vegetation indices derived from high resolution or airborne sensors for the detection of relatively small to large volumes of spill. Notwithstanding this, the Landsat 30m resolution has proven to a capability for monitoring vegetation affected by oil pollution at spill sites at a wider and temporal scale, where the size of oil spill is large e.g. at least above 300 bbl.
- Seasonality can also be a factor influencing the detection of pollution in mangrove forests like that of the Niger Delta. Oil spills that occur during the rainy season are difficult to detect due to persistent cloud cover in optical sensors. In some cases during the rainy season, vegetation at the oil polluted sites may recover, thereby

hindering the detection of oil impact on the vegetation using optical sensors. Using sensors operating at microwave wavelengths can penetrate the thick cloud cover, providing a viable option for detecting oil pollution during the wet season.

References

- Adejuwon, J. O. 2012. Rainfall seasonality in the Niger Delta Belt, Nigeria. *Journal of Geography and Regional Planning*, 5, 51-60.
- Agostini, P., Carlon, C., Critto, A., & Marcomini, A. 2007. A step toward contaminated megasite management: six European experiences at comparison in Velini, A. A. (ed) *Landfill research trends*, 47-73.
- Akners, S. 2004. *The Caspian: Politics, Energy and Security: Politics, Energy, Security*, London and New York, Routledge Curzin.
- Allen, J. R. L. 1965. Late Quaternary Niger Delta, and Adjacent Areas: Sedimentary Environments and Lithofacies. *AAPG Bulletin*, 49, 547-600.
- Amadi, P. A., Ofoegbu, C. O. & Morrison, T. 1989. Hydrogeochemical assessment of groundwater quality in parts of the niger delta, Nigeria. *Environmental Geology and Water Sciences*, 14, 195-202.
- Anejionu, O. C., Blackburn, G. A. & Whyatt, J. D. 2015. Detecting gas flares and estimating flaring volumes at individual flow stations using MODIS data. *Remote Sensing of Environment*, 158, 81-94.
- Anejionu, O. C. D., Blackburn, G. A. & Whyatt, J. D. 2014. Satellite survey of gas flares: development and application of a Landsat-based technique in the Niger Delta. *International Journal of Remote Sensing*, 35, 1900-1925.
- Anyadike, R. N. C. 1993. Seasonal and annual rainfall variations over Nigeria. *International Journal of Climatology*, 13, 567-580.
- Aregheore, E.M., 2005. Country pasture/forage resource profiles: Nigeria. Food and Agriculture Organization of the United Nations. [Accessed 23/05/2016].
- Arellano, P., Tansey, K., Balzter, H. & Boyd, D. S. 2015. Detecting the effects of hydrocarbon pollution in the Amazon forest using hyperspectral satellite images. *Environmental Pollution*, 205, 225-239.
- Astm, D., 2003. 4318-00, 2003 ASTM D 4318-00, Standard test methods for liquid limit, plastic limit, and plasticity index of soils. Annual Book of ASTM standards, pp.582-595
- Bannari, A., Morin, D., Bonn, F. & Huete, A. R. 1995. A review of vegetation indices. *Remote Sensing Reviews*, 13, 95-120.
- Baret, F. & Guyot, G. 1991. Potentials and limits of vegetation indices for LAI and APAR assessment. *Remote Sensing of Environment*, 35, 161-173.

- Barton, D. R. A. & Wallace, R. R. 1979. The effects of an experimental spillage of oil sands tailings sludge on benthic invertebrates. *Environmental Pollution*, 18, 305–312.
- Birth, G. S. & Mcvey, G. R. 1968. Measuring the Color of Growing Turf with a Reflectance Spectrophotometer¹. *Agron. J.*, 60, 640-643.
- Blackburn, G. A. 1999. Relationships between spectral reflectance and pigment concentrations in stacks of deciduous broadleaves. *Remote Sensing of Environment*, 70, 224-237.
- Blackburn, G. A. 2007. Wavelet decomposition of hyperspectral data: a novel approach to quantifying pigment concentrations in vegetation. *International Journal of Remote Sensing*, 28, 2831-2855.
- Blackburn, G. A. & Steele, C. M. 1999. Towards the remote sensing of matorral vegetation physiology: Relationships between spectral reflectance, pigment, and biophysical characteristics of semiarid bushland canopies. *Remote sensing of Environment*, 70, 278-292.
- Blumer, M. A. & Sass, J. 1972. Oil pollution: persistence and degradation of spilled fuel oil. *Science*, 9, 1120-2.
- Blunden, L. & Bahaj, A. 2006. Initial evaluation of tidal stream energy resources at Portland Bill, UK. *Renewable Energy*, 31, 121-132.
- Bowman, W. D. 1989. The relationship between leaf water status, gas exchange, and spectral reflectance in cotton leaves. *Remote Sensing of Environment*, 30, 249-255.
- BP 2011. The BP Statistical Report of World Energy Report 2011
http://www.bp.com/content/dam/bp-country/de_de/PDFs/brochures/statistical_review_of_world_energy_full_report_2011.pdf
 [accessed 23/02/2012]
- Breagh, P. 2010. Breagh Pipeline Project: Environmental Statement. Envest Limited/Gair Consulting Limited. <https://www.yumpu.com/en/document/view/9537628/breagh-pipeline-project-environmental-statement-rwecom> [accessed 12/03/2012]
- Brekke, C. & Solberg, A. H. S. 2005. Oil spill detection by satellite remote sensing. *Remote Sensing of Environment*, 95, 1-13.
- Bridge, G. 2008. Global production networks and the extractive sector: Governing resource-based development *Journal of Economic Geography*, 8, 387-419.
- Brooks, R. and Group, E., 1996. EuroQol: the current state of play. *Health policy*, 37(1), pp.53-72.
- Broge, N. H. & Leblanc, E. 2001. Comparing prediction power and stability of broadband and hyperspectral vegetation indices for estimation of green leaf area index and canopy chlorophyll density. *Remote Sensing of Environment*, 76, 156-172.

- Brown, C. E. & Fingas, M. F. 2003. Review of the development of laser fluorosensors for oil spill application. *Marine pollution bulletin*, 47, 477-484.
- Bruce, C.M. and Hilbert, D.W., 2006. Pre-processing methodology for application to Landsat TM/ETM+ imagery of the wet tropics. Rainforest CRC.
- Cáceres, T., Mesa, J. A. & Ortega, F. A. 2007. Locating waste pipelines to minimize their impact on marine environment. *European Journal of Operational Research*, 179, 1143-1159.
- Campbell, J.B. and Wynne, R.H., 2011. Introduction to remote sensing. Guilford Press.
- Carter, G. A. 1993. Responses of Leaf Spectral Reflectance to Plant Stress. *American Journal of Botany*, 80, 239-243.
- Casciello, D., Lacava, T., Pergola, N. and Tramutoli, V., 2007, July. Robust satellite techniques (RST) for oil spill detection and monitoring. In Analysis of Multi-temporal Remote Sensing Images, 2007. MultiTemp 2007. International Workshop on the (pp. 1-6). IEEE.
- Ceccato, P., Flasse, S., Tarantola, S., Jacquemoud, S. & Grégoire, J.-M. 2001. Detecting vegetation leaf water content using reflectance in the optical domain. *Remote Sensing of Environment*, 77, 22-33.
- Chander, G., Markham, B.L. and Helder, D.L., 2009. Summary of current radiometric calibration coefficients for Landsat MSS, TM, ETM+, and EO-1 ALI sensors. *Remote sensing of environment*, 113(5), pp.893-903.
- Chander, G. and Markham, B., 2003. Revised Landsat-5 TM radiometric calibration procedures and postcalibration dynamic ranges. *Geoscience and Remote Sensing, IEEE Transactions on*, 41(11), pp.2674-2677.
- Chavez, P.S., 1996. Image-based atmospheric corrections-revisited and improved. *Photogrammetric engineering and remote sensing*, 62(9), pp.1025-1035.
- CIA 2005. *World Fact Book* [Online]. Available: <https://www.cia.gov/news-information/press-releases-statements/press-release-archive-2005/pr04282005.html> [Accessed 21/10/2015].
- CIA 2011. *CIA World Factbook In: AGENCY, C. I. (ed.)*.
<https://www.cia.gov/library/publications/download/download-2011/> [Accessed 03/12/2012]
- Crawford, M., 1987. Preliminary evaluation of remote sensing data for detection of vegetation stress related to hydrocarbon microseepage- Mist Gas Field, Oregon. In Thematic Conference on Remote Sensing for Exploration Geology, 5 th, Reno, NV.
- Crunkilton, R. L., And & Duchrow, R. M. 1990. Impact of a massive crude oil spill on the invertebrate fauna of a missouri Ozark stream. *Environmental Pollution*, 63, 13-31.

- Cushman, R. M. A. & Goyert, J. C. 1984. Effects of a synthetic crude oil on pond benthic insects. *Environmental Pollution* 33, 163–186.
- Delalieux, S., Somers, B., Hereijgers, S., Verstraeten, W. W., Keulemans, W. & Coppin, P. 2008. A near-infrared narrow-waveband ratio to determine Leaf Area Index in orchards. *Remote Sensing of Environment*, 112, 3762-3772.
- Díaz, B. M. & Blackburn, G. A. 2003. Remote sensing of mangrove biophysical properties: Evidence from a laboratory simulation of the possible effects of background variation on spectral vegetation indices. *International Journal of Remote Sensing*, 24, 53-73.
- Douglas, D.H., 1986. Experiments to locate ridges and channels to create a new type of digital elevation model. *Cartographica: The International Journal for Geographic Information and Geovisualization*, 23(4), pp.29-61.
- Doust, H. 1990. Petroleum geology of the Niger Delta. *Geological Society, London, Special Publications*, 50, 365.
- Drew, R.A., 1992. Improved techniques for in vitro propagation and germplasm storage of papaya. *HortScience*, 27(10), pp.1122-1124.
- Duggin, M.J. and Robinove, C.J., 1990. Assumptions implicit in remote sensing data acquisition and analysis. *Remote Sensing*, 11(10), pp.1669-1694.
- EEA 2007. EEA environmental statement 2007.
http://www.eea.europa.eu/publications/corporate_document_2007_2 [Accessed 21/04/2013]
- Egberongbe, F. O. A., Nwilo, P. C. & Badejo, O. T. 2006. Oil Spill Disaster Monitoring Along Nigerian Coastline. *Promoting Land Administration and Good Governance 5th FIG Regional Conference*. Accra, Ghana, .
- Elliott, A. J. 1986. Shear diffusion and the spread of oil in the surface layers of the North Sea. *Deutsche Hydrografische Zeitschrift*, 39, 113-137.
- Evans, K.F., Evans, A.H., Nolt, I.G. and Marshall, B.T., 1999. The prospect for remote sensing of cirrus clouds with a submillimeter-wave spectrometer. *Journal of Applied Meteorology*, 38(5), pp.514-525.
- Fagbami, A. A., Udo, E. J. & Udo, C. T. I. 1988. Vegetation damage in an oil field in the Niger Delta of Nigeria. *Journal of Tropical Ecology*, 4, 61-75.
- Falola, T. & Heaton, M. M. 2008. *A History of Nigeria*, London, University of Cambridge Press.
- Feder, A.M. and Penfield, G.T., 1985. Remote sensing detection of microseepages in hydrocarbon exploration. In *International Symposium on Remote Sensing of Environment: The*

- Proceedings of Fourth Thematic Conference on Remote Sensing for Exploration Geology (pp. 79-92).
- Fingas, M. F. & Brown, C. E. 1997. Review of oil spill remote sensing. *Spill Science & Technology Bulletin*, 4, 199-208.
- Flood, N. 2014. Continuity of Reflectance Data between Landsat-7 ETM+ and Landsat-8 OLI, for Both Top-of-Atmosphere and Surface Reflectance: A Study in the Australian Landscape. *Remote Sensing*, 6, 7952-7970.
- Gao, B.-C. 1996. NDWI—a normalized difference water index for remote sensing of vegetation liquid water from space. *Remote sensing of environment*, 58, 257-266.
- Garbrechta, J. A. & Martzb, L. W. 1997. The assignment of drainage direction over flat surfaces in raster digital elevation models. *Journal of Hydrology*, 193, 204–213.
- Getter, C. D., Scott, G. I. & Michel, J. The effects of oil spills on mangrove forests: a comparison of five oil spill sites in the Gulf of Mexico and the Caribbean Sea. International Oil Spill Conference, 1981. American Petroleum Institute, 535-540.
- Gitelson, A. A., Gritz , Y. & Merzlyak, M. N. 2003. Relationships between leaf chlorophyll content and spectral reflectance and algorithms for non-destructive chlorophyll assessment in higher plant leaves. *Journal of Plant Physiology*, 160, 271-282.
- Gitelson, A. A., Kaufman, Y. J. & Merzlyak, M. N. 1996. Use of a green channel in remote sensing of global vegetation from EOS-MODIS. *Remote Sensing of Environment*, 58, 289-298.
- Glass, J. & Rodi, W. An explicit Hermitian finite difference scheme for pollutant transport in transient river flows. Proc. 4th GAMM Conference on Numerical Fluid Mechanics, 1981.
- Gobron, N., Pinty, B., Verstraete, M.M. and Widlowski, J.L., 2000. Advanced vegetation indices optimized for up-coming sensors: Design, performance, and applications. *Geoscience and Remote Sensing, IEEE Transactions on*, 38(6), pp.2489-2505.
- Goodman, R. 1994. Overview and future trends in oil spill remote sensing. *Spill Science & Technology Bulletin*, 1, 11-21.
- Gordon, J. S. 2007. 10 Moments That Made American Business. *American Heritage*.
- Goslee, S.C., 2011. Analyzing remote sensing data in R: the landsat package. *Journal of Statistical Software*, 43(4), pp.1-25.
- Greenle, D. D. 1987. Raster and Vector Processing for Scanned Linework. *Photogrammetric Engineering and Remote Sensing*, 53 1383–1387.
- Grimaz, S., Allen, S., Stewart, J. & Dolcetti, G. Fast prediction of the evolution of oil penetration into the soil immediately after an accidental spillage for rapid-response purposes. Proceeding of

- 3rd International Conference on Safety & Environment in Process Industry, CISAP-3, Rome (I) 11-14 May 2008, Chemical Engineering Transactions, 2008. Citeseer.
- Guyot, G., Baret, F., & Jacquemoud, S. 1992. Imaging spectroscopy for vegetation indices. *Imaging Spectroscopy: Fundamentals and Prospective Applications*, 145-165.
- Hausamann, D., Zirnig, W., Schreier, G. and Strobl, P., 2005. Monitoring of gas pipelines-a civil UAV application. *Aircraft Engineering and Aerospace Technology*, 77(5), pp.352-360.
- Henderson-Sellers, A., Yang, Z.L. and Dickinson, R.E., 1993. The project for intercomparison of land-surface parameterization schemes. *Bulletin of the American Meteorological Society*, 74(7), pp.1335-1349.
- Holly Jr, F. M. & Usseglio-Polatera, J.-M. 1984. Dispersion simulation in two-dimensional tidal flow. *Journal of Hydraulic Engineering*, 110, 905-926.
- Hongliang, F., Shunlin, L., McClaran, M. P., Van Leeuwen, W. J. D., Drake, S., Marsh, S. E., Thomson, A. M., Izaurrealde, R. C. & Rosenberg, N. J. 2005. Biophysical characterization and management effects on semiarid rangeland observed from Landsat ETM+ data. *Geoscience and Remote Sensing, IEEE Transactions on*, 43, 125-134.
- Hörig, B., Kühn, F., Oschütz, F. & Lehmann, F. 2001. HyMap hyperspectral remote sensing to detect hydrocarbons. *International Journal of Remote Sensing*, 22, 1413-1422.
- Houborg, R. & Boegh, E. 2008. Mapping leaf chlorophyll and leaf area index using inverse and forward canopy reflectance modeling and SPOT reflectance data. *Remote Sensing of Environment*, 112, 186-202.
- HRW, 1999. The Price of Oil: Corporate sibility and Violations In Nigerian Oil Producing Communities. *New York*. <https://www.hrw.org/reports/1999/nigeria/nigeria0199.pdf> [accessed 02/01/2013]
- Hu, C. and White, R.M., 1983. Solar cells: from basic to advanced systems.
- Huang, B., Duncan, R.R. and Carrow, R.N., 1997. Drought-resistance mechanisms of seven warm-season turfgrasses under surface soil drying: II. Root aspects. *Crop Science*, 37(6), pp.1863-1869.
- Huete, A., Didan, K., Miura, T., Rodriguez, E. P., Gao, X. & Ferreira, L. G. 2002. Overview of the radiometric and biophysical performance of the MODIS vegetation indices. *Remote Sensing of Environment*, 83, 195-213.
- Huete, A., Justice, C. & Van Leeuwen, W. 1999. MODIS vegetation index (MOD13). *Algorithm theoretical basis document*, 3, 213.

- Huete, A. R. 1988. A soil-adjusted vegetation index (SAVI). *Remote Sensing of Environment*, 25, 295-309.
- Huete, A. R., Hua, G., Qi, J., Chehbouni, A. & Van Leeuwen, W. J. D. 1992. Normalization of multidirectional red and NIR reflectances with the SAVI. *Remote Sensing of Environment*, 41, 143-154.
- Huete, A. R. & Jackson, R. D. 1987. Suitability of spectral indices for evaluating vegetation characteristics on arid rangelands. *Remote Sensing of Environment*, 23, 213-IN8.
- Hunt Jr, E. R. & Rock, B. N. 1989. Detection of changes in leaf water content using Near- and Middle-Infrared reflectances. *Remote Sensing of Environment*, 30, 43-54.
- Hussein, M., Jin, M. & Weaver, J. W. 2002. Development and verification of a screening model for surface spreading of petroleum. *Journal of Contaminant Hydrology*, 57
- IEA 2011. World Energy Outlook. <http://www.worldenergyoutlook.org/weo2011/> [accessed 27/02/2013]
- Ikwegbu, N. 2007. Impact of oil Development Activities on the Physico-socio-economic Sustainability of the Niger Delta of Nigeria. [publisher not identified]
- Jensen, R. J. 2014. *Remote sensing of the environment - An earth resource perspective*, Essex UK, Pearson Education Ltd. Essex, UK.
- Jenson, S. K. & Domingue, J. O. 1988. Extracting topographic structure from digital elevation data for geographic information system analysis. *Photogrammetric Engineering and Remote Sensing*, 54, 1593-1600.
- Jha, M. N., Levy, J. & Gao, Y. 2008. Advances in remote sensing for oil spill disaster management: state-of-the-art sensors technology for oil spill surveillance. *Sensors*, 8, 236-255.
- Jiang, Z., Huete, A. R., Didan, K. & Miura, T. 2008. Development of a two-band enhanced vegetation index without a blue band. *Remote Sensing of Environment*, 112, 3833-3845.
- Karnieli, A., Kaufman, Y. J., Remer, L. A. & Wald, A. 2001. Afri — aerosol free vegetation index. *Remote Sensing of Environment*, 77, 10-21.
- Kaufman, Y. J. & Tanre, D. 1992. Atmospherically resistant vegetation index (ARVI) for EOS-MODIS. *IEEE Transactions on Geoscience and Remote Sensing*, 30, 261-270.
- Key, C. H., Benson, N., Ohlen, D., Howard, S., Mckinley, R. & Zhu, Z. 2002. The normalized burn ratio and relationships to burn severity: ecology, remote sensing and implementation. *Proceedings of the Ninth Forest Service Remote Sensing Applications Conference. American Society for Photogrammetry and Remote Sensing, Bethesda, MD. San Diego, CA.*

- Khanna, S., Santos, M. J., Ustin, S. L., Koltunov, A., Kokaly, R. F. & Roberts, D. A. 2013. Detection of Salt Marsh Vegetation Stress and Recovery after the Deepwater Horizon Oil Spill in Barataria Bay, Gulf of Mexico Using AVIRIS Data. *PLoS ONE*, 8, e78989.
- Kostecki, P. T. 1991. *Hydrocarbon Contaminated Soils and Groundwater: Analysis, Fate, Environmental & Public Health Effects, & Remediation*, Florida, USA., CRC Press.
- Krylov, N., Boksernan, A. & Stavrovsky, E. 1998. *Oil Industry of the Former Soviet Union - Reserves, Extraction and Transportation: Reserves, Extraction and Transportation*, CRC Press. Boca Raton, Florida, United States.
- Landgrebe, D. A. 2005. *Signal theory methods in multispectral remote sensing*, John Wiley & Sons. Hoboken, New Jersey, United States.
- Li, L., Ustin, S. L. & Lay, M. 2005. Application of AVIRIS data in detection of oil-induced vegetation stress and cover change at Jornada, New Mexico. *Remote Sensing of Environment*, 94, 1-16.
- Li, Z., Cihlar, J., Zheng, X., Moreau, L. and Ly, H., 1996. The bidirectional effects of AVHRR measurements over boreal regions. *Geoscience and Remote Sensing, IEEE Transactions on*, 34(6), pp.1308-1322.
- Lillesand, T. M., Kiefer, R. W. & Chipman, J. W. 2008. *Remote Sensing and Image Interpretation*, New Jersey, John Wiley & Sons, Inc. Hoboken, New Jersey, United States.
- Lillesand, T.M., Kiefer, R.W. and Chipman, J.W., 2008. Digital image interpretation and analysis. *Remote Sensing and Image Interpretation*, 6, pp.545-81.
- Lin, Q., Mendelsohn, I.A., Suidan, M.T., Lee, K. and Venosa, A.D., 2002. The dose-response relationship between No. 2 fuel oil and the growth of the salt marsh grass, *Spartina alterniflora*. *Marine Pollution Bulletin*, 44(9), pp.897-902.s
- Liu, H. Q. & Huete, A. 1995. Feedback based modification of the NDVI to minimize canopy background and atmospheric noise. *IEEE Transactions on Geoscience and Remote Sensing*, 33, 457-465.
- Liu, W. X., Luo, Y. M., Teng, Y., Li, Z. G. & Wu, L. H. 2007. A survey of petroleum contamination in several Chinese oilfield soils. *Soils*, 39, 247-251.
- López, G. M. J. & Caselles, V. 1991. Mapping burns and natural reforestation using thematic Mapper data. *Geocarto International*, 6, 31-37.
- Lubin, D. and Massom, R., 2006. *Polar Remote Sensing: Volume I: Atmosphere and Oceans*. Springer Science & Business Media.

- Luis, S. J., And Zemba, S.G. 1993. *Estimating the impact of source depletion on long-term risk assessments. In: Calabrese, E.J., Kostecki, P.T. (Eds.), Hydrocarbon Contaminated Soils.*, Massachusetts, USA, CRC Press.
- Lyon, J. G., Yuan, D., Lunetta, R. S. & Elvidge, C. D. 1998. A Change Detection Experiment Using Vegetation Indices. *Photogrammetric Engineering & Remote Sensing*, 64, 143-150.
- Mackay, D. & Matsugu, R. S. 1973. Evaporation rates of liquid hydrocarbon spills on land and water. *The Canadian Journal of Chemical Engineering*, 51, 434-439.
- Mackay, D. A. & Mohtadi, M. 1975. The area affected by oil spills on land. *The Canadian Journal of Chemical Engineering*, 53, 140–143.
- Mack, G. and Petkova, V.B., 1979. Comparison of lattice gauge theories with gauge groups Z_2 and $SU(2)$. *Annals of Physics*, 123(2), pp.442-467.
- Main, R., Cho, M. A., Mathieu, R., O’kennedy, M. M., Ramoelo, A. & Koch, S. 2011. An investigation into robust spectral indices for leaf chlorophyll estimation. *ISPRS Journal of Photogrammetry and Remote Sensing*, 66, 751-761.
- Marshall, M., Thenkabail, P., Biggs, T. & Post, K. 2016. Hyperspectral narrowband and multispectral broadband indices for remote sensing of crop evapotranspiration and its components (transpiration and soil evaporation). *Agricultural and Forest Meteorology*, 218–219, 122-134.
- Masnik, M. T., Stauffer, J. R., Hocutt, C. H. & Wilson, J. H. 1976. Effects of an oil spill on the macroinvertebrates and fish in a small southwestern Virginia creek. *Journal Name: Journal Environmental Science and Health, Part A; (United States); Journal Volume: A11:4-5, Medium: X; Size: Pages: 281-296.*
- Mather, P. M. & Koch, M. 2011. *Computer processing of remotely-sensed images - An Introduction*, New York, Wiley-Blackwell. New York, United States.
- Metternicht, G. 2003. Vegetation indices derived from high-resolution airborne videography for precision crop management. *International Journal of Remote Sensing*, 24, 2855-2877.
- Motohk, T., Nasahara, K. N., Oguma, H. A. & Tsuchida, S. 2010. Applicability of Green-Red Vegetation Index for Remote Sensing of Vegetation Phenology. *Remote Sensing*, 2, 2369-2387.
- Myneni, R. B., Hoffman, S., Knyazikhin, Y., Privette, J. L., Glassy, J., Tian, Y., Wang, Y., Song, X., Zhang, Y., Smith, G. R., Lotsch, A., Friedl, M., Morisette, J. T., Votava, P., Nemani, R. R. & Running, S. W. 2002. Global products of vegetation leaf area and fraction absorbed PAR from year one of MODIS data. *Remote Sensing of Environment* 83, 214–231.

- NASA. [Accessed 20/03/2014].
- NASA. *Earth's Energy Budget* <http://nasawavelength.org/resource/nw-000-000-001-680> [Online]. [Accessed 20/11/2015].
- Nduka, J. K. & Orisakwe, O. E. 2011. Water-quality issues in the Niger Delta of Nigeria: a look at heavy metal levels and some physicochemical properties. *Environmental Science Pollution Research International*, 18, 237-46.
- NEB 2006. Canadian Energy Overview - An Energy Market Assessment May 2007. http://publications.gc.ca/collections/collection_2008/neb-one/NE2-4-2007E.pdf [accessed 30/02/2013]
- NNPC 2011. Annual Statistical Bulletin. First Edition ed. <http://www.nnpcgroup.com/Portals/0/Monthly%20Performance/2011%20ASB%201st%20edition.pdf>[accessed 12/12/2012]
- NNPC/Petroleum Economist. 2005. *Energy Map of Nigeria*. London: Petroleum Economist. <http://store.petroleum-economist.com/Map-Gas-Power-Infrastructure-Map-of-Nigeria-p/mpem309.htm>
- Noomen, M.F., 2007. Hyperspectral reflectance of vegetation affected by underground hydrocarbon gas seepage, Enschede, ITC 151p. ISBN 978-90-8504-671-4.
- Noomen, M. F., Hakkarainen, A., Van Der Meijde, M. & Van Der Werff, H. M. A. 2015. Evaluating the feasibility of multitemporal hyperspectral remote sensing for monitoring bioremediation. *International Journal of Applied Earth Observation and Geoinformation*, 34, 217-225.
- Noomen, M. F. & Skidmore, A. K. 2008. The effects of high soil CO₂ concentrations on leaf reflectance of maize plants. *International Journal of Remote Sensing*, 30, 481-497.
- Noomen, M. F., Smith, K. L., Colls, J. J., Steven, M. D., Skidmore, A. K. & Van Der Meer, F. D. 2008. Hyperspectral indices for detecting changes in canopy reflectance as a result of underground natural gas leakage. *International Journal of Remote Sensing*, 29, 5987-6008.
- Noomen, M. F., Van Der Werff, Herald, M. A. & Van Der Meer, F. D. 2012. Spectral and spatial indicators of botanical changes caused by long-term hydrocarbon seepage. *Ecological Informatics*, 5, 55-64
- Obire, O. & Nwaubeta, O. 2002. Effects of refined petroleum hydrocarbon on soil physiochemical and bacteriological characteristics. *Journal of Applied Science Environment*, 6, 39-44.
- Odjugo, P. A. O. 2005. An analysis of rainfall patterns in Nigeria. *Global Journal of Environmental Sciences*, 4, 139-145.

- Oguntunde, P. G., Abiodun, B. J. & Lischeid, G. 2011. Rainfall trends in Nigeria, 1901–2000. *Journal of Hydrology*, 411, 207-218.
- Ohimain, E. 2004. Environmental impacts of dredging in the Niger Delta. *Terra et Aqua*, 97, 9-19.
- Ohimain, E. I., Bamidele, J. F. & Omisore, O. O. 2010. The Impacts of Micro-Topographic Changes on Mangroves in the Lower Reaches of the Benin River, Niger Delta. *Environmental Research Journal*, 4, 167-172.
- Okoro, D., Oviasogie, P. O. & Oviasogie, F. E. 2011. Soil quality assessment 33 months after crude oil spillage and clean-up. *Chemical Speciation and Bioavailability*, 23, 1-6.
- Oliveira, W.J., Crosta, A. and Goncalves, J.L.M., 1997, November. Spectral characteristics of soils and vegetation affected by hydrocarbon gas: a greenhouse simulation of the Remanso do Fogo seepage. In Applied Geologic Remote Sensing-International Conference- (Vol. 1, pp. I-83).
- OPEC 2011. Annual Statistical Bulletin.
https://www.opec.org/opec_web/static_files_project/media/downloads/publications/ASB2010_2011.pdf[accessed 15/12/2012]
- Osuji, L. C. & Ezebuoro, P. E. 2006. Hydrocarbon contamination of a typical mangrove floor in Niger Delta, Nigeria. *International Journal of Environmental Science Technology* 3, 313-320.
- Osuji, L. C. & Opiah, U. C. 2007. Hydrocarbon contamination of a terrestrial ecosystem: the case of Oshire-2 oil spill in Niger Delta, Nigeria. *The Environmentalist*, 27, 337-340.
- Osuji, L. C., Udoetok, I. A. & Ogali, R. E. 2006. Attenuation of Petroleum Hydrocarbons by Weathering: A Case Study. *Chemistry & Biodiversity*, 3, 422-433.
- Otterman, J. & Fraser, R. S. 1979. Adjacency effects on imaging by surface reflection and atmospheric scattering: cross radiance to zenith. *Applied Optics*, 18, 2852-2860.
- Penuelas, J., Pinol, J., Ogaya, R. & Filella, I. 1997. Estimation of plant water concentration by the reflectance Water Index WI (R900/R970). *International Journal of Remote Sensing*, 18, 2869-2875.
- Pezeshki, S., Hester, M., Lin, Q. & Nyman, J. 2000. The effects of oil spill and clean-up on dominant US Gulf coast marsh macrophytes: a review. *Environmental Pollution*, 108, 129-139.
- Purkis, S. & Klemas, V. 2011. *Remote Sensing and Global Environmental Change*, West Sussex UK, Wiley-Blackwell & Sons Ltd. West Sussex UK.
- Qi, J., Cabot, F., Moran, M. S. & Dedieu, G. 1995. Biophysical parameter estimations using multidirectional spectral measurements. *Remote Sensing of Environment*, 54, 71-83.

- Qi, J., Chehbouni, A., Huete, A. R., Kerr, Y. H. & Sorooshian, S. 1994. A modified soil adjusted vegetation index. *Remote Sensing of Environment*, 48, 119-126.
- Raghavan, V. 2000. Developmental Biology of Flowering Plants. *Plant Growth Regulation* 33, 245–246.
- Rajitha, K., Prakash Mohan, M.M. and Varma, M.R., 2015, January. Effect of cirrus cloud on normalized difference Vegetation Index (NDVI) and Aerosol Free Vegetation Index (AFRI): A study based on LANDSAT 8 images. In *Advances in Pattern Recognition (ICAPR), 2015 Eighth International Conference on* (pp. 1-5). IEEE.
- Rondeaux, G., Steven, M. & Baret, F. 1996. Optimization of soil-adjusted vegetation indices. *Remote Sensing of Environment*, 55, 95-107.
- Rosenberg, D.M., Wiens, A.P. and Flannagan, J.F., 1980. Effects of crude oil contamination on Ephemeroptera in the Trail River, Northwest Territories, Canada (pp. 443-455). Springer US.
- Rosso, P. H., Pushnik, J. C., Lay, M. & Ustin, S. L. 2005. Reflectance properties and physiological responses of *Salicornia virginica* to heavy metal and petroleum contamination. *Environmental Pollution*, 137, 241-252.
- Rouse, J. W., Jr.; Haas, R. H., Schell, J. A. & Deering, D. W. 1973. Monitoring the vernal advancement and retrogradation (green wave effect) of natural vegetation *Prog. Rep. RSC 1978-1* 93.
- Roy, D.P., Kovalsky, V., Zhang, H.K., Vermote, E.F., Yan, L., Kumar, S.S. and Egorov, A., 2016. Characterization of Landsat-7 to Landsat-8 reflective wavelength and normalized difference vegetation index continuity. *Remote Sensing of Environment*. in press, available online <http://www.sciencedirect.com/science/article/pii/S0034425715302455> [accessed 31/05/2016]
- Running, S. W., C. O. Justice, V. Salomonson, D. Hall, J. B., Y. J. Kaufmann, A. H. Strahler, A. R. Huete, J.-P. Muller, V. Vanderbilt, Z. M. Wan, P. Teillet & Carneggie, D. 1994. Terrestrial remote sensing science and algorithms planned for EOS/MODIS. *International Journal of Remote Sensing*, 15, 3587-3620.
- Saiko, T. 2001. *Saiko, T., 2001*. Environmental crises: geographical case studies in post-Socialist Eurasia. Pearson Education. England, UK.
- Saleska, S. R., Didan, K., Huete, A. R. & Da Rocha, H. R. 2007. Amazon Forests Green-Up During 2005 Drought. *Science*, 318, 612.
- Schumacher, D. 1996. Hydrocarbon-induced alteration of soils and sediments. 71-89.
- Scott, J.S., 1966. Report on the fisheries of the Niger Delta special area. NDDB 109pp.

- Schaepman-Strub, G., Schaepman, M.E., Painter, T.H., Dangel, S. and Martonchik, J.V., 2006. Reflectance quantities in optical remote sensing—Definitions and case studies. *Remote sensing of environment*, 103(1), pp.27-42.
- Schowengerdt, R.A., 2006. *Remote sensing: models and methods for image processing*. Academic press. Cambridge, Massachusetts, USA.
- Schneider, S.H., 1972. Cloudiness as a global climatic feedback mechanism: The effects on the radiation balance and surface temperature of variations in cloudiness. *Journal of the Atmospheric Sciences*, 29(8), pp.1413-1422.
- Sekuler, R. and Blake, R., 1985. *Perception*. Alfred A. Kopf NY.
- Shell Petroleum. <http://www.shell.com/> [Accessed 14/08/2014].
- Shippert, P. 2013. <http://m.exelisvis.com/Blogs/TabId/1524/PageID/3/PgrID/5703/PID/5703/authorid/562/AuthorName/PegShippert/Default.aspx>
- Simmons, C. & Keller, J. 2005. Liquid Spills on Permeable Soil Surfaces: Experimental Confirmations. PNNL-15408. *Pacific Northwest National Laboratory, Richland, Washington*.
- Simmons, C. S., Keller, J. M. & Hylden, J. L. 2004. *Spills on Flat Inclined Pavements*, United States. Department of Energy. http://www.pnl.gov/main/publications/external/technical_reports/PNNL-14577.pdf[accessed 20/04/2015]
- Simmons, C. S. A. & Keller, J. M. 2003. Status of Models for Land Surface Spills of Nonaqueous Liquids. *In: ENERGY, U. S. D. O. (ed.)*. Washington: Pacific Northwest National Laboratory.
- Simonich, S.L. and Hites, R.A., 1995. Global distribution of persistent organochlorine compounds. *Science*, 269(5232), p.1851.k
- Sims, D. A. 2002. Relationship between leaf pigment content and spectral reflectance across a wide range of species, leaf structures and developmental stages. *Remote Sensing of Environment* 18, 337-354
- Singh, C. & Lin, J. 2008. Isolation and characterization of diesel oil degrading indigenous microorganisms in Kwazulu-Natal, South Africa. *African Journal of Biotechnology*, 7.
- Slonecker, T., Fisher, G. B., Aiello, D. P. & Haack, B. 2010. Visible and Infrared Remote Imaging of Hazardous Waste: A Review. *Remote Sensing*, 2, 2474-2508.
- Smil, V. 2010. *Energy Transitions: History, Requirements, Prospects*, Oxford, England, Praeger An Imprint of ABC-CLIO, LLC.

- Smith, K. L., Steven, M. D. & Colls, J. J. 2004. Use of hyperspectral derivative ratios in the red-edge region to identify plant stress responses to gas leaks. *Remote Sensing of Environment*, 92, 207-217.
- Smith, K. L., Steven, M. D. & Colls, J. J. 2005. Plant spectral responses to gas leaks and other stresses. *International Journal of Remote Sensing*, 26, 4067-4081.
- Song, J.J., Lee, C.I. and Seto, M., 2001. Stability analysis of rock blocks around a tunnel using a statistical joint modeling technique. *Tunnelling and underground space technology*, 16(4), pp.341-351.
- Sripada, R. P., Heinigerb, R. W., Whitec, J. G. A. & Meijer, A. D. 2005. Aerial Color Infrared Photography for Determining Early In-Season Nitrogen Requirements in Corn *Agronomy Journal*, 98 968-977.
- Studer, S., Stöckli, R., Appenzeller, C. & Vidale, P. L. 2007. A comparative study of satellite and ground-based phenology. *International Journal of Biometeorol*, 51, 405–414.
- Sweet, F., Kauffman, M., Pellerin, T., Espy, D. & Mills, M. An estimate of the national cost for remediation of MTBE releases from existing leaking underground storage tank sites. *Proceedings of the Annual International Conference on Soils, Sediments, Water and Energy*, 2006 University of Massachusetts.
- Tishchenko, A.V., 2000. Generalized source method: new possibilities for waveguide and grating problems. *Optical and quantum electronics*, 32(6-8), pp.971-980.
- Teillet, P. M., Staenz, K. & Williams, D. 1997. Effects of spectral, spatial and radiometric characteristics on remote sensing vegetation indices. *Remote Sensing of Environment*, 18, 139-149.
- Tucker, C. J. 1979. Red and photographic infrared linear combinations for monitoring vegetation. *Remote Sensing of Environment*, 8, 127-150.
- UNEP 2007. Mangroves of Western and Central Africa.
http://www.unep.org/regionalseas/publications/otherpubs/pdfs/Mangroves_of_Western_and_Central_Africa.pdf[accessed 20/02/2014]
- UNEP 2011. Environmental Assessment of Ogoniland. UNEP Nairobi.
<http://www.unep.org/disastersandconflicts/CountryOperations/Nigeria/EnvironmentalAssessmentofOgonilandreport/tabid/54419/Default.aspx>[accessed 15/12/2011]
- Ustin, S. L., Roberts, D. A., Pinzón, J., Jacquemoud, S., Gardner, M., Scheer, G., Castañeda, C. M. & Palacios-Orueta, A. 1998. Estimating canopy water content of chaparral shrubs using optical methods. *Remote Sensing of Environment*, 65, 280-291.

- Van Der Meer, F., Van Dijk, P., Kroonenberg, S., Hong, Y. & Lang, H. 2000. Hyperspectral hydrocarbon microseepage detection and monitoring: potentials and limitations. *Second EARsel Workshop on Imaging Spectroscopy, Enschede, 2000*.
- Van Der Meer, F., Van Dijk, P., Van Der Werff, H. & Yang, H. 2002. Remote sensing and petroleum seepage: a review and case study. *Terra Nova*, 14, 1-17.
- Van Der Meijde, M., Van Der Werff, H. M. A., Jansma, P. F., Van Der Meer, F. D. & Groothuis, G. J. 2009. A spectral-geophysical approach for detecting pipeline leakage. *International Journal of Applied Earth Observation and Geoinformation*, 11, 77-82.
- Van Der Werff, H., Van Der Meijde, M., Jansma, F., Van Der Meer, F. & Groothuis, G. J. 2008. A Spatial-Spectral Approach for Visualization of Vegetation Stress Resulting from Pipeline Leakage. *Sensors*, 8, 3733-3743.
- Van Der Werff, H. M. A., Noomen, M. F., Van Der Meijde, M. & Van Der Meer, F. D. 2007. Remote sensing of onshore hydrocarbon seepage: problems and solutions. *Geological Society, London, Special Publications*, 283, 125-133.
- Van Persie, M., Van der Kamp, A. and Algra, T., 2004. Simulation and optimisation of a high resolution optical remote sensing system for monitoring of the European gas pipeline network. In XXth ISPRS Congress, Istanbul, Turkey (Vol. 113, No. 1, pp. 46-54).
- Wang, C., Chen, B., Zhang, B., He, S. and Zhao, M., 2013. Fingerprint and weathering characteristics of crude oils after Dalian oil spill, China. *Marine pollution bulletin*, 71(1), pp.64-68.
- Wang, F.-M., Huang, J.-F., Tang, Y.-L. & Wang, X.-Z. 2007. New Vegetation Index and Its Application in Estimating Leaf Area Index of Rice. *Rice Science*, 14, 195-203.
- Weston, D.C. and Gibson Jr, G.E., 1993. Partnering-project performance in US Army Corps of Engineers. *Journal of Management in Engineering*, 9(4), pp.410-425.
- Wiedemeier, T.H., 1999. Natural attenuation of fuels and chlorinated solvents in the subsurface. John Wiley & Sons.
- Wu, C., Niu, Z., Tang, Q. & Huang, W. 2008. Estimating chlorophyll content from hyperspectral vegetation indices: Modeling and validation. *Agricultural and Forest Meteorology*, 148, 1230-1241.
- Wulder, M.A., White, J.C., Magnussen, S. and McDonald, S., 2007. Validation of a large area land cover product using purpose-acquired airborne video. *Remote Sensing of Environment*, 106(4), pp.480-491.
- Wynn, C., 2000. An introduction to BRDF-based lighting. Nvidia Corporation.

- Xu, D.Q., Ni, G.Q., Jiang, L.L., Shen, Y.T., Li, T., Ge, S.L. & Shu, X.B. 2008. Exploring for natural gas using reflectance spectra of surface soils. *Advances in Space Research*, 41, 1800-1817.
- Xu, Z. & Ratha, D. 2008. *Migration and remittances factbook 2008*, World Bank Publications.
- Yang, H., Meer, F. V. D., Zhang, J. & Kroonenberg, S. B. 2000. Direct detection of onshore hydrocarbon microseepages by remote sensing techniques. *Remote Sensing Reviews*, 18, 1-18.
- Yang, X. and Lo, C.P., 2000. Relative radiometric normalization performance for change detection from multi-date satellite images. *Photogrammetric Engineering and Remote Sensing*, 66(8), pp.967-980.
- Yoder, B. J. A. & Waring, R. H. 1994. The normalized difference vegetation index of small Douglas-fir canopies with varying chlorophyll concentrations. *Remote Sensing of Environment*, 49, 81-91.
- Zarco-Tejada, P. J., Berjón, A., López-Lozano, R., Miller, J. R., Martín, P., Cachorro, V., González, M. R. & De Frutos, A. 2005. Assessing vineyard condition with hyperspectral indices: Leaf and canopy reflectance simulation in a row-structured discontinuous canopy. *Remote Sensing of Environment*, 99, 271-287.
- Zhang, G., Zheng, Z., Shen, X., Zou, L. & Huang, K. 2011. Remote sensing interpretation of areas with hydrocarbon microseepage in northeast China using Landsat-7/ETM+ data processing techniques. *International Journal of Remote Sensing*, 32, 6695-6711.
- Zhao, Q. & Li, Y. Monitoring Marine Oil-spill Using Microwave Remote Sensing Technology. *Electronic Measurement and Instruments*, 2007. ICEMI '07. 8th International Conference on, Aug. 16 2007-July 18 2007 2007. 4-69-4-72.
- Zhou, J., Murray, A. and Abes, J., 2008, January. Implementation of Alternative Integrity Validation on a Large Diameter Pipeline Construction Project. In 2008 7th International Pipeline Conference (pp. 153-165). American Society of Mechanical Engineers.
- Zhu, L., Zhao, X., Lai, L., Wang, J., Jiang, L., Ding, J., Liu, N., Yu, Y., Li, J., Xiao, N., Zheng, Y. & Rimmington, G. M. 2013. Soil TPH concentration estimation using vegetation indices in an oil polluted area of eastern China. *PLoS One*, 8, e54028.

Appendix

This thesis comprises introduction, literature, methodology and three results chapters, 4, 5 and 6 has been published. The co-authors, including the PhD candidate and their respective contributions are detailed below.

Journal publications:

Ch. 4 – Investigating BMVIs for detection and analysis of vegetation stress over time and space in polluted areas.

Parts of the work presented in this chapter have been published as:

Adamu, B., Tansey, K. and Ogutu, B. (2015). "Using vegetation spectral indices to detect oil pollution in the Niger Delta." *Remote Sensing Letters* 6(2): 145-154. doi: 10.1080/2150704X.2015.1015656

Respective co-author contributions: Appendix I. Contributions of co-authors

Adamu, B. (University of Leicester): Carried out the research planning with advice of co-authors, performed data preparation and analysis, vegetation indices extraction for statistical analysis, production of tables and figures, chapter and publication writing and revisions from co-authors.

Tansey, K. (University of Leicester) provided supervision, advice and feedbacks throughout the initial planning process to completion of this work.

Ogutu, B. (University of Leicester 2013-2015; University of Southampton 2015 - date) contributed in the formal supervision, advice on selection of vegetation spectral indices, feedbacks at the mid part of this work.

Ch. 5 – Analysis of factors influencing detectability of oil pollution using BMVIs.

Parts of the work presented in this chapter have been published as:

Adamu, B., Tansey, K. and Ogutu, B., (2016). “An investigation into the factors influencing the detectability of oil spills using spectral indices in an oil-polluted environment”. *International Journal of Remote Sensing*, 37(10), pp.2166-2185. DOI: 10.1080/01431161.2016.1176271

Respective co-author contributions: Appendix I. Contributions of co-authors

Tansey, K. (University of Leicester) provided supervision, advice and feedbacks throughout the initial planning process to completion of this work.

Ogutu, B. (University of Leicester 2013-2015; University of Southampton 2015 - date) contributed in the preparation of the manuscript and feedbacks on this work.

Ch. 6 – Validation of vegetation spectral techniques for detection of oil pollution on vegetation.

Parts of the work a manuscript has been submitted for publication as:

Adamu, B., Tansey, K. and Ogutu, B., (2016). Remote sensing for detection and monitoring of vegetation affected by oil spills. *Remote Sensing Special Edition* on the 9/06/2016 (under review).

Respective co-author contributions: Appendix I. Contributions of co-authors

Tansey, K. (University of Leicester) provided supervision, advice and feedbacks throughout the initial planning process to completion of this work.

Ogutu, B. (University of Leicester 2013-2015; University of Southampton 2015 - date) contributed in the preparation of the manuscript and feedbacks on this work.

Conference proceedings:

Initial results from this work have been presented at conferences and published:

Adamu, B., Tansey, K. and Ogutu, B. (2014). Detection of oil pollution along the pipeline routes in tropical ecosystem from multi-spectral data. *Multisensor, Multisource Information Fusion: Architectures, Algorithms, and Applications 2014*. Braun J. J., ed. Proc. of SPIE. , Baltimore, Maryland, USA.

Adamu, B., Tansey, K. and Bradshaw, M.J. (2013). Investigating vegetation spectral reflectance for detecting hydrocarbon pipeline leaks from multispectral data. *Image and Signal Processing for Remote Sensing XIX*, edited by Lorenzo Bruzzone, Proc. of SPIE. , Dresden, Germany.

Appendix: Copyright Permission from publisher

Adamu, Bashir

From: Masheter, Aimee - Chichester <amasheter@wiley.com> on behalf of Wiley Global Permissions <permissions@wiley.com>
Sent: 04 April 2016 10:25
To: Adamu, Bashir
Subject: RE: Request for permission to use of figures/images

Dear Bashir,

Thank you for your request.

Permission is granted for you to use the material requested for your thesis/dissertation subject to the usual acknowledgements (author, title of material, title of book/journal, ourselves as publisher) and on the understanding that you will reapply for permission if you wish to distribute or publish your thesis/dissertation commercially. You must also duplicate the copyright notice that appears in the Wiley publication in your use of the Material; this can be found on the copyright page if the material is a book or within the article if it is a journal.

Permission is granted solely for use in conjunction with the thesis, and the material may not be posted online separately.

Any third party material is expressly excluded from this permission. If any of the material you wish to use appears within our work with credit to another source, authorisation from that source must be obtained.

Best wishes,

Sophie Flude
Permissions Assistant
John Wiley & Sons Ltd
The Atrium
Southern Gate, Chichester
West Sussex, PO19 8SQ
UK

WILEY

From: Adamu, Bashir [mailto:ba108@leicester.ac.uk]
Sent: 17 March 2016 15:47
To: Wiley Global Permissions
Cc: 'purkis@nova.edu'; 'klemas@udel.edu'
Subject: Request for permission to use of figures/images

Dear Authors/Publisher,

I am currently in the process of finalising my PhD thesis on "*Broadband multispectral indices for remote sensing of vegetation affected by oil spills in the mangrove forest of the Niger Delta, Nigeria*", which I am shortly due to submit to the University of Leicester.

During my research, I came across the following article/image "*Remote sensing and global environmental change*": Figure 5.1 p64 and Figure 5.2 p65 and would like to request your permission to include it in an electronic copy of my thesis.

The University of Leicester requires their students to submit an electronic copy to their institutional repository, Leicester Research Archive (<https://lra.le.ac.uk/>), which is a digital archive of research outputs from the University. By submitting my thesis to the LRA it will be available in full, to anyone, free of charge ("open access").

I believe that the inclusion of image is integral to my thesis and would therefore be extremely grateful if you could grant permission for me to use these images/figures in the manner detailed above. Naturally, I would fully reference your work and include any acknowledgement you deem appropriate.

Please let me know if you require any further information, otherwise thank you in advance for your kind consideration.

Thank you in anticipation to your response.

Bashir Adamu
PhD Research

Centre for Landscape and Climate Research
Department of Geography
University of Leicester, University Road, Leicester, LE1 7RH, UK

t: +44 (0)116
m: +44 (0) 7931905092
e: ba108@le.ac.uk
w: www.le.ac.uk



Follow us on [Twitter](#) or visit our [Facebook](#) page



Elite without being elitist

John Wiley & Sons Limited is a private limited company registered in England with registered number 641132. Registered office address: The Atrium, Southern Gate, Chichester, West Sussex, United Kingdom. PO19 8SQ.
